# Using partially specified models to detect and quantify structural sensitivity in biological systems

Thesis submitted for the degree of
Doctor of Philosophy
at the University of Leicester

by

**Matthew William Adamson**

*Department of Mathematics*

*University of Leicester*

**June 2015**

*“To be uncertain is to be uncomfortable, but to be certain is to be ridiculous.”*

-Chinese proverb

# *Abstract*

Mathematical models in ecology and evolution are highly simplified representations of a complex underlying reality. For this reason, there is always a high degree of uncertainty with regards to the model specification—not just in terms of parameters, but also in the form taken by the model equations themselves. This uncertainty becomes critical for models in which the use of two different functions fitting the same dataset can yield substantially different model predictions—a property known as structural sensitivity. In this case, even if the model is purely deterministic, the uncertainty in the model functions carries through into uncertainty in the model predictions, and new frameworks are required to tackle this fundamental problem. Here, we construct a framework that uses partially specified models: ODE models in which unknown functions are represented not by a specific functional form, but by an entire data range and constraints of biological realism. Partially specified models can be used to rigorously detect when models are structurally sensitive in their predictions concerning the character of an equilibrium point by projecting the data range into a generalised bifurcation space formed of equilibrium values and derivatives of any unspecified functions. The key question of how to carry out this projection is a serious mathematical challenge and an obstacle to the use of partially specified models. We address this challenge by developing several powerful techniques to perform such a projection.

# *Acknowledgements*

I owe a great debt of gratitude to my supervisor Andrew Morozov for his constant support and guidance over the course of my PhD. Through our many meetings his keen insights, broad knowledge and readiness to help have proved to be invaluable assets in the completion of this work, and his passion for research has time and again inspired me to push myself in my studies.

I would also like to thank the staff of the Department of Mathematics for all that they have taught me and the excellent research environment they have provided. In particular, I would like to extend my gratitude to Sergei Petrovskii for always being ready to offer sound advice and words of encouragement.

Thanks also to my fellow residents of Michael Atiyah 126 and the many other friends who have made my time in Leicester so enjoyable, and were always there to provide welcome distraction from my research when it was needed, which was often. I'm also grateful to the bar staff at the Criterion, who were always there to provide beer and pizza when it was needed, which was even more often.

Finally, and most of all, I would like to thank my parents for their unwavering love and support over the years. There can be no doubt that without them I wouldn't be the person I am today or have achieved any of the things I have done. This thesis is for them (even though they probably won't understand a word of it).

# Contents

# Chapter 1

# Introduction

Mathematical models of biological systems based on differential equations often have the troublesome property of structural sensitivity—in which the use of two functional forms that are quantitatively close and qualitatively similar yields contradictory dynamical behaviour (Myerscough et al., 1996; Wood and Thomas, 1999; Cordoleani et al., 2011). Perhaps the best introduction to structural sensitivity would be by way of an example–a particularly striking example of structural sensitivity in a biological model was provided by Fussmann and Blasius (2005). In this paper they considered three different equations for the functional response term— the per-capita feeding rate of the predator as a function of prey density—in a Rosenzweig-MacArthur predator-prey model (this model is shown and discussed later on, in Section 3.3 of this thesis). The three functional forms considered were

$$f(x) = \frac{a_1 x}{1 + b_1 x}, \tag{1.1}$$

$$f(x) = a_2 \tanh(b_2 x), \tag{1.2}$$

$$f(x) = a_3\big(1 - \exp(-b_3 x)\big), \tag{1.3}$$

called the Monod, hyperbolic tangent, and Ivlev functional responses, respectively. Crucially, (1.1), (1.2) and (1.3) are qualitatively similar, and their parameters were chosen so that they all took close values, as can be seen from their graphs in Fig. 1.1. Nevertheless, when used in the Rosenzweig-MacArthur model, they were found to yield completely different model predictions, as is shown by the predicted time series in Figure 1.2. Use of the hyperbolic tangent function (1.2), shown in red, gives us a stable equilibrium. Use of the Ivlev function (1.3) on the other hand, shown in black, exhibits low amplitude oscillations. Most strikingly, use of the Monod function, as shown in blue, yields oscillations with a huge amplitude, with the prey population dropping to dangerously low levels that would lead to its extinction in the real world. Notably, such sensitivity can be observed around a wide range of parameters—not solely in the vicinity of a bifurcation.

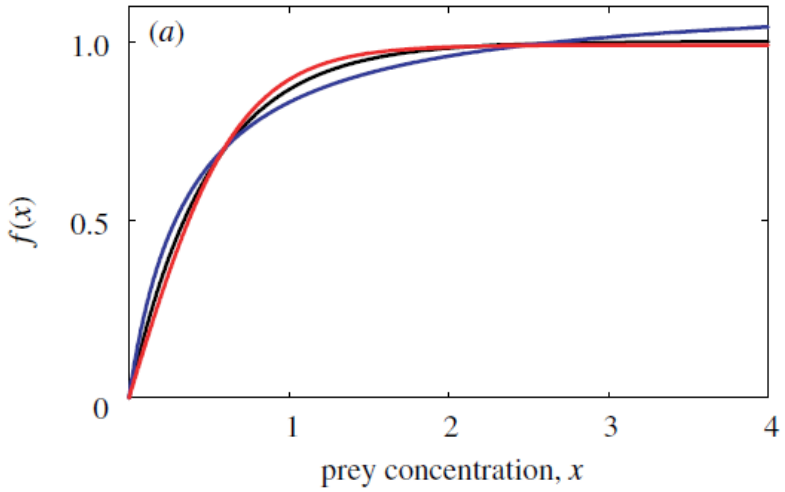


Figure 1.1: Graphs of three different Holling-type II functional responses. The Monod function (1.1) is shown in blue, the hyperbolic tangent function (1.2) is shown in red and the Ivlev function (1.3) is shown in black. Figure originally from (Fussmann and Blasius, 2005).

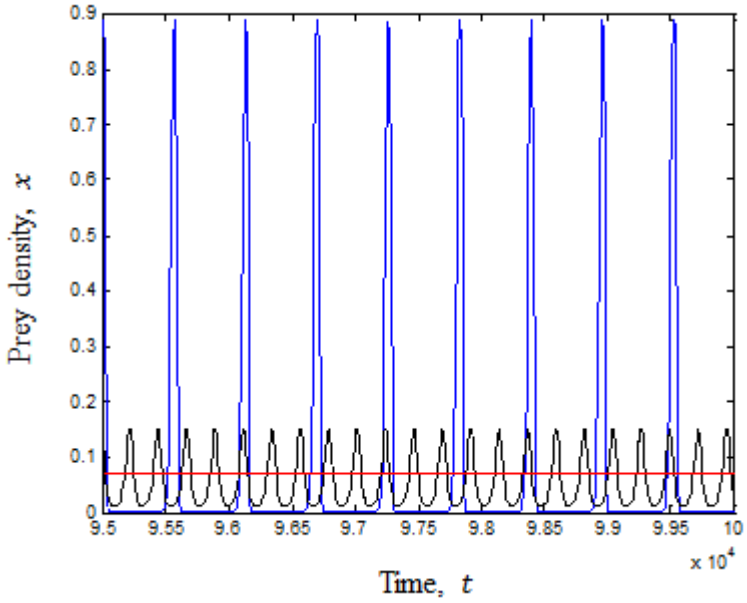


Figure 1.2: Structural sensitivity in the Rosenzweig-MacArthur predator-prey model. Simulated time-series data for the prey species in the Rosenzweig-MacArthur model with the three different functional responses shown in Fig. 1.1.

Models are particularly vulnerable to structural sensitivity when we cannot derive or justify their constituent functions. This is especially the case in biological models, because biological processes have a high level of complexity, involving huge numbers of diverse and heterogeneous individuals interacting across wildly differing spatial and temporal scales in a fluctuating environment. For this reason, any mathematical function

used in the biological sciences is necessarily a highly simplified representation of the process it is intended to represent, and so cannot be justified a priori.

Indeed, even if a particular choice of functional representation is supported by experiments on populations at a laboratory scale, there is no reason the same representation should be valid after aggregating over a heterogeneous population and scaling up to the size of real ecosystems (Chesson, 1998 ; Poggiale, 1998; Pascual et al., 2001; Englund and Leonardsson, 2008; Morozov et al., 2008; Morozov, 2010). Consider, for instance, the famous Monod equation used to describe the feeding rate of a consumer/predator, which has a concrete theoretical basis in ecology (Holling, 1966; Jeschke et al., 2002; Begon et al., 2002). Since we often deal with the dynamics of a population, and not of an individual, we need to use the averaged response over the entire population of consumers, so even in the case where the consumption of each individual is described exactly by a Monod formulation, averaging this non-linear function over the whole population can result in a different mathematical expression.

Another factor which can potentially cause variation in the underlying model functions is evolution of the life traits of animals, which can take place over a relatively short period of time (Thompson, 1998; Duffy and Sivars-Becker, 2007; Kinnison and Hairston, 2007). Finally, to describe species interactions in a real ecosystem, we need to take into account other important factors such as feeding history, complex feeding behaviour, adaptation to food and even short term evolution (Yoshida et al., 2003; Morozov, 2012). Including each of these factors can also seriously alter the well-known Monod formulation, and clearly the same can hold true for any other functional relation such as a closure term, growth rate, etc.

The fact that we cannot justify our precise functions in dynamical systems would seem to have been previously addressed in investigations of structural stability (Kuznetsov, 2004). Structural stability, however, is not particularly relevant in biology: a system is structurally stable if *for some sufficiently small* $\varepsilon$ all perturbations of magnitude less than $\varepsilon$ preserve the topological dynamics of the system, while on the other hand, most biological data is quite noisy and cannot be measured to an arbitrary degree of accuracy. In fact, in most experiments and observations we are unable to distinguish between close functions which differ from each other by less than 5-10% (Canale et al., 1973; Halbach and Halbach-Keup, 1974; DeMott, 1982; Hansen et al., 1990; Wood and Nisbet, 1991; Jost and Ellner, 2000; Morozov et al., 2008). Since we can't take our perturbations to be *sufficiently* small, we should rather ask whether our model predictions

are consistent for all perturbations within a small but finite magnitude determined *a priori* from the accuracy of our data. Structural sensitivity takes this into account by admitting all perturbations within a finite, predetermined magnitude $\varepsilon$, which is taken from the accuracy of available data.

Generally, although structural sensitivity is fairly well acknowledged, the conventional way to assess the possibility of errors in model predictions consists of checking the sensitivity of the results to variation in the model parameters (Lim et al., 1989; Janssen et al., 1996; Bendoricchio and Jorgensen, 2001) by carrying out a standard bifurcation analysis on models (e.g. Bazykin, 1998; Berezovskaya et al., 2001; Kooi and Boer, 2001). The sensitivity in the system can be quantified in this way by finding the distance, in parameter space, to the nearest bifurcation hypersurface—which is the smallest parameter perturbation that can alter the qualitative dynamics of the system. Provided that a particular choice of the constituent model functions is well justified, or that considering different mathematical parameterizations does not influence the general model behaviour, such an approach is valid. In the case where we cannot justify our model functions, however, this approach is inadequate to check for and deal with structural sensitivity, because models have been shown to be highly sensitive to the formulation of model functions whilst remaining robust with respect to parameter perturbations (Fussmann and Blasius, 2005; Cao et al., 2008; Cordoleani et al., 2011).

Indeed, mathematically speaking, checking sensitivity in this way with a particular choice of function which has $p$ parameters amounts to considering only an arbitrary $p$-dimensional (at most) subset of the infinite-dimensional space of potential model functions. Therefore the approach of varying parameters of a fixed model function amounts to exploring an arbitrary, co-dimension infinity, subset of the space of valid model functions, so we shouldn't be surprised that it is incomplete. For this reason, we should aim to develop frameworks for detecting structural sensitivity, and carrying out bifurcation analysis, in which the uncertainty in model specifications is not ignored, but is instead carried through our analysis.

We can achieve this, and explicitly include the uncertainty in model functions by considering partially specified models (Wood, 2001; Adamson and Morozov, 2012a, 2014a, 2014b). In such models, we leave unknown functions unspecified apart from requiring that they satisfy some qualitative criteria inherited from the biological problem being modelled—we may require a function to be increasing, for instance, or to pass

through the origin, etc. This approach is based on similar ideas to the seminal works of Gause and Kolmogorov as early as the 1930s (Gause, 1934, Kolmogorov, 1936). Many properties of models are locally determined, such as the number and stability of equilibrium points, and it is quite easy to deal with such properties in partially specified models. For example, near an equilibrium point the system behaviour is solely determined by the value of the equilibrium density and the local values of the unknown functions and their derivatives at this point (Kuznetsov, 2004). We can then treat these values as independent parameters and construct a generalised bifurcation diagram in this new parameter space.

Construction of a generalised bifurcation diagram in a generalised parameter space consisting of local function derivatives etc. is also the basis of the approach known as 'Generalized modelling' (Gross and Feudel, 2006; Kuehn et al. 2012). In this way, possible dynamics of a system can be explored independently of functional forms. Generalized modelling can be linked with data by considering a transformation of model functions in which the Jacobian depends not on the derivatives of unspecified functions at the equilibrium, but on the 'elasticities', which can theoretically be measured from data. However, all the resulting parameters still need to be measured at equilibrium states, and obtaining these measurements can be impossible in the case of an unstable equilibrium. There is also the potential issue with this approach that the model is only linked with data obtained at a single population density.

An alternative way to link models with unspecified functions and data is to limit our choice of model functions to those functions which stay within a certain possible range of data points—given by upper and lower bounds between which any valid functions must pass. These upper and lower bounds could be constructed by fitting a particular function to data, and allowing all functions which pass within a given distance $\varepsilon$ of this fitted function, where $\varepsilon$ is given by the error in the data. We can also restrict our model functions qualitatively so that they are biologically reasonable—we may have reason to demand them to be positive, or increasing, for instance. In order to detect sensitivity in this way we should consider all valid perturbations of the model functions—even though this set is in general infinitely dimensional. However, consider the case where we can determine, for any set of values in the generalised bifurcation space, whether or not there is a valid function taking these values. If we can do this, we can map out the entire closed region of the generalised bifurcation space corresponding to qualitatively appropriate functions that remain between our error bounds. In this way, we

can *project* the entire set of valid model functions into the generalised bifurcation space, and detect structural sensitivity by exploring the entire range of possible model behaviour admitted by valid functions. Therefore, finding such a projection is extremely powerful, and is the main mathematical question addressed in this thesis.

The thesis is organised as follows. In Chapter 2, we shall introduce precise definitions of structural sensitivity of dynamical systems, discuss its relation to the property of structural stability, and compare and contrast several different metrics of dynamical systems, and their usefulness (or otherwise) when detecting and quantifying structural sensitivity in biological systems. In Chapter 3, we shall introduce a general approach to using partially specified models to detect and quantify structural sensitivity in biological systems by considering the example of structural sensitivity in a Rosenzweig-MacArthur predator-prey model. Here we shall introduce the idea of projecting the set of valid functions into the generalised bifurcation space using geometric arguments, and provide theorems to do this in two cases. In Chapter 4, we shall extend the theorems stated in Chapter 3, and provide a more general theorem that allows us to obtain this projection in the case we are considering an unknown function with $n$ inflection points. We shall then apply this theorem to several more complicated systems from the literature. Finally, in Chapter 5, we shall consider the implications of structural sensitivity for bifurcation analysis—when we have uncertainty in our model functions, the resulting uncertainty in the model dynamics means that we no longer have concrete bifurcations. Instead, we should carry the uncertainty through our analysis by performing probabilistic bifurcation analysis. We shall illustrate this by performing such an analysis - we shall calculate the probability of having a supercritical or a subcritical Hopf bifurcation in a ratio-dependent predator-prey model with an unknown prey growth function.

# Chapter 2

# Definitions of structural sensitivity and appropriate metrics of dynamics systems

*This chapter is based on parts of the paper (Adamson and Morozov, 2014a)*

In this chapter, we shall introduce the general concept of structural sensitivity of ODE-based models, and then consider several definitions of structural sensitivity based on different metrics of dynamical systems, and discuss the strengths and shortcomings of each when applied to the problem of dealing with uncertainty in biological models with respect to both theory and experimental data.

## 2.1 General definition of structural sensitivity

To better understand the formal concept of structural sensitivity, it is essential to recall the definition of the related property of structural stability. We use the definition provided in the seminal book by Kuznetsov (2004):

**Definition 2.1 (Andronov's structural stability)**
Consider a continuous-time system

$$\dot{x} = f(x), \quad x \in \mathbb{R}^n, \tag{2.1}$$

with smooth $f$, a closed region $\Omega \subset \mathbb{R}^n$. Further, let us consider a certain metric $d_M$ on the space of $C^1$ functions on $\Omega$. System (2.1) is *structurally stable* in a region $\Omega_0 \subset \Omega$ if there exists some $\varepsilon > 0$ such that for any system

$$\dot{x} = g(x), \quad x \in \mathbb{R}^n, \tag{2.2}$$

such that $d_M(f, g) < \varepsilon$, there are regions $U, V \subset \Omega$, $\Omega_0 \subset U$ such that (2.2) in $U$ is topologically equivalent to (2.1) in $V$.

Recall (see Kuznetsov, 2004) that two systems are topologically equivalent if there is a continuous bijection with continuous inverse (homeomorphism) which maps the orbits of one system to those of the other whilst preserving the direction of time.

Now we define the closely related property of structural sensitivity as follows. Our general definition is largely based on the one provided in Cordoleani et al. (2011), with the important distinction that we ignore deformation of attractors with basins of measure zero:

**Definition 2.2 (Structural sensitivity)**

Let us consider system (2.1) together with two positive real numbers $\sigma$ and $\varepsilon$, and a closed region $\Omega \subset \mathbb{R}^n$. Further, let us consider a certain metric $d_M$ on the space of $C^1$ functions on $\Omega$. We denote by $B_\varepsilon(f)$ the set of functions $g$ such that $d_M(f,g) < \varepsilon$ over $\Omega$. For a given initial condition $x \in \mathbb{R}^n$, and function $g \in B_\varepsilon(f)$, we denote by $\omega(x)$ its $\omega$-limit in model (2.1) and by $\omega_g(x)$ its $\omega$-limit in the model

$$\dot{x} = g(x), \quad x \in \mathbb{R}^n. \tag{2.3}$$

We say that (2.1) is $\varepsilon$-structurally $\sigma$-sensitive in $\Omega_0 \subset \Omega$ if there exists $g \in B_\varepsilon(f)$ such that one of the following conditions is fulfilled:

(i) (2.3) is not structurally stable over $\Omega_0$;

(ii) there exists a set $X \subseteq \mathbb{R}^n$ of positive measure, such that given any initial condition $x_0 \in X$, then for all $x \in \Omega_0$ satisfying $\omega(x_0) = \omega(x)$, we have $d_H\left(\omega(x), \omega_g(x)\right) \geq \sigma$, where $d_H$ is the *Hausdorff distance*.

In other words, (2.1) is structurally sensitive if there is either a structurally unstable model in the vicinity of (2.1), or if a small size perturbation of (2.1) can sufficiently deform at least one attractor of the resulting model (2.3). The values $\varepsilon$ and $\sigma$ are parameters which can be interpreted as the *accuracy* of available data and the desired *tolerance* of our model predictions, respectively (see Cordoleani et al. 2011 for details). We should emphasize again the differences between structural sensitivity and structural instability. Condition (i) is similar to structural instability, but there is an important difference: the term *sufficiently $C^1$-close* in the definition of structural stability. For structural sensitivity we consider every system within the *fixed* distance, $\varepsilon$. With regard to part (ii) of Defn. 2.2., we note that it may be of interest to consider the case when *transient* dynamics differ by a sufficiently large distance, instead of just attractors, in

which case we would need to modify Defn. 2.2 (ii) to consider deformation of the orbits of a positive-measure set across the entire time interval. We shall not consider such a modification here for the sake of brevity.

In this thesis, we shall only consider structural sensitivity with respect to the qualitative dynamics of models. Therefore, we shall not consider part (ii) of Definition 2.2, and it is helpful to define the following:

**Definition 2.3 (Qualitative structural sensitivity)**

Consider system (2.1) together with a positive real number $\varepsilon$ and a closed region $\Omega \subset \mathbb{R}^n$. Further, let us consider a certain metric $d_M$ on the space of $C^1$ functions on $\Omega$, (with acceptable model functions potentially being restricted to comply with prior theoretical knowledge—as discussed along with the possible choices of such a metric in Section 2.2). We denote by $B_\varepsilon(f)$ the set of functions $g$ such that $d_M(f,g) < \varepsilon$ over $\Omega$.

We say that (2.1) is qualitatively $\varepsilon$-structurally sensitive in $\Omega_0 \subset \Omega$ if there exists $g \in B_\varepsilon(f)$ such that the model

$$\dot{x} = g(x), \quad x \in \mathbb{R}^n \tag{2.4}$$

is not structurally stable over $\Omega_0$.

## 2.2 Specific definitions of structural sensitivity

We have introduced the general definition of structural sensitivity, but in practice there are several particular definitions arising from this general definition: the metric $d_M$ used in Definitions 2.1-2.3 is unspecified, and choosing various metrics will determine different types of structural sensitivity. In dynamical systems theory, the most commonly found such metric is the following (or some variation thereof), taken from Kuznetsov (2004) or any other fundamental manuals:

**Definition 2.4 ($C^1$-distance)**

Consider two continuous-time systems

$$\dot{x} = \boldsymbol{f}(x), \quad x \in \mathbb{R}^n, \tag{2.5}$$

$$\text{and } \dot{x} = \boldsymbol{g}(x), \quad x \in \mathbb{R}^n, \tag{2.6}$$

where $\boldsymbol{f}, \boldsymbol{g}: \mathbb{R}^n \to \mathbb{R}^n$ are $C^1$ functions. The $C^1$-*distance* between (2.5) and (2.6) over a closed, bounded, region $\Omega \subset \mathbb{R}^n$ is the positive number given by

$$d_1 \coloneqq \sup_{x \in \Omega} \{ \| \boldsymbol{f}(x) - \boldsymbol{g}(x) \| + \| D_{\boldsymbol{f}}(x) - D_{\boldsymbol{g}}(x) \| \}$$

where $\| \boldsymbol{f}(x) - \boldsymbol{g}(x) \|$ denotes a vector norm over $\mathbb{R}^n$ and $\| D_{\boldsymbol{f}}(x) - D_{\boldsymbol{g}}(x) \|$ denotes a matrix norm over $\mathbb{R}^n$. $D_{\boldsymbol{f}}(x)$ is the Jacobian matrix of $\boldsymbol{f}$.

In a large number of biological models, $\boldsymbol{f}$ and $\boldsymbol{g}$ in (2.5) and (2.6) are composed of linear combinations of potentially non-linear model functions, some of which have parameterisations we are certain of, through theoretical reasoning or established laws etc. In such a situation, it makes little sense to consider a distance over the space of all systems, but only those systems which fix the model functions we are sure of:

**Definition 2.5 (Fixed function $C^1$-distance)**

Consider two continuous-time systems

$$\dot{x} = \boldsymbol{G}\left(g_1(x), \dots, g_m(x), h_1(x), \dots, h_p(x)\right), \quad x \in \mathbb{R}^n, \tag{2.7}$$

$$\text{and } \dot{x} = \boldsymbol{G}\left(g_1(x), \dots, g_m(x), \tilde{h}_1(x), \dots, \tilde{h}_p(x)\right), \quad x \in \mathbb{R}^n, \tag{2.8}$$

where $\boldsymbol{G}: \mathbb{R}^{m+p} \to \mathbb{R}^n$ is linear and $g_1, \dots, g_m, h_1, \dots, h_p, \tilde{h}_1, \dots, \tilde{h}_p \in C^1(\mathbb{R}^n)$. The *fixed function $C^1$-distance* between (2.7) and (2.8) over a closed, bounded, region $\Omega \subset \mathbb{R}^n$ is the $\mathrm{C}^1$-distance between them over $\Omega$ i.e. the fixed function $C^1$-distance is the $C^1$-distance defined only on systems with the model functions $g_1, \dots, g_m$ fixed.

In many practical cases when the exact formulation of a model function is unknown, we have no information regarding the derivatives of the unknown functions. All the information we have is given by data points from experiments. In such a case, use of a $C^1$-metric may be impractical, and we may wish to use the following metrics:

**Definition 2.6 (Absolute $d_Q$-distance)**

Consider two continuous-time systems

$$\dot{x} = \boldsymbol{G}\left(g_1(x), \dots, g_m(x), h_1(x), \dots, h_p(x)\right), \quad x \in \mathbb{R}^n, \tag{2.9}$$

$$\text{and } \dot{x} = \boldsymbol{G}\left(g_1(x), \dots, g_m(x), \tilde{h}_1(x), \dots, \tilde{h}_p(x)\right), \quad x \in \mathbb{R}^n, \tag{2.10}$$

where $\boldsymbol{G}$: $\mathbb{R}^{m+p} \to \mathbb{R}^n$ is linear, $g_1, \dots, g_m \in C^1(\mathbb{R}^n)$, and $\{h_1, \dots, h_p\}, \{\tilde{h}_1, \dots, \tilde{h}_p\} \in Q = \{Q_1, \dots, Q_p\}$ where the $Q_i \subsetneq C^1(\mathbb{R}^n)$ are classes of functions with *Lipschitz continuous first derivatives* with Lipschitz constant $A$, satisfying certain conditions. The *absolute $d_Q$-distance* between (2.9) and (2.10) over a closed, bounded, region $\Omega \subset \mathbb{R}^n$ is the positive number given by

$$d_Q \coloneqq \sup_{x \in \Omega} \sqrt{\left(h_1(x) - \tilde{h}_1(x)\right)^2 + \cdots + \left(h_p(x) - \tilde{h}_p(x)\right)^2}. \qquad (2.11)$$

**Remark:** It is also of interest that the system may somehow be sensitive to the choice of linear composition of nonlinear terms, i.e. if $G$ is replaced by some $\tilde{G}$ and the nonlinear terms changed accordingly. However, we can usually justify our choice of model composition to an extent— e.g. $G$ representing a breakdown of the functional operator into average per-capita growth rates, mortality terms, functional responses, etc. and, as with the use of $C^1$-metrics, allowing variation of the linear composition makes the model potentially unrealistic, and any sensitivity analysis difficult to interpret. For these reasons, we consider this discussion to be beyond the scope of this thesis, although it should certainly be considered elsewhere.

**Definition 2.7 (Relative $d_Q$-distance)**

The *relative $d_Q$-distance* between (2.9) and (2.10) over a closed, bounded, region $\Omega \subset \mathbb{R}^n$ is the positive number given by

$$d_Q \coloneqq \sup_{x \in \Omega} \sqrt{\frac{\left(h_1(x) - \tilde{h}_1(x)\right)^2 + \cdots + \left(h_p(x) - \tilde{h}_p(x)\right)^2}{\max\{h_1(x)^2 + \cdots + h_p(x)^2, \tilde{h}_1(x)^2 + \cdots + \tilde{h}_p(x)^2\}}}. \qquad (2.12)$$

Note that the requirement that we only include model functions with Lipschitz continuous first derivatives is vital. Because in $C^0$ metrics there are no limitations on the derivatives, the Jacobian matrices of two systems can be arbitrarily far apart, no matter how small the $C^0$ distance between them. This can lead to absurd behaviour such as, for instance, the possibility of transforming a system with a single equilibrium into one with a million equilibria through a perturbation of any size. Provided that we restrict ourselves to functions with $A$ as a Lipschitz constant, however, then the second derivatives will be contained within some interval $(-A, A)$ and the compactness of $\Omega$ ensures that any systems within a given $d_Q$ distance of each other must have a bounded difference between

their first derivatives. Therefore the metrics in Defns. 2.6 and 2.7 are implicitly $C^1$-metrics, rather than $C^0$ metrics as it initially seems, and they are therefore not susceptible to the usual problems with $C^0$ metrics.

Finally, in terms of practical tests for structural sensitivity, the most common approach (Janssen et al., 1994; Bendoricchio and Jorgensen, 2001) is to choose a fixed parameterisation of all model functions, and check for sensitivity to variation of parameters of these model functions. Such an approach uses the following notion of distance:

**Definition 2.8 (Parameter variation distance)**

Consider two continuous-time systems composed of the same parameterised function with different parameters:

$$\dot{x} = f(x, \alpha_1, \dots, \alpha_m), \qquad x \in \mathbb{R}^n, \qquad \alpha \in \Theta \subset \mathbb{R}^m \tag{2.13}$$

$$\text{and } \dot{x} = f(x, \hat{\alpha}_1, \dots, \hat{\alpha}_m), \qquad x \in \mathbb{R}^n, \qquad \hat{\alpha} \in \Theta \subset \mathbb{R}^m \tag{2.14}$$

The *parameter variation distance* between (2.13) and (2.14) over a closed, bounded, region $\Omega \subset \mathbb{R}^n$ is the positive number given by

$$d_4 \coloneqq \sup_{x \in \Omega} \| f(x, \alpha_1, \dots, \alpha_m) - f(x, \hat{\alpha}_1, \dots, \hat{\alpha}_m) \|, \tag{2.15}$$

where $\|\cdot\|$ denotes a vector norm in $\mathbb{R}^n$.

## 2.3 Conclusions. Comparison of definitions of structural sensitivity.

Given the wide range of notions of model distance to choose from, it is natural to ask whether there is one in particular which we should use when testing for structural sensitivity. The answer depends on the information we have concerning the constituent functions that ought to be used. By far the main approach used in the literature is based on Definition 2.8, i.e. considering sensitivity of model outputs to the variation of parameters values for fixed model functions (Janssen et al., 1994; Bendoricchio and Jorgensen, 2001). The main drawback of this definition is that even in fairly simple models, robustness of the results to variation of parameters for fixed functions does not indicate that the model is not sensitive to small variations of the functional forms themselves (Myerscough et al., 1996; Wood and Thomas, 1999; Fussmann and Blasius, 2005; Gross et al., 2009; Cordoleani et al., 2011; Adamson and Morozov, 2012a).

On the other hand, in the case where we want to consider the effect of *all* possible perturbations of a given model function, the use of the $C^1$-metric ensures that all possible model perturbations are considered, so no viable systems are missed. However, this can be rather a disadvantage in structural sensitivity investigations since the perturbations considered may include a large portion of models which are meaningless with respect to the original problem. For instance, if we have strong biological evidence that the mortality rate of a population increases with the population density, we should not consider the case where it is a decreasing function. Another drawback of the use of the $C^1$-metric is that in the case an investigation indicates the presence of structural sensitivity, the sheer scope of the systems considered makes it difficult to deduce a practically meaningful conclusion regarding the mechanisms through which the structural sensitivity takes place, whereas using other metrics, we may find which particular function (e.g. a growth rate term) will cause the observed sensitivity. Finally, use of a $C^1$-metric necessitates prior knowledge of the first derivatives of the system, but obtaining an accurate estimate of derivatives from empirical data is usually impossible (Bendoricchio and Jorgensen, 2001), in which case a sensitivity analysis using the $C^1$-metric may itself be sensitive to the initial derivative functions chosen—taking us back to where we started.

Our knowledge of the biological systems we are modelling is often rather limited, but we may have more information for some functions than others: we may know that certain function properties can be supported by theory, e.g. the growth rate of a population at zero should be zero, an increase in prey density ought to correspond to an increase (or at least, not a decrease) in the rate of consumption by a predator etc. Furthermore, experiments can be performed to provide data sets which the function should to some extent conform to. Aside from this, however, we cannot know anything else about such functions for sure.

In this situation, let us consider use of the $d_Q$-distance based on Definitions 2.6 and 2.7—either the absolute or relative distance, depending on whether we are considering absolute or relative error in our data measurements. Using such definitions of distance, we do not need to consider all possible perturbations in the $\varepsilon$-neighbourhood of the initial model functions, but only those which will conserve the generic qualitative properties of those functions. Such a definition allows us to treat our models as what are known in the literature as 'partially specified models' (Wood, 2001). The properties of

the viable set of functions $Q$ in Definitions 2.6 and 2.7 can be taken as those that are justified from theory or 'common sense' or, less commonly, experimental data. If we can then choose an initial model which fits the available data, and construct the neighbourhood $B_\varepsilon(f; d_Q)$—with $\varepsilon$ being derived from the accuracy of the experimental data, usually quite large due to the large errors present in biological data— then it will contain all theoretically valid models that fit the data set, and nothing more. For this reason, we shall consider that the definition of structural sensitivity using the $d_Q$-distance is the most natural when modelling biological systems and shall hereon explore the sensitivity of models considering the $d_Q$-distance only. The use of this concept of distance between models essentially limits us to considering models of the form (2.7). This type of model is known as a partially specified model, which naturally leads us to consider how we can use partially specified models to detect structural sensitivity. We shall now consider this in the next chapter.

# Chapter 3

# A general approach to using partially specified models to detect and quantify structural sensitivity.

*This chapter is based on the paper (Adamson and Morozov, 2012a)*

## 3.1 Introduction

The major problem with checking for structural sensitivity in models is that for a given mathematical formulation of any single functional dependence *f* we need to somehow check for a difference in the model outcomes for 'all' functions that fit our qualitative criteria and fit the data range. Such a procedure may seem impossible in principle: the set of valid model functions will in general be infinite dimensional. For this reason, up until now, investigation of structural sensitivity has usually been done by choosing a few concrete parameterizations of *f* and comparing the resultant model outcomes in each case (e.g. Fussmann and Blasius, 2005), but clearly such a sensitivity analysis is rather subjective, since it strongly depends on the choice of the forms of *f* which are compared.

A better approach is to explicitly include the uncertainty in model functions by considering partially specified models (Wood, 2001; Adamson and Morozov, 2012a). In such models, we leave unknown functions unspecified apart from requiring that they satisfy some qualitative criteria inherited from the biological problem being modelled—we may require a function to be increasing, for instance, or to pass through the origin, etc. This approach is based on similar ideas to the seminal works of Gause and Kolmogorov as early as the 1930s (Gause, 1934, Kolmogorov, 1936). As regards the analysis of such systems, many properties of models are locally determined, such as the number and stability of equilibrium points, and it is quite easy to deal with such properties in partially specified models. For example, near an equilibrium point, provided a system is structurally stable, the qualitative system behaviour is solely determined by the value of the equilibrium density and the local values of the unknown functions and their derivatives at this point (Kuznetsov, 2004). We can then treat these values as independent

parameters—called ‘generalised parameters’—and construct a bifurcation diagram in this new generalised parameter space.

A crucial question, however, is how we can restrict our generalised bifurcation analysis to the space of qualitatively valid functions that fit our data range. In this chapter we shall introduce a method to do this. The crux of the method is the use of geometric methods to build a precise projection of the infinite dimensional space of functions admitted by the data into the generalised bifurcation space while respecting the global constraints of biological realism. This will give us a closed region in the bifurcation space that corresponds to the generalised parameters taken by functions that are admitted by the data range. Notably, this new method of structural sensitivity analysis can rigorously cover all possible model functions, which makes it particularly useful when modelling biological systems with a high degree of uncertainty. Using this principle, we can work in this closed region of generalised bifurcation space to quantify the uncertainty in the system by introducing a concept of the ‘degree’ of sensitivity.

We demonstrate our test by using it to reveal structural sensitivity in the seminal Rosenzweig–MacArthur predator-prey model, with respect to variation in both the functional response of the predator/consumer and the per capita growth rate of the prey, and show why the conventional methods of structural sensitivity analysis based solely on variation of the parameters can be misleading in certain cases. In addition to this extensive example, we discuss the implementation of our test for a number of ecological models published previously in the literature, for which it is possible to demonstrate the existence of structural sensitivity.

## 3.2 General framework

We consider a biological model based on a system of autonomous ODEs given by

$$\frac{d\boldsymbol{x}}{dt} = \boldsymbol{F}(\boldsymbol{x}), \quad \boldsymbol{x} \in \Omega \subset \mathbb{R}^n, \tag{3.1}$$

where the vector function $\boldsymbol{F} = (F_1, F_2, \dots, F_n)$ is taken to be sufficiently smooth and $\Omega$ is compact. Each $F_i$ is the summation of terms describing the inflow and outflow of biomass, energy or individuals on a different trophic level, and depends on a set of functions $f_{i_j}$, representing growth rates, numerical and functional responses, closure terms etc.

$$F_i = G_i\left(f_{i_1}(\boldsymbol{x}), f_{i_2}(\boldsymbol{x}), \dots, f_{i_m}(\boldsymbol{x})\right). \tag{3.2}$$

We assume that the mathematical formulation of some of these $f_{i_j}$ is well known (or postulated), and we denote these functions by $g_{i_j}$, so that we obtain a partially specified model. The only potential uncertainty regarding these functions consists in the correct choice of their parameters. We denote by $\tilde{h}_{i_j}$ the functions whose exact shape/formulation is unknown, and for which we only have information on i) general qualitative properties such as the sign of their derivatives, whether they vanish at zero, the existence of any thresholds etc. and ii) some data sets which these functions should fit somehow. To incorporate the general qualitative properties into our model, we introduce the class of all functions taking these properties, $Q$, and require that the set of $\tilde{h}_{i_j}$ belongs to this class.

To obtain a concrete biological system from (3.1), we need to specify all functions in the model by choosing parameters in the known functions $g_{i_j}$, and by specifying the parameterisation of the $\tilde{h}_{i_j}$, as well as the corresponding parameters. The resultant model will have a set of attractors—which can be stationary states, periodic, quasiperiodic or chaotic—which is determined by the choice of the functions. Here we shall focus on how alternative formulations of the unknown functions $\tilde{h}_{i_j}$ affect the stability of any stationary states in the model.

Let us assume for now that there are $p$ functions in the model with an unknown mathematical formulation, which we denote by $\tilde{h}_1, \dots, \tilde{h}_p$ (dropping the $\tilde{h}_{i_j}$-notation here for simplicity), and there are $q$ known functions is the model. Firstly, to complete the system, we choose particular realizations of the functions $\tilde{h}_1, \dots, \tilde{h}_p$ as usual, using empirical observation or theoretical reasoning to obtain the 'base system':

$$\frac{d\boldsymbol{x}}{dt} = \boldsymbol{F}\left(g_1(\boldsymbol{x}), \dots, g_q(\boldsymbol{x}), h_1(\boldsymbol{x}), \dots, h_p(\boldsymbol{x})\right), \quad \boldsymbol{x} \in \Omega \subset \mathbb{R}^n, \tag{3.3}$$

We shall refer to the initial choice of functions $h_1, \dots, h_p$ as the base functions. Ideally, these functions should be fitted to data, so we shall assume this is the case, and that the total error bound is given by $\varepsilon$ (if not, we can always treat $\varepsilon$ as a parameter of the investigation). The question is, how sensitive are the model outcomes to the choice of $\tilde{h}_1, \dots, \tilde{h}_p$, where these functions are taken only from the set of functions in $Q$ that fit the data range determined by $h_1, \dots, h_p$ and $\varepsilon$?

This set of functions is precisely the ball of radius $\varepsilon$ around the base system in the absolute or relative $d_Q$-distance as defined in Def. 2.6 and 2.7, depending whether we're considering an absolute or relative error in our data:

$$B_{\varepsilon_Q}(\boldsymbol{h}) = \{\boldsymbol{f} \in Q | d_Q(f, h) < \varepsilon\}. \tag{3.4}$$

Hereon, we shall denote the neighbourhood of radius $\varepsilon$ in either the absolute or relative $d_Q$-distance the '$\varepsilon_Q$-neighbourhood' of the base system. We don't distinguish between the two because the framework we shall develop here works similarly for both types of distance—with the only difference being some minor details in the proofs.

Here we shall only consider sensitivity of systems to the existence and linear stability of equilibria. In the case of a given equilibrium, $\boldsymbol{x}_0{}^*$, we know from the implicit function theorem that, provided the system is structurally stable, if we replace the function set $\boldsymbol{h} \coloneqq \{h_1, \dots, h_p\}$ in the system by some other sufficiently close function set, $\widetilde{\boldsymbol{h}} \coloneqq \{\tilde{h}_1, \dots, \tilde{h}_p\}$, the new system will have a corresponding equilibrium $\boldsymbol{x}^*$ close to $\boldsymbol{x}_0{}^*$, and we can ask whether the stability of the new equilibrium $\boldsymbol{x}^*$ is altered from the stability of $\boldsymbol{x}_0{}^*$. In the case that systems are not sufficiently close, we can check for persistence of the equilibrium under perturbations that are not sufficiently small by considering the isocline equation:

$$\boldsymbol{F}\left(g_1(\boldsymbol{x}^*), \dots, g_q(\boldsymbol{x}^*), \tilde{h}_1(\boldsymbol{x}^*), \dots, \tilde{h}_p(\boldsymbol{x}^*)\right) = 0$$

and checking whether there are sets $\left(\boldsymbol{x}^*, \tilde{h}_1(\boldsymbol{x}^*), \dots, \tilde{h}_1(\boldsymbol{x}^*)\right)$ satisfying this equation, while $\left(\tilde{h}_1(\boldsymbol{x}^*), \dots, \tilde{h}_p(\boldsymbol{x}^*)\right)$ is within the distance $\varepsilon$ of $\left(h_1(\boldsymbol{x}^*), \dots, h_p(\boldsymbol{x}^*)\right)$.

As far as stability goes, in a non-degenerate case, the stability of an equilibrium is given by the characteristic equation of the corresponding linearised system:

$$\lambda^n + \lambda^{n-1}R_{n-1} + \cdots + \lambda^1 R_1 + R_0 = 0\,, \tag{3.5}$$

where the $R_i\left(\boldsymbol{x}^*, \widetilde{\boldsymbol{h}}(\boldsymbol{x}^*), \widetilde{\boldsymbol{h}}'(\boldsymbol{x}^*)\right)$ are functions that can be analytically computed based on the Jacobian matrix for a specified function set $\widetilde{\boldsymbol{h}}(\boldsymbol{x}^*)$. The equilibrium $\boldsymbol{x}^*$ is stable if and only if the roots of (3.5), $\lambda_1, \dots, \lambda_n$, have negative real parts (Kuznetsov, 2003), and this gives us the condition of stability in terms of $\boldsymbol{x}^*$, $\widetilde{\boldsymbol{h}}(\boldsymbol{x}^*)$ and the vector of $p \cdot m$ partial derivatives

$$\widetilde{\boldsymbol{h}}'(\boldsymbol{x}^*) = \left(\frac{\partial \tilde{h}_1}{\partial x_1}(\boldsymbol{x}^*), \dots, \frac{\partial \tilde{h}_1}{\partial x_m}(\boldsymbol{x}^*), \frac{\partial \tilde{h}_2}{\partial x_1}(\boldsymbol{x}^*), \dots, \frac{\partial \tilde{h}_2}{\partial x_m}(\boldsymbol{x}^*), \frac{\partial \tilde{h}_3}{\partial x_1}(\boldsymbol{x}^*), \dots, \frac{\partial \tilde{h}_p}{\partial x_m}(\boldsymbol{x}^*)\right),$$ where

$m$ is the dimension of the union of the domains of the unknown functions. Although it is

generally impossible to solve (3.5) analytically, it is easy to do it numerically for fixed $\boldsymbol{x}^*$, $\widetilde{\boldsymbol{h}}(\boldsymbol{x}^*)$ and $\widetilde{\boldsymbol{h}}'(\boldsymbol{x}^*)$. In particular, if $n$=2, we only need to check the sign of the determinant and trace of the Jacobian.

In order to check for structural sensitivity in an unspecified system, it would initially seem that we need to test each single function set $\widetilde{\boldsymbol{h}}$ in the $\varepsilon_Q$-neighbourhood of $\boldsymbol{h}$. The space of such function sets has infinite dimension in general—even if they only consist of one unknown function—but we see from (3.5) that the only values given by the function set which determine the stability of a given fixed point $\boldsymbol{x}^*$ are the $(n + p + m \cdot p)$ values $\boldsymbol{x}^*$, $\widetilde{\boldsymbol{h}}(\boldsymbol{x}^*)$ and $\widetilde{\boldsymbol{h}}'(\boldsymbol{x}^*)$ (recall that $n$ is the dimension of the state space, $p$ is the number of unknown functions and $m$ is the dimension of the domain of the unknown function set $\boldsymbol{h}$). Additionally, since from (3.1) $\boldsymbol{F}(\boldsymbol{x}^*) = 0$ must hold if $\boldsymbol{x}^*$ is to be an equilibrium, this gives us $n$ of these values—either analytically or numerically—provided that the others are specified. Instead of considering the functions themselves, we can consider the remaining $(p + m \cdot p)$ unknown values and proceed as follows. We consider the range of possible $\boldsymbol{x}^*$ in the vicinity of ${\boldsymbol{x}_0}^*$ which are the stationary states of the system with some $\widetilde{\boldsymbol{h}}$ from the $\varepsilon_Q$-neighbourhood of $\boldsymbol{h}$, i.e.

$$X = \left\{ \boldsymbol{x}^* \in \mathbb{R}^n \middle| \exists\, \widetilde{\boldsymbol{h}} \in Q \text{ s.t } \sqrt{\left(\left|h_1(\boldsymbol{x}^*) - \tilde{h}_1(\boldsymbol{x}^*)\right|\right)^2 + \cdots + \left(\left|h_p(\boldsymbol{x}^*) - \tilde{h}_p(\boldsymbol{x}^*)\right|\right)^2} < \varepsilon \right\}$$
$$\text{and } \boldsymbol{F}(\boldsymbol{x}^*) = 0, \tag{3.6}$$

where $F$ is the system specified by choosing the function set $\boldsymbol{h}$. Similarly, for each possible $\boldsymbol{x}^* \in X$, we can then consider the range of values $\widetilde{\boldsymbol{h}}(\boldsymbol{x}^*)$ that can be taken by functions $\widetilde{\boldsymbol{h}}$ in the $\varepsilon_Q$-neighbourhood of $\boldsymbol{h}$, and for any permissible combination of $\boldsymbol{x}^*$ and $\widetilde{\boldsymbol{h}}(\boldsymbol{x}^*)$, we can consider the range of values $\widetilde{\boldsymbol{h}}'(\boldsymbol{x}^*)$ which can be taken by functions $\widetilde{\boldsymbol{h}}$ in the $\varepsilon_Q$-neighbourhood of $\boldsymbol{h}$. This range will necessarily be finite, since we have chosen $Q$ such that its functions have second derivatives that do not exceed some range $(-A, A)$, so the Jacobian of the system clearly cannot vary arbitrarily. In this way, we outline

$$V_\varepsilon \coloneqq \left\{ (\boldsymbol{x}^*, \boldsymbol{\eta}, \boldsymbol{\zeta}) \middle| \boldsymbol{x}^* \in X, \exists \widetilde{\boldsymbol{h}} \in B_{\varepsilon_Q}(\boldsymbol{h}) \text{ s.t } \widetilde{\boldsymbol{h}}(\boldsymbol{x}^*) = \boldsymbol{\eta}, \widetilde{\boldsymbol{h}}'(\boldsymbol{x}^*) = \boldsymbol{\zeta} \right\}, \tag{3.7}$$

This approach gives us the projection of the $\varepsilon_Q$-neighbourhood of $\boldsymbol{h}$ into the generalised bifurcation space or ($X$-$H$-$H'$) space—that is, the space with elements $(\boldsymbol{x}^*, \boldsymbol{\eta}, \boldsymbol{\zeta})$—and since we can use the characteristic equation (3.5) to verify the stability of $\boldsymbol{x}^*$, we can then check the entire projected neighbourhood for values which alter the stability of the equilibrium from that of ${\boldsymbol{x}_0}^*$ in model (3.1) with the base function set $\boldsymbol{h}$.

If the stability is altered for certain values of $\boldsymbol{x}^*$, $\boldsymbol{\eta}$ and $\boldsymbol{\zeta}$, in the projection of the $\varepsilon_Q$-neighbourhood of $\boldsymbol{h}$, we can conclude that the model exhibits structural sensitivity.

The key advantage of this approach is that the projected $\varepsilon_Q$-neighbourhood of $\boldsymbol{h}$ in ($X$-$H$-$H'$) parameter space has at most $p + m \cdot p$ dimensions, and so may be covered numerically, whereas the corresponding neighbourhood in function space, being infinite dimensional, is impossible to check numerically. The main challenge with the approach is determining how to actually project the correct $\varepsilon_Q$-neighbourhood into the generalised bifurcation ($X$-$H$-$H'$) space, since even though the qualitative analysis is local, the definition of the $\varepsilon_Q$-neighbourhood is non-local: we require $\sqrt{\left(\left|h_1(\boldsymbol{x}) - \tilde{h}_1(\boldsymbol{x})\right|\right)^2 + \cdots + \left(\left|h_p(\boldsymbol{x}) - \tilde{h}_p(\boldsymbol{x})\right|\right)^2} < \varepsilon$ for *all* $\boldsymbol{x} \in \Omega$, and there may be other global constraints in $Q$. We shall use some examples to illustrate how we can do this in the next section.

One other issue faced by this approach is how to quantify the *degree* of structural sensitivity which is exhibited by a system. Ideally, we would like the degree of structural sensitivity in a system to reflect the probability that any two function sets—independently chosen from the $\varepsilon_Q$-neighbourhood at random—yield different predictions for the stability of the given equilibrium. In order to achieve this, we first need to choose a suitable probability distribution over the $\varepsilon_Q$-neighbourhood in the generalised bifurcation space in order to determine the probability of choosing a point in the stable or unstable region. One of the simplest approaches we can take is to assume the probability distribution is uniform over the projected $\varepsilon_Q$-neighbourhood, in which case the probability of selecting a function projecting to a point in a region of the projected $\varepsilon_Q$-neighbourhood in generalised bifurcation space corresponding to a certain kind of dynamics is simply given by the proportion of its area/volume to the total area/volume of the projected $\varepsilon_Q$-neighbourhood, $V_\varepsilon$.

The next logical step in finding an improved probability distribution would be to, where possible, weight each point in the generalised bifurcation space by some measure of the density of functions which we are projecting onto this point. The problem here, however, is that we are dealing with a projection from an infinite dimensional function space into an at-most $(p + m \cdot p)$-dimensional space. As a pragmatic solution to this difficulty, we propose a measure of the density of functions $\rho$, projected to a point $(\boldsymbol{x}^*, \boldsymbol{\eta}, \boldsymbol{\zeta})$ in $V_\varepsilon$, the projected $\varepsilon_Q$-neighbourhood of $\boldsymbol{h}$, that only relies on the space $\Omega \times$

$\mathbb{R}^p$: we consider the area/volume of points $(\boldsymbol{x}, y_1, \dots, y_p)$ in $\Omega \times \mathbb{R}^p$ through which the graphs of at least one set of functions in the $\varepsilon_Q$-neighbourhood of $\boldsymbol{h}$ can pass—i.e for which there exists some set of functions, $\boldsymbol{f}$, in the $\varepsilon_Q$-neighbourhood of $\boldsymbol{h}$ such that $(\boldsymbol{x}, y_1, \dots, y_p) = (\boldsymbol{x}, f_1(\boldsymbol{x}), \dots, f_p(\boldsymbol{x}))$—*whilst also satisfying* $\boldsymbol{f}(\boldsymbol{x}^*) = \boldsymbol{\eta}$ and $\boldsymbol{f}'(\boldsymbol{x}^*) = \boldsymbol{\zeta}$. That is if we specify the volume

$$\Gamma \coloneqq \left\{(\boldsymbol{x}, \boldsymbol{y}) | \exists \boldsymbol{f} \in B_{\varepsilon_Q}(\boldsymbol{h}), \boldsymbol{f}(\boldsymbol{x}) = \boldsymbol{y}, \boldsymbol{f}(\boldsymbol{x}^*) = \boldsymbol{\eta}, \boldsymbol{f}'(\boldsymbol{x}^*) = \boldsymbol{\zeta}\right\},$$

then we define the functional density as

$$\rho_1 \coloneqq \int_\Gamma 1 \, dV. \tag{3.8}$$

Thus, the probability of selecting a function which yields stable dynamics can be defined as

$$\mathcal{V} = \frac{\int_{V_1} \rho_1 \, dV}{\int_{V_\varepsilon} \rho_1 \, dV}, \tag{3.9}$$

where $V_1$ is the domain corresponding to linear stability, defined as

$$V_1 \coloneqq \left\{(\boldsymbol{x}^*, \eta, \zeta) \in V_\varepsilon | \mathrm{Re}\left(\lambda_i(\boldsymbol{x}^*, \eta, \zeta)\right) < 0, i = 1, \dots, n\right\}.$$

The case where the probability distribution is taken to be uniform over the $\varepsilon_Q$-neighbourhood can be obtained from (3.9) by integrating a probability density 1, instead of $\rho_1$. Once $\mathcal{V}$ is computed for a given probability distribution, the probability of two randomly chosen functions yielding different predictions will be given by $2\mathcal{V} \cdot (1 - \mathcal{V})$, since the choice is considered to be independent. This value will range from 0 (the $\varepsilon_Q$-neighbourhood will consist of only stable or only unstable regions) to 0.5 (there is an equal probability that a function from the $\varepsilon_Q$-neighbourhood will predict a stable or unstable equilibrium), so we scale this value by two to obtain the degree of structural sensitivity:

**Definition 3.1 The degree of structural sensitivity with respect to stability of an equilibrium**

If $V_\varepsilon$ is the total projected $\varepsilon_Q$-neighbourhood in the generalised bifurcation space, $V_1$ is the subset of this neighbourhood for which a given equilibrium is stable, and $\rho$ is a probability density function on $V_\varepsilon$, then the *degree of structural sensitivity* is defined as

$$\Delta \coloneqq 4 \cdot \frac{\int_{V_1} \rho \, dV}{\int_{V_\varepsilon} \rho \, dV} \cdot \left(1 - \frac{\int_{V_1} \rho \, dV}{\int_{V_\varepsilon} \rho \, dV}\right). \tag{3.10}$$

Note that the degree of sensitivity: i) will equal 0 if the measure of the stable region is either the measure of all the projected $\varepsilon_Q$-neighbourhood, or is 0; ii) has a maximum of 1, which is attained whenever the probability of having a stable equilibrium is exactly $1/2$; iii) essentially only depends on $\frac{\int_{V_1} \rho \, dV}{\int_{V_\varepsilon} \rho \, dV}$, which is the probability of having a stable equilibrium; iv) will be unaltered if we replace the volume of the stable region with the volume of the unstable region, $V_2$, in the calculation, since we necessarily have

$$\frac{\int_{V_2} \rho \, dV}{\int_{V_\varepsilon} \rho \, dV} = 1 - \frac{\int_{V_1} \rho \, dV}{\int_{V_\varepsilon} \rho \, dV}, \tag{3.11}$$

and therefore get the same degree of sensitivity whether we use the probability of a stable equilibrium or an unstable equilibrium, as should be expected.

In the next section we shall show a few examples of how our investigation can be carried out in simple cases in which there is a single unknown function, and shall address the problem of finding a projection from the $\varepsilon_Q$-neighbourhood of a given base function into the generalised bifurcation space.

## 3.3 Implementation of structural sensitivity test in models.

Here we demonstrate our method by using it to reveal structural sensitivity in the classical Rosenzweig–MacArthur predator-prey model (Rosenzweig and MacArthur, 1963) given by

$$\frac{dP}{dt} = \tilde{r}(P) \cdot P - \tilde{h}(P) \cdot Z \,, \tag{3.12}$$

$$\frac{dZ}{dt} = k \cdot \tilde{h}(P) \cdot Z - m \cdot Z \,, \tag{3.13}$$

where *P* and Z are the densities of prey and predator respectively. $\tilde{r}(P)$ is the per capita growth rate of prey; $\tilde{h}(P)$ is the predator functional response, $k$ is the trophic efficiency coefficient and $m$ is the predator mortality

### 3.3.1 Investigation of structural sensitivity with respect to the functional response of the predator

Following the work of Fussmann and Blasius (2005), who previously uncovered structural sensitivity in such a system, we first consider that the only unknown function

is $\tilde{h}$, the functional response of the predator. In this case we consider that the prey growth rate is fixed as the logistic function $\tilde{r}(P) = r \cdot \left(1 - \frac{P}{K}\right)$, and that the mortality term is constant. We obtain the function class $Q$ by imposing the following constraints on $\tilde{h}$:

$$\begin{cases} \tilde{h}(0) = 0, \\ \tilde{h}'(P) > 0, \quad \forall\ P \in [0, P_{\max}] \\ A < \tilde{h}''(P) < 0. \end{cases} \tag{3.14}$$

which characterise a general Holling type II functional response over $\Omega = [0, P_{\max}]$ (Myerscough et al., 1996; Gentleman et al., 2003)—an increasing function with decelerating intake rate—note that the term 'Holling type II' is also often used to refer to the particular function $h(P) = \frac{aP}{b+P}$. The second derivative is bounded below by the parameter $A < 0$ to ensure that $\tilde{h}$ is Lipschitz continuous with $|A|$ as a Lipschitz constant. To test structural sensitivity of the model we consider the functions from the $\varepsilon_Q$-neighbourhood of a certain base function $h$, where the class of functions $Q$ consists of all functions satisfying (3.14). Figs 3.1A and 3.1B show a standard base functional response, together with the upper and lower bounds of any functions within its $\varepsilon_Q$-neighbourhood—using absolute and relative $d_Q$-distance as defined in Definitions 2.8 and 2.9, respectively. The upper and lower limits of $\tilde{h}$ in these cases are constructed by plotting the boundaries $h_{\varepsilon+} \coloneqq h + \varepsilon, \quad h_{\varepsilon-} \coloneqq \max\{0, h - \varepsilon\}$ and $h_{\varepsilon+} \coloneqq h \cdot (1 + \varepsilon), \quad h_{\varepsilon-} \coloneqq h \cdot (1 - \varepsilon)$, respectively (As with the two types of $\varepsilon_Q$-neighbourhood, we use $h_{\varepsilon+}$ and $h_{\varepsilon-}$ to refer to either of boundary). The possible range of values taken by the stationary prey density $P^*$ is defined by the intersection between the horizontal line $\frac{m}{k}$ and the curves $h_{\varepsilon+}$ and $h_{\varepsilon-}$, which follows from considering the nontrivial predator isocline from equation (3.13). Clearly, for every $\tilde{h}$, the value $\tilde{h}(P^*)$ is uniquely defined in this case by $\tilde{h}(P^*) = \frac{m}{k} = \text{const.}$, so we do not need to consider variation of this value. Also, it is of note that because we only consider monotonically increasing functions, it is only possible for us to have one nontrivial prey equilibrium density $P^*$.

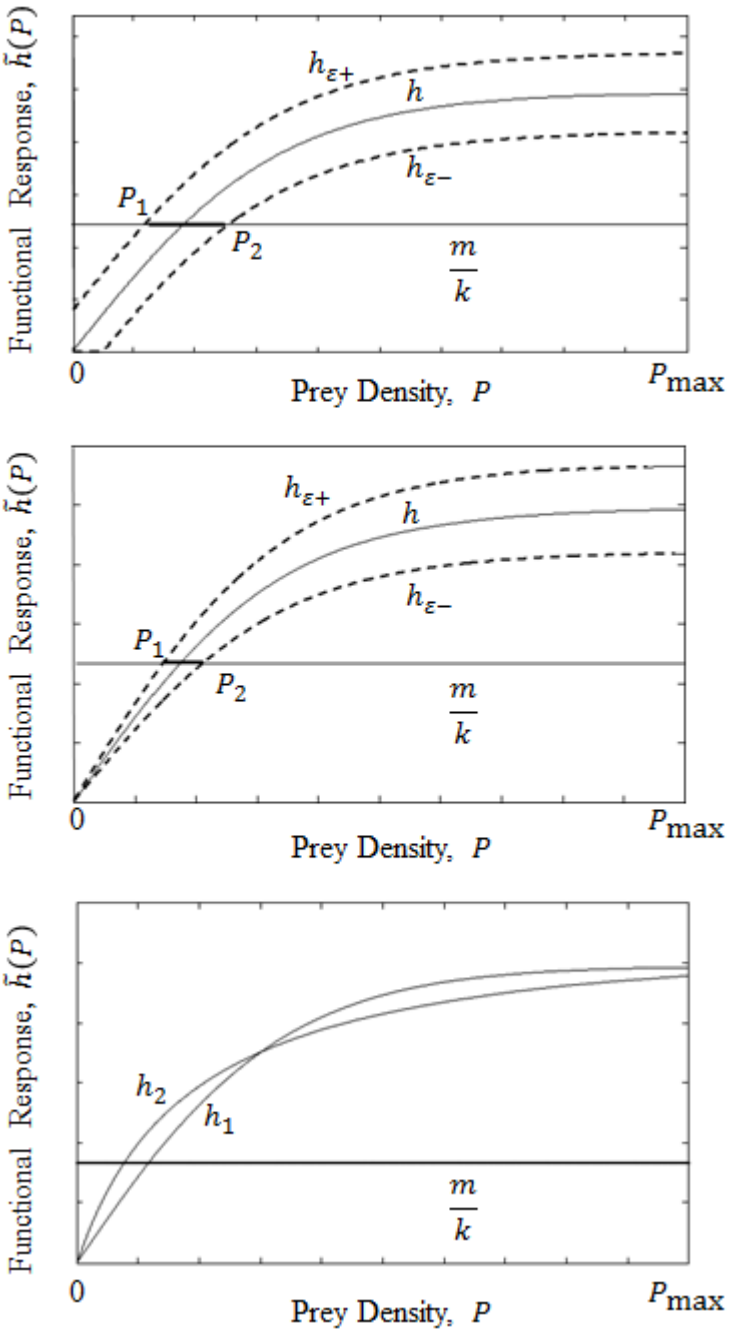


Figure 3.1.: Revealing the range of possible stationary densities $P^*$ for the $\varepsilon_Q$ neighbourhood of the predator functional response $\tilde{h}$ in model (3.12)-(3.13). The value of $P^*$ is obtained as the intersection of the functional response and the horizontal line $\tilde{h}(P) = \frac{m}{k}$. The curves $h_{\varepsilon\pm}$ indicate the upper and the lower bounds of variation of the base function $h$. (A) The $\varepsilon_Q$-neighbourhood based on Definition 2.6 of distance, the absolute difference between $h$ and its perturbations. (B) The $\varepsilon_Q$-neighbourhood, based on the relative difference between $h$ and its perturbations, Definition 2.7. (C). The two base functional responses used in the analysis of model (3.12)-(3.13) given by $h_1$, the Monod function (3.15), and $h_2$, the hyperbolic tangent parameterization (3.16). The parameters in the functional responses are $a_1 = 3.05; b_1 = 2.68$ and $a_2 = 0.99; b_2 = 1.48$. The other parameters are $m = 0.1; k = 0.3$.

For each stationary $P^* \in (P_1, P_2)$ there exists a range of possible derivatives, $DP \equiv \tilde{h}'(P^*) > 0$, but clearly not all of them are feasible. Necessary and sufficient conditions for the existence of a function $\tilde{h}$ in the $\varepsilon_Q$-neighbourhood of $h$ such that $\tilde{h}(P^*) = \frac{m}{k}$ and $\tilde{h}'(P^*) = DP$ are given by the following theorem:

**Theorem 3.1**

There exists an infinite class of functions $\tilde{h}$ satisfying (3.14), such that $h_{\varepsilon-}(P) < h(P) < h_{\varepsilon+}(P)\ \forall P \in [0, P_{\max}]$, $\tilde{h}(P^*) = \frac{m}{k}$ and $\tilde{h}'(P^*) = DP$ if and only if the following conditions are met:

$$\begin{aligned} U(P) &= \frac{m}{k} + DP(P - P^*) > h_{\varepsilon-}(P), \\ L(P) &= \frac{m}{k} + DP(P - P^*) + \frac{1}{2}A(P - P^*)^2 < h_{\varepsilon+}(P), \\ L(0) &= \frac{m}{k} - P^* \cdot DP - \frac{1}{2}A \cdot P^{*2} < 0. \end{aligned} \qquad (3.15)$$

**Proof**

To prove that conditions (3.15) are necessary, we first note that $U(P)$ is, by definition, the tangent line to any viable $\tilde{h}$ at $P = P^*$. Since from (3.14) any valid function $\tilde{h}$ must be convex, it must be bounded above by this tangent line. Secondly, we note that $L(P)$ is the unique function satisfying $L(P^*) = \frac{m}{k}$, $L'^{(P^*)} = DP$ and $L''(P) = A \forall P \in [0, P_{\max}]$. Since we have specified $A$ as the lowest second derivative of any suitable functional response, it is easy to see—by considering any alternate second derivative—that the admissible functional responses are bounded below by $L$, we necessarily have $L(P) < \tilde{h}(P) < U(P)$ for any $\tilde{h}$ satisfying (3.14) and $\tilde{h}(P^*) = \frac{m}{k}$, $\tilde{h}'(P^*) = DP$. Conditions (3.15) are therefore clearly necessary conditions for $h_{\varepsilon-} < \tilde{h} < h_{\varepsilon+}$ to exist. Fig. 3.2 illustrates an example of the tangent line and parabola which bound any function satisfying (3.14). To prove that (3.15) are sufficient conditions, we need to describe a method that can produce infinitely many such functions provided that (3.15) holds. Our method and a resultant function is illustrated in Fig. 3.3. For the sake of brevity, in this proof we loosen the constraints on $\tilde{h}''$ to $A \leq \tilde{h}''(P) \leq 0$, but we note that the proof remains valid in the case that the inequality is strict—in this case we can modify the proof by replacing $U$ and $L$ with $\hat{U}(P) = \frac{m}{k} + DP \cdot (P - P^*) + \frac{\gamma}{2}(P - P^*)^2$ and $\hat{L}(P) = \frac{m}{k} + DP \cdot (P - P^*) + \frac{1}{2}(A + \gamma)(P - P^*)^2$ where $0 < \gamma \ll 1$ is chosen to be small enough that

(3.15) hold for the new $\widehat{U}$ and $\widehat{L}$. Note that such a $\gamma$ must exist because $\widehat{U}$ and $\widehat{L}$ are continuous with respect to $\gamma$ and (3.15) holds for $\gamma = 0$.

Firstly, we choose some $\delta$ such that $0 < \delta < \varepsilon$, and (3.14) holds for $h_{\delta-}$ and $h_{\delta+}$, defined in the same way as $h_{\varepsilon-}$ and $h_{\varepsilon+}$. As with $\gamma$, it is easy to show that such a $\delta$ must exist due to continuity arguments. We first define $\tilde{h}$ over $P \in [0, P^*]$. Starting from $P = \tilde{P}$, we set $\tilde{h}$ to be equal to the parabola of maximum curvature, $\tilde{h}(P) = L(P)$. At each point along this parabola, we consider how the tangent line changes. Initially, this tangent line is $U$, which lies above $h_{\delta-}$ and intersects the axis $P = 0$ above the origin. For lower $P$ values, this intersection decreases continuously, so there must come a point $P_1$ from which the tangent line either passes through the origin without crossing $h_{\delta-}$ first, or must lie tangent to $h_{\delta-}$ at a lower value $P_2$.

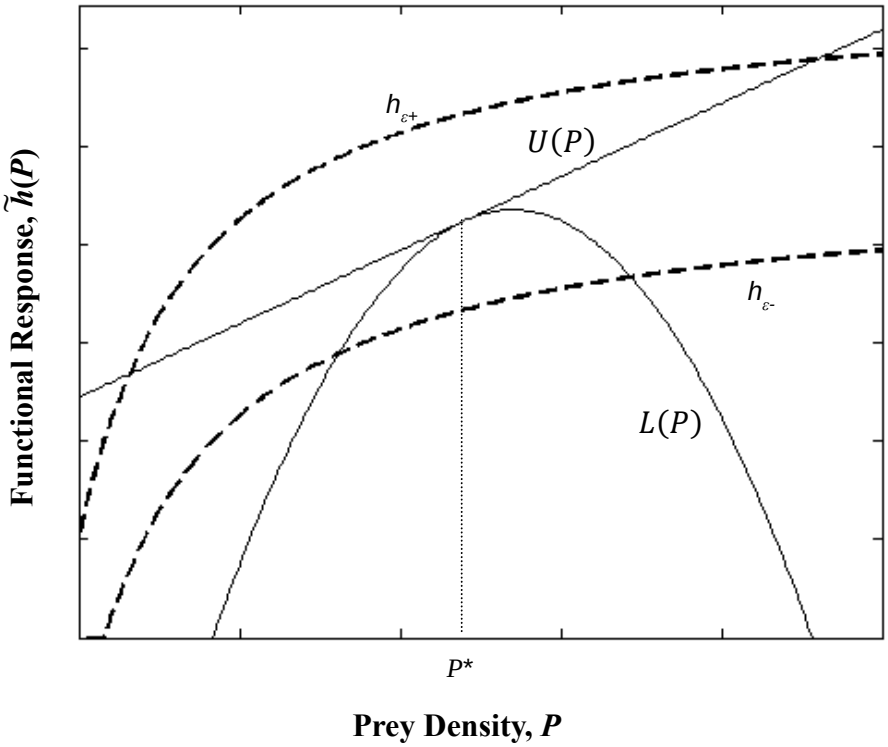


Figure 3.2: Graphical representation of conditions (3.15). The tangent line $U(P)$ and parabola $L(P)$ which form the upper and lower bounds of a function $\tilde{h}$ taking the values $\tilde{h}(P^*) = \frac{m}{k}$, $\tilde{h}'(P^*) = DP$ and satisfying conditions (3.14). There will exist at least one such function in the $\varepsilon_Q$-neighbourhood of $h$ (i.e which stays between $h_{\varepsilon+}$ and $h_{\varepsilon-}$) if and only if $U$ lies above $h_{\varepsilon-}$ and $L$ lies below $h_{\varepsilon+}$ over the whole interval $(0, P_{\max}]$, with the origin being between them.

Now for $P \in (P_2, P_1)$, we set our function equal to this tangent line. If it passes through the origin, we are done. If instead it lies tangent to $h_{\delta-}$ at the point $P_2$, we set

$\tilde{h}(P) = h_{\delta-}(P)$ for values $P \in (P_3, P_2)$, where $P_3$ is the unique value from which the line tangent to $h_{\delta-}$ passes through 0, so for $P \in [0, P_3)$ we set $\tilde{h}(P)$ equal to this tangent line. We note that $P_3 \leq P_2$ necessarily: $P_3 > P_2$ is not possible because in this case $P_3$ would have been set as $P_1$ in an earlier step. Therefore we are done.

For $P \in (P^*, P_{\max}]$, we can define $\tilde{h}$ in a similar manner: we follow the tangent line from $P^*$ and at each point check the parabola of curvature $A$ which is tangent to this line. There must be a point at which this parabola is also tangent to $h_{\delta+}$ (unless the tangent line doesn't intersect $h_{\delta+}$—in which case we are done). At this point we can let our function follow the parabola until it is tangent to $h_{\delta+}$, and then follow $h_{\delta+}$ until it reaches $P_{\max}$, then we are done. Finally, we note that there are uncountably many valid values of $\delta$ to choose at the start of the method. Therefore an infinite class of viable functions exists■

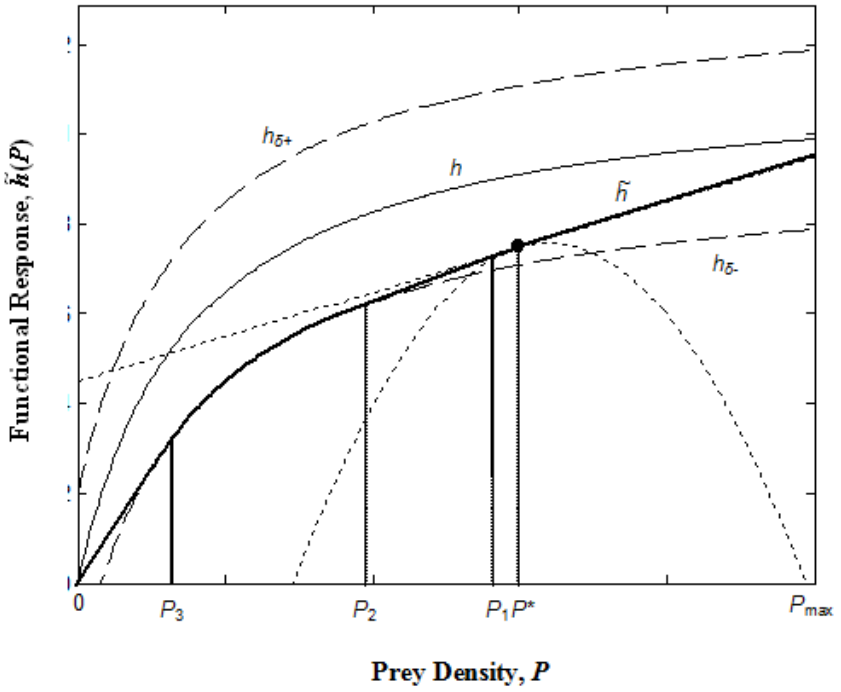


Figure 3.3: Example of a functional response $\tilde{h}$ satisfying criterion (3.14) constructed using the method described in Theorem 3.1—depending only on conditions (3.15) being satisfied. The light dashed curves represent the tangent line at $\left(\tilde{P}, \frac{m}{k}\right)$, $U$, and the parabola with second derivative $A$ that is tangent to the function at $\left(\tilde{P}, \frac{m}{k}\right)$, $L$. These form upper and lower bounds, respectively, on any potential function. See the text for more details of the method.

Using Theorem 3.1, by scanning all feasible values of $P^*$ and $DP$ we can check the stability of the interior stationary state $(P^*, Z^*)$ for all functions in the $\varepsilon_Q$-neighbourhood of $h$. The stability condition for this equilibrium (based on a simple analysis of the Jacobian) is given by (Rosenzweig and MacArthur, 1963):

$$\frac{m}{k}\left(1-\frac{2P^*}{K}\right)-DP\cdot P^*\cdot\left(1-\frac{P^*}{K}\right)<0. \tag{3.16}$$

The generic behaviour of model (3.12)-(3.14) with a predator functional response satisfying (3.14) is well known. For a fixed $\tilde{h}$, the stability of the stationary state is determined by the carrying capacity $K$: for a small $K$, the interior stationary state is stable; an increase in $K$ will eventually result in the system's destabilization via a Hopf bifurcation—a phenomenon known as the 'paradox of enrichment' (Rosenzweig, 1971; Gilpin, 1972).

We shall implement our test for structural sensitivity with respect to the functional response using two different base functions: the Monod parameterization (3.17) and the hyperbolic tangent function (3.18), two of the most commonly used Holling type-II functional response terms in the literature (Jassby and Platt 1976; Jeschke et al., 2002; Fussmann and Blasius, 2005).

$$h_1(P)=a_1\frac{P}{1+b_1P}, \tag{3.17}$$

$$h_2(P)=a_2\tanh(b_2P), \tag{3.18}$$

where $a_i$ and $b_i$ are parameters with standard meanings. It is easy to see that both $h_1$ and $h_2$ satisfy conditions (3.14). The parameters in the expressions are chosen in such a way that functions $h_1$ and $h_2$ are close to each other in terms of absolute difference, which does not exceed $\varepsilon = 1.2$. The pair of actual base functions used are shown in Fig. 3.1C.

To perform our investigation, we used the conditions (3.15) to numerically compute the region in $(P^*\text{-}\,DP)$ space which corresponds to the projected $\varepsilon_Q$-neighbourhood of $h$, and then used criterion (3.16) to determine the regions of stability and instability of the fixed point $(P^*, Z^*)$ in this space. We then calculate the degree of structural sensitivity $\Delta$, assuming $\rho\equiv1$ in (3.10) for simplicity. Fig. 3.4A shows the dependence of $\Delta$ on the carrying capacity, $K$, for different base functions and values of $\varepsilon$, using Definition 2.6 of the distance between two functions, based on an absolute error. We see that in all cases, $\Delta$ is low for small values of $K$—this is because, initially, the $\varepsilon_Q$-neighbourhood is dominated by the region of stability—but as $K$ is increased, $\Delta$ increases

to 1 as the region of stability in the $\varepsilon_Q$-neighbourhood shrinks, before dropping off again as the region of instability starts to dominate. This follows the paradox of enrichment, since for all choices of functional response, increasing $K$ will destabilise the equilibrium *eventually* ($\Delta$ reaches zero if we consider higher values of $K$ than those shown in Fig. 3.4A), but significantly, $\Delta$ is far from zero across a large range of $K$, which indicates that there are significant regions of stability and instability in these cases (c.f. Figure 3.5), and therefore structural sensitivity of the model. So, while in this model the paradox of enrichment does take place, the exact carrying capacity, $K$, at which the Hopf bifurcation happens is strongly dependent upon the formulation of the functional response, and can vary across a huge range. Crucially for the method, the degree of structural sensitivity observed is similar regardless of whether the Monod or hyperbolic tangent base function is used, indicating that for close base functions the structural sensitivity test does not depend upon the choice between them.

Fig. 3.4B shows the dependence of the degree of structural sensitivity on $K$ when Definition 2.7 of the distance between functions is used—the relative $d_Q$-distance. One can see that for small $\varepsilon$ the results depend on the base function chosen—the Monod function in this case exhibits structural sensitivity for a much smaller range of $K$. This discrepancy can be explained by noting that while the absolute error between the two base functions is small, the relative error is $\varepsilon \approx 0.5$ or $\varepsilon \approx 1$, depending which of the two functions is considered the base function, so they are quite far removed from each other's $\varepsilon_Q$-neighbourhood in terms of relative distance. Therefore this result is not an inconsistency on the part of the method: when $\varepsilon$ is large enough ($\varepsilon = 0.7$) to compare with the relative distance between the two base functions, the Monod and hyperbolic tangent base functions again exhibit similar degrees of structural sensitivity. It is of interest that using different concepts of the closeness of functions to define the $\varepsilon_Q$-neighbourhood of a given base function $h$ can result in different predictions regarding structural sensitivity. This can be seen from comparison of the Monod curves in Figs 3.4A and 3.4B: when relative closeness is considered (Fig. 3.4B), the system with a Monod base function only exhibits structural sensitivity for values of $K$ between 0.3 and 3—a much smaller range of $K$ than for the same system when absolute distance is used.

In Figs 3.5A and 3.5B we have plotted the stability portrait in ($P^*$-$DP$) space for the Monod and hyperbolic tangent base functions, respectively, where the absolute distance is used with $\varepsilon = 0.1$, and $K = 1.2$ (c.f. Fig. 3.4A). In the green region, $(P^*, Z^*)$

is a stable equilibrium, the red region indicates an unstable equilibrium and the dark blue region corresponds to the values of $P^*$ and $DP$ which are not found for any function $\tilde{h}$ in the $\varepsilon_Q$-neighbourhood of $h$—i.e. lying outside the projection of the $\varepsilon_Q$-neighbourhood. It should be noted that all regions are actually projections of the corresponding regions in infinite dimensional function space.

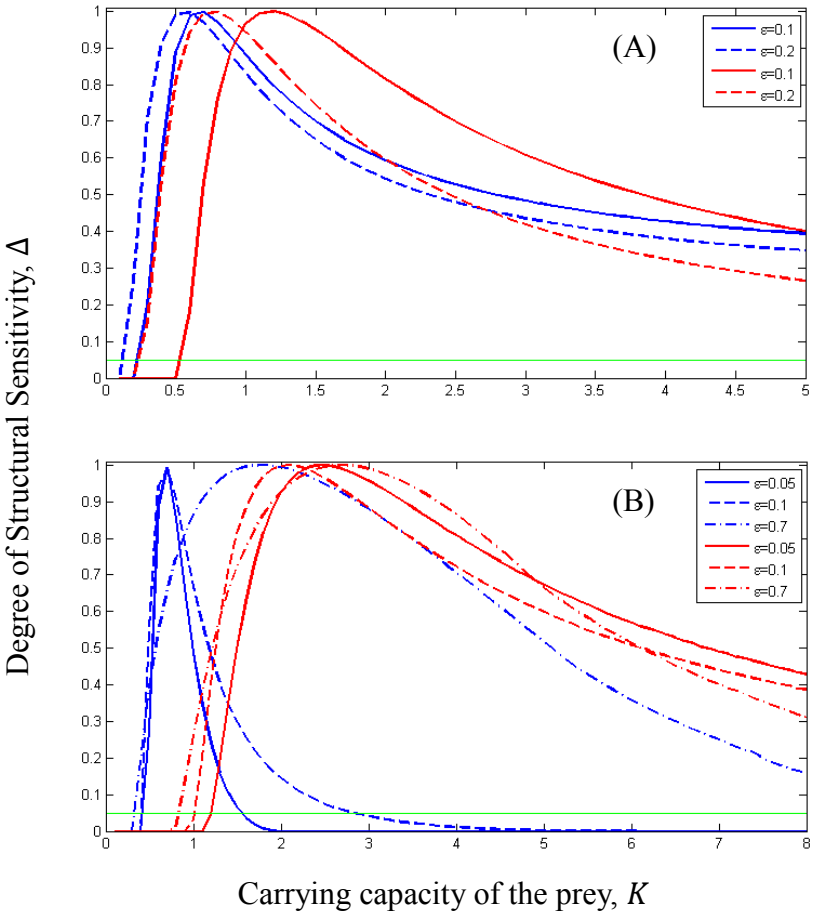


Figure 3.4: The degree of structural sensitivity of the predator-prey model (3.12)-( 3.13) to variation of the functional response, plotted against the carrying capacity $K$. Two different base functions are used: blue curves correspond to the Monod functional response (3.17) and red curves to the hyperbolic tangent functional response (3.18), c.f. Fig. 3.1C. The degree of sensitivity $\Delta$ is computed based on (3.10) with $\rho \equiv 1$, and a sample 'threshold sensitivity' of 5% is shown by the green line. A Hopf bifurcation takes place at $K \approx 0.67$ in the system with the Monod base function and $K \approx 2.01$ with the hyperbolic tangent base function. (A) The $\varepsilon_Q$ neighbourhood of $h$ is defined based on the absolute difference between $h$ and its perturbations. (B) The $\varepsilon_Q$ neighbourhood of $h$ is defined based on the relative difference between $h$ and its perturbations. The other model parameters are $m$=0.1 and $k$=0.3.

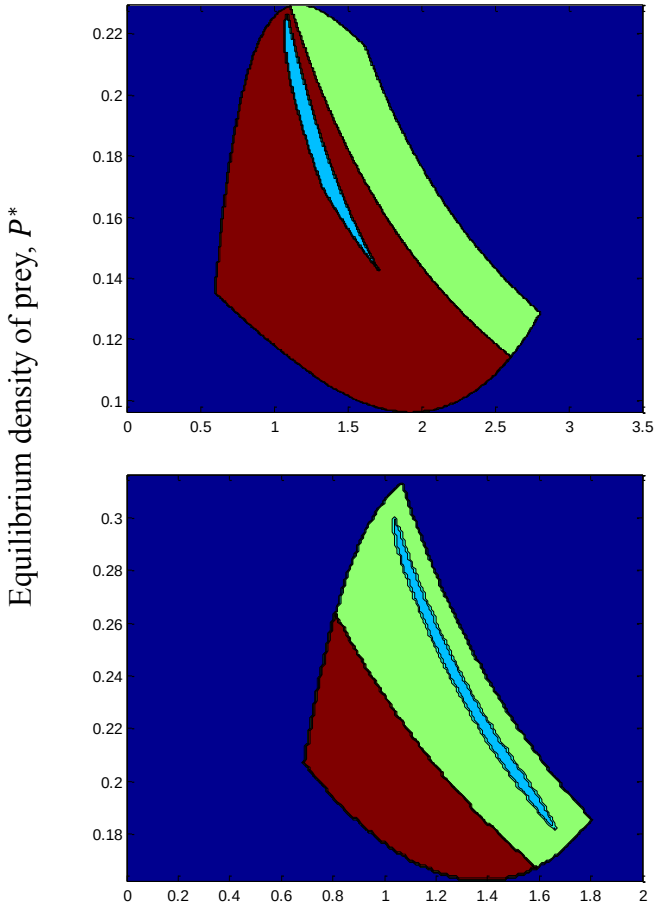


Figure 3.5: Testing structural sensitivity of predator-prey model (3.12)-(3.12) to variation of the functional response of the predator. The $\varepsilon_Q$ neighbourhood of $h$ is projected from function space into the ($P^*$-$DP$) space—with the dark blue region denoting areas outside of the $\varepsilon_Q$ neighbourhood. The $\varepsilon_Q$ neighbourhood of $h$ is defined based on the absolute difference between $h$ and its perturbations, with $\varepsilon = 0.1$. Diagram (A) corresponds to the Monod base function whereas diagram (B) corresponds to the hyperbolic tangent functional response. Red and green domains describe, respectively, the unstable and stable stationary state. The azure domain corresponds to the region covered by conventional sensitivity analysis obtained by varying only parameters $a$, $b$ in the base functions. Both diagrams are plotted for a carrying capacity $K$=1.2. The other model parameters are $m$=0.1 and $k$=0.3.

The ($P^*$-$DP$) representation can shed some light on the limitations of conventional sensitivity analysis—which is only based on a variation of the model parameters for a fixed functional form. We can vary the parameters $a_i$ and $b_i$ in equations (3.17) and (3.18) and consider all possible combinations which belong to the corresponding $\varepsilon_Q$-neighbourhoods: these regions in ($P^*$-$DP$) space are denoted by the azure domains in Figs

3.5A and 3.5B. In the cases shown, varying the model parameters does not indicate any structural sensitivity, but it is clear from the more complete analysis that there is extensive structural sensitivity which variation of parameters misses completely. This is because variation of the parameters for a fixed functional form only allows us to vary the values $P^*$ and $DP$ in a thin strip directed in a direction roughly parallel to the Hopf bifurcation line. This 'blinkered' approach therefore gives a misleading representation of the degree of structural sensitivity in the system, and so we can only rely on a conventional parameter-based analysis of sensitivity when the carrying capacity *K* is close to the Hopf bifurcation value for a given $h$, since in this case the azure domain will intersect the boundary between the stability and instability domains.

### 3.3.2 Investigation of structural sensitivity with respect to the growth term of the prey

We now consider the structural sensitivity of the system with respect to variation in the formulation of the growth term of the prey, in the cases where the functional response is fixed as either the Monod or hyperbolic tangent functional response with the same parameters $a_i$ and $b_i$ as used for the base functions in section 3.3.1. We impose the following constraints on $\tilde{r}(P)$:

$$\begin{aligned} &\tilde{r}'(P) < 0, \\ &A_1 < \tilde{r}''(P) < A_2 \ \ \forall P \in [0, P_{\max}], \end{aligned} \tag{3.19}$$

where $A_1 < 0$ and $A_2 > 0$, which defines a logistic-type growth term, with the magnitude of the second derivative bounded by $max\{|A_1|, |A_2|\}$. We take our base function to be the classic logistic growth function

$$r(P) = r \cdot \left(1 - \frac{P}{K}\right), \tag{3.20}$$

which clearly satisfies conditions (3.19) (for any $A_1$, $A_2$). We require that $\tilde{r}$ is within an absolute distance $\varepsilon$ of this base function, that is, it must satisfy

$$r_{\varepsilon-}(P) < \tilde{r}(P) < r_{\varepsilon+}(P) \ \ \forall\, P \in (0, P_{\max}], \tag{3.21}$$

where $r_{\varepsilon-}(P) \coloneqq r(P) + \varepsilon$, and $r_{\varepsilon+}(P) \coloneqq r(P) - \varepsilon$.

When varying the growth term, since the functional response $h$ is fixed, the equilibrium prey density $P^*$ is given by the constant $h^{-1}\left(\frac{m}{k}\right)$, and the stability condition in the case of an arbitrary growth function $\tilde{r}$ is given by

$$\frac{m}{k}\left(\tilde{r}(P^*) + P^* \cdot \tilde{r}'(P^*)\right) - \tilde{r}'(P^*) \cdot P^* \cdot \tilde{r}(P^*) < 0\,. \qquad (3.22)$$

Our generalised bifurcation space now considers of the values $rP \coloneqq \tilde{r}(P^*)$ and $DP \coloneqq \tilde{r}'(P^*)$, and the $\varepsilon_Q$-neighbourhood of $r$ consists of all functions satisfying (3.19) and (3.21). To obtain the projection of the $\varepsilon_Q$-neighbourhood into the generalised bifurcation space, we use the following theorem:

**Theorem 3.2**

There exists a valid function $\tilde{r}$ satisfying conditions (3.19) and (3.21) such that $\tilde{r}(P^*) = rP$ and $\tilde{r}'(P^*) = DP$ if and only if the following conditions hold:

$$U(P) \coloneqq rP + DP \cdot (P - P^*) + \frac{A_2}{2}(P - P^*)^2 > r_{\varepsilon-}, \quad \text{and}$$

$$L(P) \coloneqq rP + DP \cdot (P - P^*) + \frac{A_1}{2}(P - P^*)^2 < r_{\varepsilon+}. \qquad (3.23)$$

**Proof**

Firstly, note that, as in Theorem 3.1, (3.23) are necessary conditions because $L(P)$ is the parabola of minimum second derivative satisfying $L(P^*) = rP$ and $L'(P^*) = DP$—so is a lower bound for a suitable function—and $U(P)$ is the parabola of maximum second derivative satisfying $U(P^*) = rP$ and $U'(P^*) = DP$—so is an upper bound.

To prove that (3.23) are sufficient conditions, we need to find a method to construct a valid function that depends only on (3.23) being satisfied. We illustrate such a method for absolute distance in Fig. 3.6 and for relative distance in Fig. 3.7. For brevity, we will relax the constraints on $\tilde{r}''$ such that $A_1 \leq \tilde{r}'' \leq A_2$ is allowed (as in Theorem 3.1, the proof can easily be modified to hold for the strict inequality). We consider two cases for $DP$: $DP \geq r'(P)$ and $DP < r'(P)$, where $r$ is the base (logistic) function, which has constant derivative. If $DP \geq r'(P)$, then for $P < P^*$ we initially set $\tilde{r}(P) = U(P)$, so that $\tilde{r}$ initially follows the parabola of maximum second derivative. $U$ lies above $r_{\varepsilon-}$, so in the range $P \in [0, P^*)$, $U$ either reaches the axis $P = 0$ without intersecting $r_{\varepsilon+}$, in which case we set $\tilde{r}(P) = U(P)\ \forall P \in [0, P^*)$, and we are done, or at some $P_1 > 0$ it crosses $r_{\varepsilon+}$ from below as $P \downarrow P_1$ (where $\downarrow$ denotes the one-sided limit from the right hand side)—in which case we must have $\tilde{r}'(P_1) < r'(P_1)$. Since the derivative of the parabola is continuous, by the intermediate value theorem there must be some point $P_2 \in [P_1, P_0]$ where $\tilde{r}'(P_2) = r'(P_2)$. Over the interval $[0, P_2]$, we then set $\tilde{r}$ to equal the tangent line

at $U(P_2)$. Whether we're using Definition 2.6 or 2.7 of distance, this tangent line running parallel to $r(P)$ will not intersect $r_{\varepsilon+}$ or $r_{\varepsilon-}$, for $P \in [0, P_2]$, so we are done.

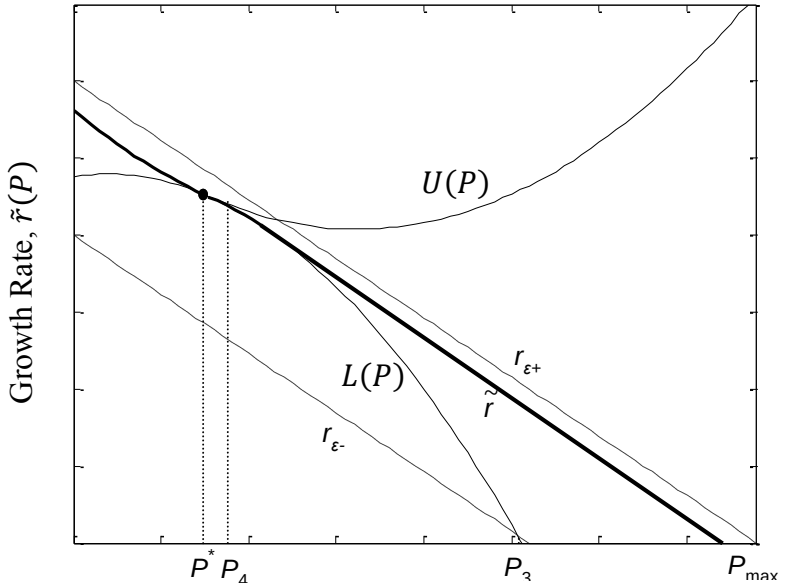


Figure 3.6: Example of a growth rate $\tilde{r}$ satisfying criterion (3.19) constructed using the method described in Theorem 3.2 for the case in which Definition 2.6 of distance (absolute distance) is used. The method depends only on conditions (3.23) being satisfied. The thin solid parabolas $U$ and $L$ are those of maximum and minimum (signed) curvature, respectively, which are tangent to the growth function at $(P^*, rP)$. These form upper and lower bounds on any potential function.

For $P > P^*$, if we initially set $\tilde{r}(P) = L(P)$, to follow the parabola with (signed minimum) curvature $A_1$, the same holds: this parabola either reaches the $P$-axis—in which case we set $\tilde{r}(P) = L(P)\ \forall P \in (P^*, P_{\max}]$ and we are done—or at some $P_3 > P^*$ it crosses $r_{\varepsilon-}$ from above as $P \uparrow P_3$, in which case again we must have $\tilde{r}'(P_3) < r'(P_3)$. In this second case, if we are using Definition 2.6 of distance (absolute distance), we can use the intermediate value theorem to find $P_4$, where the tangent line at $L(P_4)$ lies parallel to $r(P)$. We can then take $\tilde{r}$ to be equal to this tangent over $(P_4, P_{\max}]$, and we are done. If we are using Definition 2.7 (relative distance), then whether we initially set $\tilde{r}(P) = L(P)$ or $\tilde{r}(P) = U(P)$ depends whether their shared tangent line from $P^*$ intersects the $P$-axis at $P > P_{\max}$—in which case we follow $L$, the parabola of minimum curvature—or $P < P_{\max}$—in which case we follow $U$. If $P = P_{\max}$ we can follow the tangent itself and we are done. In the first (second) case, where this parabola crosses $r_{\varepsilon-}$ ( $r_{\varepsilon+}$) the tangent line must intersect the $P$-axis at $P < P_{\max}$ ($P > P_{\max}$)—or not at all for $P > P^*$— so since

the tangent line varies continuously along the parabola, there must be a point $P_4$ at which the tangent line to the parabola intersects the $P$-axis exactly at $(P_{\max}, 0)$. Clearly this tangent line lies between $r_{\varepsilon-}$ and $r_{\varepsilon+}$, so we set $\tilde{r}$ to be equal to it over $[P_4, P_{\max}]$, and we are done.

In the other case, where $DP < r'(P)$, then the only differences to the proof are: i) We need to swap the parabolas the functions is initially equal to from $L$ to $U$ (and vice-versa) *except* the parabola initially followed for $P > P^*$ in the case where we are considering relative distance. This is necessary since we require a change in the sign of $\tilde{r}'(P) - r'(P)$ in order to use the IVT to find a line tangent to $r'(P)$. ii) A parabola of negative curvature can intercept the $P$-axis with a positive derivative in this case, but this is easily fixed: since $DP < r'(P) < 0$ initially, it necessitates a change in the sign of $\tilde{r}'(P) - r'(P)$, so we can use the IVT to find a line tangent to $r'(P)$ and then proceed as in previous cases■

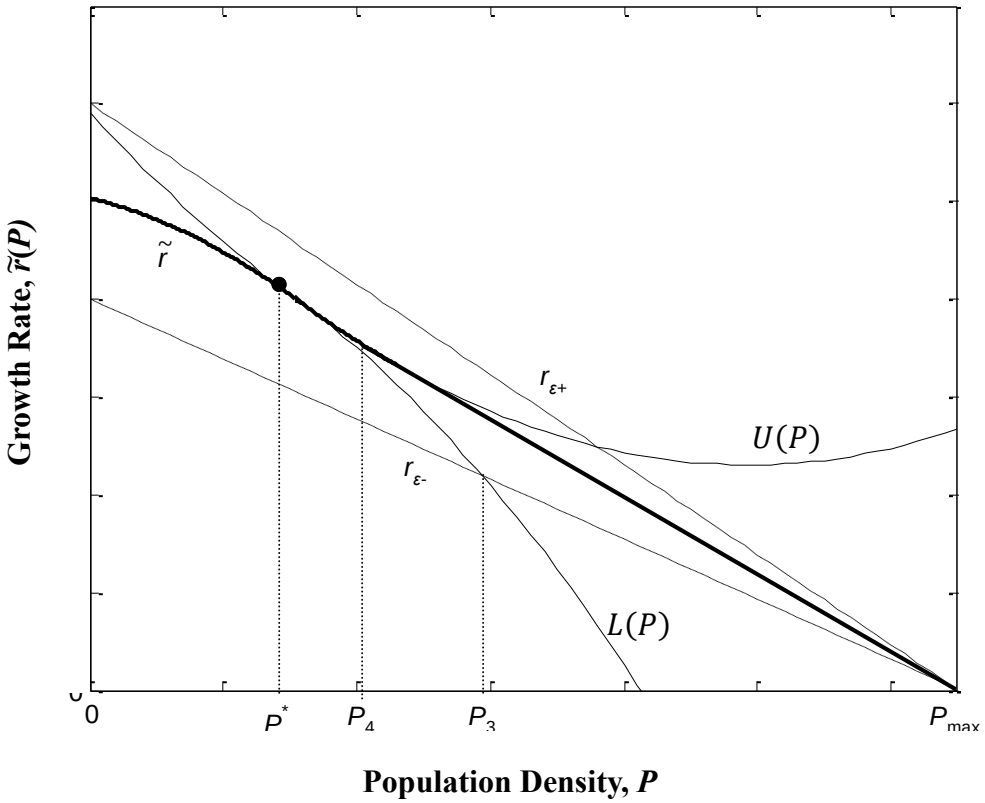


Figure 3.7: Example of a growth rate $\tilde{r}$ satisfying criterion (3.19) constructed using the method described in Theorem 3.2 for the case in which Definition 2.7 of distance (relative distance) is used. The method depends only on conditions (3.23) being satisfied. As in Fig. 3.6, the thin solid parabolas $U$ and $L$ are those of maximum and minimum (signed) curvature, which are tangent to the growth function at $(P^*, rP)$. These form upper and lower bounds, respectively, on any potential function.

Using conditions (3.23), we can check the stability of $(P^*, Z^*)$ for all functions in the $\varepsilon_Q$ neighbourhood of $r$, and plot the corresponding regions in ($rP$-$DP$) space. We can then use these regions to compute the degree of structural sensitivity in the system. Fig. 3.8 shows the degree of structural sensitivity $\Delta$ (constructed for $\rho \equiv 1$) plotted against the carrying capacity, $K$ (c.f. Fig. 3.4). Several values of $\varepsilon$ are considered, and both the Monod and hyperbolic tangent functional responses from section 3.3.1 were used. The degree of structural sensitivity shown by the system with respect to variation of the growth term is completely different depending on which functional response is taken—with the Monod functional response: varying the growth term will only alter the stability of the equilibrium for $K$ between 0.5 and 2, while with the hyperbolic tangent functional response there is a high degree of structural sensitivity even when $K = 16$. This substantial difference is in spite of the fact that the two functional responses used are very close together, and it suggests that if we have two unknown functions, performing analysis of structural sensitivity with respect to each in turn will not be enough to determine the extent of structural sensitivity with respect to variation of *both* of them together.

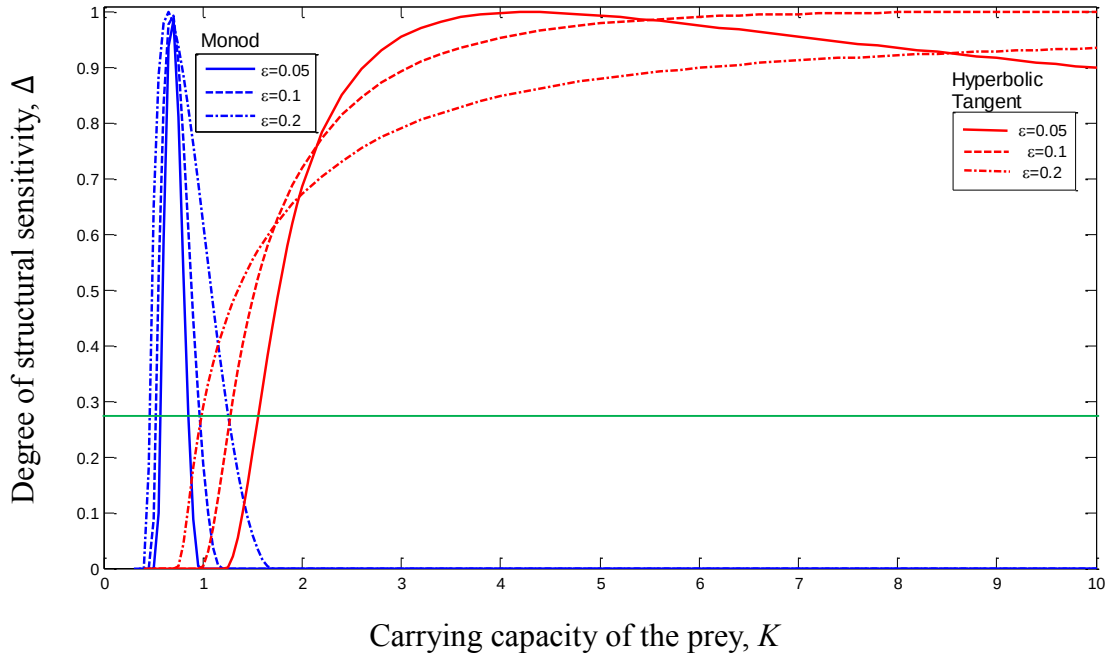


Figure 3.8: The degree of structural sensitivity of model (3.12)-(3.13) to the choice of parameterization of the growth rate for varying values of carrying capacity, *K*. The base function is taken to be the logistic function (3.20) and two different predator functional responses are used: blue curves correspond to the Monod function (3.17) and red curves correspond to the hyperbolic tangent function (3.18). The degree of sensitivity $\Delta$ is computed based on (3.10) with $\rho \equiv 1$, and a sample 'threshold sensitivity' of 5% is shown by the green line – values of $\Delta$ below this can essentially be considered 'not sensitive'. The $\varepsilon_Q$ neighbourhood of *h* is defined based on the absolute difference between *h* and its perturbations. The other model parameters are $m$=0.1 and $k$=0.3.

In Figs 3.9A, 3.9B and 3.9D, 3.9E, we present the $\varepsilon_Q$ neighbourhood of $r$ (with $\varepsilon = 0.1$) along with its regions of stability and instability in ($rP$-$DP$) space for two values of $K$ with the Monod and hyperbolic tangent functional responses respectively. These figures show us that an increase in $K$ does not affect the Hopf bifurcation line in this space, but instead shifts the $\varepsilon_Q$-neighbourhood towards the $DP = 0$ axis. The difference in structural sensitivity between the Monod and hyperbolic tangent functional responses is entirely due to the resultant change in the value of $P^*$.

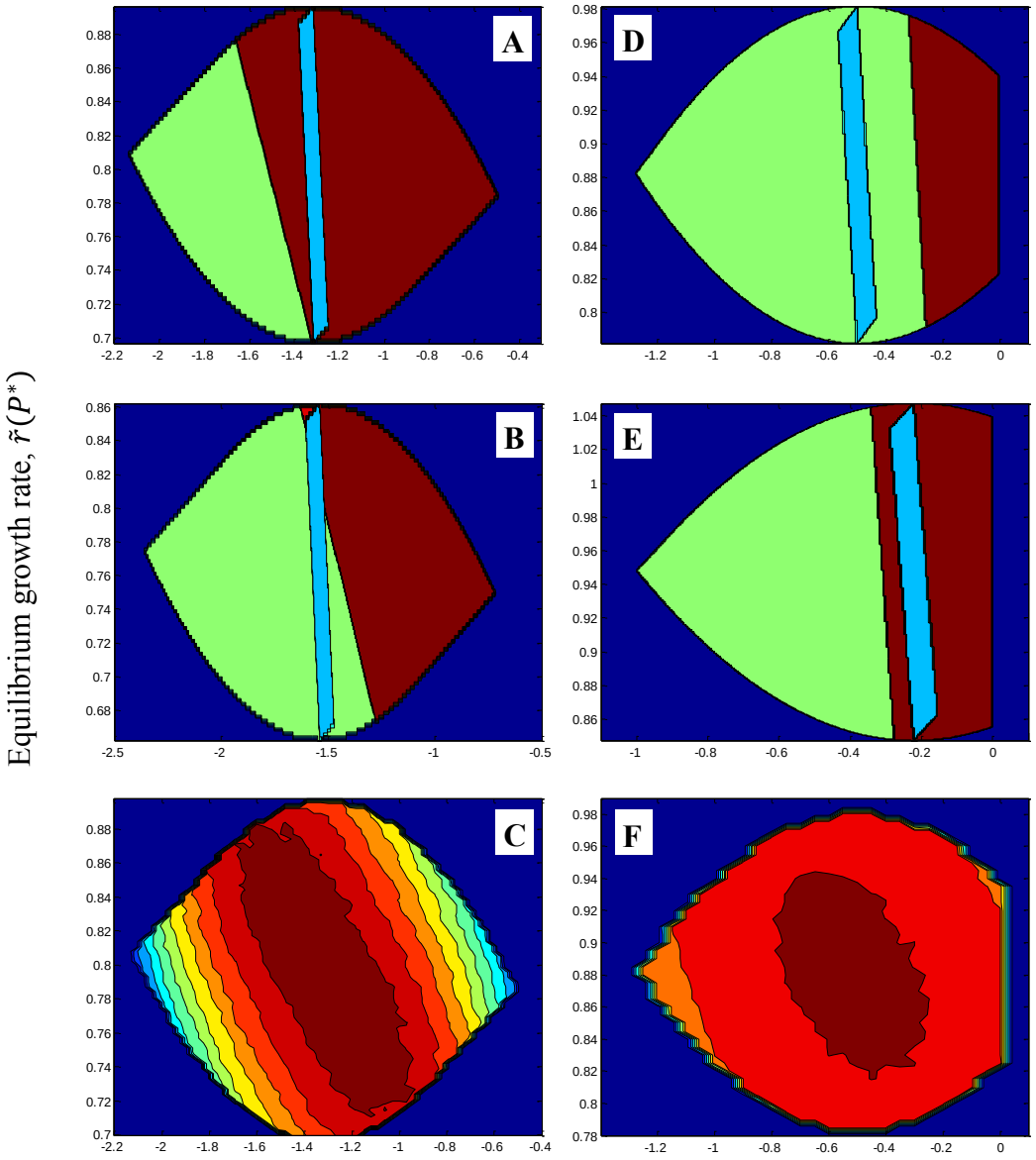


Figure 3.9: Testing structural sensitivity of model (3.12)-(3.13) to variation of the per capita growth rate of prey $\tilde{r}$. The whole space of functions $\tilde{r}$ is projected into ($rP$-$DP$) space. The $\varepsilon_Q$ neighbourhood is defined based on the absolute difference between $r$ and its perturbations. Diagrams (A, B) correspond to the Monod functional response and are constructed for $K$=0.65 and $K$=0.8, respectively. Diagrams (D, E) correspond to the hyperbolic tangent functional response of the predator and are constructed for $K$=2 and $K$=4.5. The meaning of the coloured domains is the same as in Fig. 3.5. Diagrams C, F show the functional density, $\rho(rP, DP)$, in the ($rP$-$DP$) space for the cases corresponding to diagrams B and D respectively. In Fig. 3.9C $\rho$ ranges from 0.13 in the azure regions to 0.59 in the central dark red region, and in Fig. 5F $\rho$ ranges from 0.6 in the orange regions to 0.82 in the central dark red region. Dark blue indicates a functional density of 0, indicating that no functions in the $\varepsilon_Q$-neighbourhood correspond to this point.

## 3.4 Computation of the functional density

For the growth function, it is quite simple to compute the 'functional density' $\rho$ of each point in ($rP$-$DP$) space, as discussed at the end of Section 3.2: as the domain of the function is one dimensional, we can bound the functions passing through a point by the parabolas of maximum positive and negative curvature, and use this approach to decide which points have functions passing through them which also pass through $(P^*, rP)$ with derivative $DP$.

We do this by considering all points in the strip between $r_{\varepsilon+}$ and $r_{\varepsilon-}$, and determining whether there is a function $\tilde{r}$ with $\tilde{r}(P^*) = rP$, and $\tilde{r}'(P^*) = DP$ such that the curve $\tilde{r}$ passes through the point and $\tilde{r}'(P) < 0 \quad \forall \; P \in [0, P_{max}]$. The proportion of points between $r_{\varepsilon+}$ and $r_{\varepsilon-}$ which do have such functions passing through them then gives us a numerically computable measure of the set of functions which project onto the point $(rP, DP)$.

Given the values $rP$ and $DP$, and a point $(Q, r_Q)$, we determine whether there is a function $\tilde{r}$ passing through this point as follows: firstly, we check that $(Q, r_Q)$ lies between the minimum and maximum parabolas $L$ and $U$ used in our proof of Theorem 3.2:

$$L(P) \coloneqq rP + DP(P - P^*) + \frac{A_1}{2}(P - P^*)^2,$$

$$U(P) \coloneqq rP + DP(P - P^*) + \frac{A_2}{2}(P - P^*)^2$$

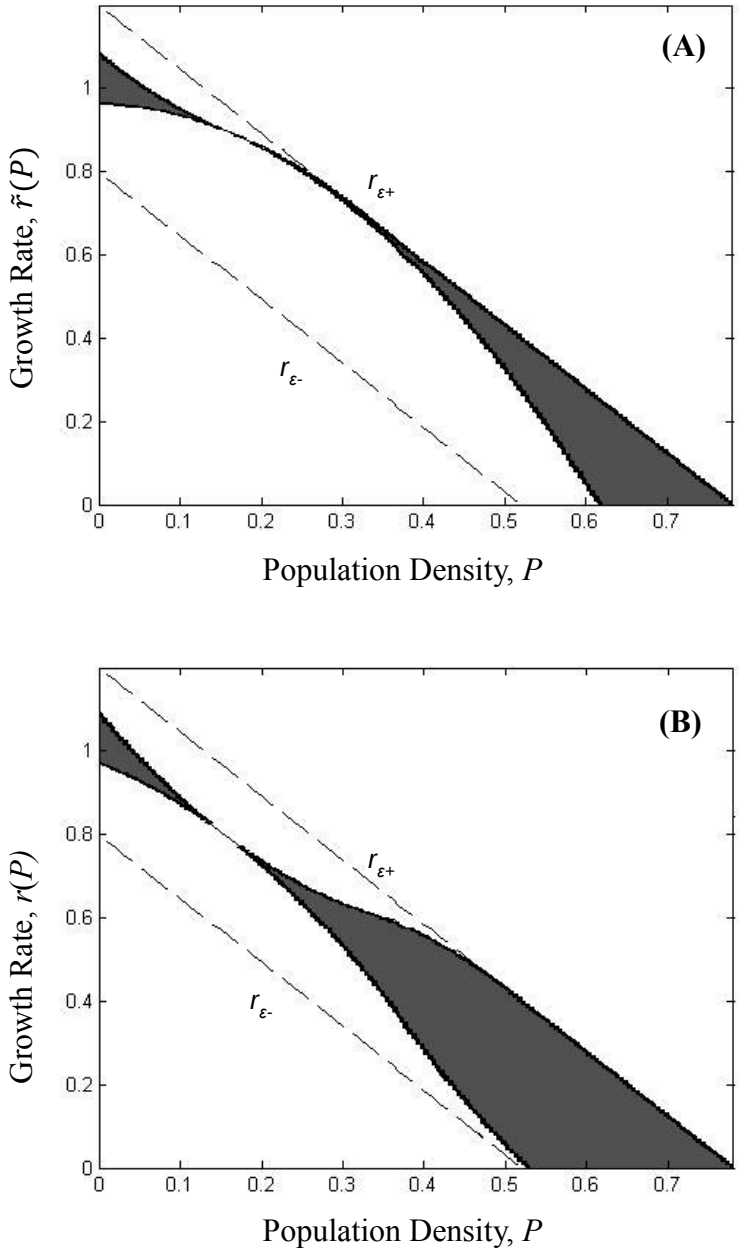


Figure 3.10: Computing the functional density $\rho$ of growth rate function variation in the ($rP$-$DP$) space. The definition of the functional density is given in section 3.2 of the text. In this figure for each fixed pair $rP$, $DP$ we show in grey the region of points bounded by $r_{\pm\varepsilon}$ such that there exists at least one curve passing through any of those points and having a slope $DP$ at the point ($P$, $rP$). (A) The functional density is low ($rP$=0.8; $DP$ =1.0): graphs of functions $\tilde{r}$ satisfying $\tilde{r}(P^*) = rP$, $\tilde{r}'(P^*) = DP$ can only pass through a limited number of points $(P, \tilde{r}(P))$ between $r_{\varepsilon+}$ and $r_{\varepsilon-}$. (B) The functional density is high ($rP$=0.6; $DP$ =1.5): graphs of functions $\tilde{r}$ satisfying $\tilde{r}(P^*) = rP$, $\tilde{r}'(P^*) = DP$ can pass through many points $(P, \tilde{r}(P))$ between $r_{\varepsilon+}$ and $r_{\varepsilon-}$. The other model parameters are $K$=0.65; $m$=0.1 and $k$=0.3.

If $(Q, r_Q)$ doesn't lie between $L$ and $U$, there can be no valid $\tilde{r}$. If $(Q, r_Q)$ does lie between these parabolas, then we need to choose a derivative at $(Q, r_Q)$, $D_Q$, and define the parabolas

$$\hat{L}(P) \coloneqq r_Q + D_Q(P - Q) + \frac{A_1}{2}(P - Q)^2, \text{ and}$$

$$\hat{U}(P) \coloneqq r_Q + D_Q(P - Q) + \frac{A_2}{2}(P - Q)^2,$$

which define the upper and lower bounds for functions $\tilde{r}$ satisfying $A_1 < \tilde{r}''(P) < A_2 \ \forall P \in [0, P_{\max}]$, and passing through $(Q, r_Q)$ with derivative $D_Q$. We need to check several conditions on the 4 parabolas: firstly, we need $\hat{L}(P) < r_{\varepsilon+}(P)$ and $\hat{U}(P) > r_{\varepsilon-}(P) \ \forall \ P \in [0, P_{max}]$ (otherwise there are no valid functions having derivative $D_Q$ at $(Q, r_Q)$ at all). Secondly, we require that $\hat{L}(P) < U(P)$ and $L(P) < \hat{U}(P) \ \forall \ P \in [0, P_{max}]$.

These conditions are enough to ensure that there is a function $\tilde{r}''$ passing through $(P^*, rP)$ with derivative $DP$ that also passes through $(Q, r_Q)$, while satisfying the restriction on the second derivative in (3.19), but in some cases we need one more condition to ensure that such a function exists which also satisfies $\tilde{r}'(P) < 0 \ \forall P \in [0, P_{max}]$. If $Q > P^*$, then in the case that $Q - \frac{D_Q}{A_1} > P^* - \frac{DP}{A_2}$, we need the third condition $rP - \frac{DP^2}{A_2} + \frac{1}{2}A_2 \cdot DP^2 > r_Q - \frac{{D_Q}^2}{A_1} + \frac{1}{2}A_1 \cdot {D_Q}^2$—in words, if the minimum of the parabola $U$ occurs at a lower value of $P$ than the maximum of the parabola $\hat{L}$, we require $\min\{U(P)\} > \max\{\hat{L}(P)\}$, otherwise any function between $(P^*, rP)$ and $(Q, r_Q)$ with the given $D_Q$ will have to have a positive derivative at some point because once it has passed below the minimum of $U$, it will have to rise above the higher maximum of $\hat{L}$. If, instead, we have $P^* > Q$, then the condition is the same, except now the function needs to pass below the minimum of $\hat{U}$ and be able to pass above the maximum of $L$ without a positive derivative. Thus if $P^* - \frac{DP}{A_1} > Q - \frac{D_Q}{A_2}$, we require $r_Q - \frac{{D_Q}^2}{A_2} + \frac{1}{2}A_2 \cdot {D_Q}^2 > rP - \frac{DP^2}{A_1} + \frac{1}{2}A_1 \cdot DP^2$.

All of these conditions depend on $D_Q$, and we note that there is always one 'optimal' value $D_Q$ for each condition to be satisfied—i.e. it is necessary for the condition to hold for this $D_Q$, for it to hold for any derivative at $(Q, r_Q)$ at all—for example, if $\hat{L}(P) < r_{\varepsilon+}(P)$ doesn't hold when $\hat{L}$ is defined for $D_Q = \frac{dr_{\varepsilon+}}{dP}(P)$, it will not hold for any

other derivative. So we proceed as follows: starting from $D_Q = DP$, we check all the conditions. If one of the conditions is not satisfied, then we either decrease or increase $D_Q$ by a small increment until either the condition is satisfied or the optimal $D_Q$ is reached without satisfying the condition—in which case we can conclude that there is no valid function passing through $(Q, r_Q)$. If the given condition is satisfied, we continue checking the others and making adjustments until either we find a $D_Q$ such that all conditions are satisfied—in which case we are done—or we find an unsatisfied condition which, in order to rectify, we have to undo the changes we have already made to $D_Q$ to ensure it satisfies another condition—in which case there can be no valid function. If at any point we reach the optimal $D_Q$ for a given condition (or a sufficiently large/small $D_Q$ when the optimal derivative is $\pm\infty$) without satisfying it, we should stop■

Fig. 3.10 illustrates the points that have functions passing through them which also pass through $(P^*, rP)$ with derivative $DP$, for two given values of $(rP, DP)$. Figs 3.9C and 3.9F show the functional density of the $\varepsilon_Q$-neighbourhood in the case of Fig. 3.9B and 3.9D, respectively. The functional density is shown to be greater towards the centre of the domain, but does not vary a great deal (the range is 0.13-0.59 in Fig. 3.9C, but only falls below 0.5 in non-red regions, and the range is 0.6-0.82 in Fig. 3.9F) so including this information will not significantly change the character of the graphs in Fig. 3.8 in this particular model.

## 3.5 Discussion and conclusions

Although it is well recognized that biological models can be quite sensitive to the mathematical formulation of the model functions (Myerscough et al., 1996; Wood and Thomas, 1999; Fussmann and Blasius, 2005; Cao et al., 2008; Cordoleani et al., 2011), the conventional sensitivity analysis is mostly undertaken by varying the model parameters for fixed functional forms (Lim et al., 1989; Janssen et al., 1996; Bendoricchio and Jorgensen, 2001 and many other references). This is mainly because it has been held as 'evident' that we cannot check all possible mathematical formulations of a given functional dependence *f*, since the functional space to which *f* belongs has an infinite number of dimensions. In this chapter, we've introduced a simple but rigorous test of structural sensitivity, which reveals the effect of the choice of the mathematical

formulation of model functions on the local stability of equilibria. The main idea is to project the infinite-dimensional functional space onto a finite low-dimensional space consisting of the values of the functions and their derivatives at the equilibrium. The method is exhaustive, in the sense that no valid model function which alters the stability conditions will be missed, provided the resolution of the mesh is high enough. Importantly, the use of a partially specified model means we only consider functions with the same qualitative global properties as the initial model function (e.g., monotonically increasing/decreasing, sign of curvature, etc.), so the observed violations of stability are more surprising than they would be if we allowed perturbations of the model functions that changed fundamental qualitative properties.

Implementation of our sensitivity test reveals the main reason for the limitations of the conventional parameter-based methods of sensitivity. As is shown, for instance, in Figs 3.5 and 3.9, varying only the model parameters for a fixed mathematical formulation can result in a displacement in the functional space confined to a limited number of directions, and if the main direction of displacement in the functional space is roughly parallel to the bifurcation hyper surface, then variation of the model parameters will not result in a crossing of this bifurcation hyper surface (Fig. 3.5A, B, Fig. 3.9B, D, F), unless the base function lies very close to it in the first place (Fig. 3.9A). Therefore, this limited approach can reach a misleading conclusion that the stability of the given equilibrium will be consistent across a large range of parameters, while considering perturbations of the base function in the $\varepsilon_Q$ neighbourhood in the direction traversal to the bifurcation hyper surface will reveal a stability change (Fig. 3.5A, B and Fig. 3.9B, D, F). As an example, in Appendix A we analytically construct the $\varepsilon_Q$ neighbourhood corresponding to variation of parameters for a fixed mathematical formulation $f$ and derive the conditions of structural sensitivity for small $\varepsilon_Q$ when the number of parameters is equal to two.

Projecting the infinite dimensional function space onto a low dimensional space of generalised parameters—containing only the equilibrium points and the values of the functions and their derivatives at the equilibrium—has a drawback in that information about the measure of the $\varepsilon_Q$-neighbourhood in the function space, and that of its sub-domains of stability and instability, may be lost. Formally, we can solve this problem by introducing certain weights of the points in the considered subspace to represent their impact. In this chapter, we've introduced the functional density $\rho$, which characterises

the relative amount of functions which can be potentially constructed to take the given values and derivatives at the equilibrium (e.g. Fig. 3.10). Another important issue arises from the fact that some parameterizations can have more biological significance than others, and so when computing the degree of sensitivity $\Delta$ we would ideally give more consideration to those functions which are more biologically relevant and disregard less meaningful parameterizations. However, weighting the possible parameterizations according to their biological significance requires detailed information about the nature of the underlying processes which is often not available.

Our sensitivity test requires the choice of a certain base function, which defines the $\varepsilon_Q$ neighbourhood in which we will consider all possible functions. Therefore it is pertinent to ask whether the choice of base function influences the outcome of our structural sensitivity test. The answer to this fundamental question depends on how the magnitude of the perturbation of the base function compares with $\varepsilon$. In any case, very small perturbations of the base function shouldn't influence the qualitative behaviour, since the model is assumed to be structurally stable, but additionally the investigations presented here lead us to conclude that provided the perturbation of the base function is smaller than $\varepsilon$, the result of the structural sensitivity test will not change significantly (c.f. Fig. 3.4). In practice, the base function should be fitted to an experimental data set, with the tolerance $\varepsilon$ being constructed using the error terms, so our sensitivity test can be assumed to be independent of the base function.

To summarise, in this chapter, we've presented a general overview of how to use partially specified models to detect and quantify structural sensitivity in biological models. We've illustrated this by considering the Rosenzweig-MacArthur model, and checking its sensitivity to the formulation of both the growth rate of the prey and the functional response term. On the way, we've proved ways to obtain a projection of the $\varepsilon_Q$-neighbourhood of model functions into the generalised bifurcation space considering of the equilibrium value, and the value of the function and its derivative at this equilibrium, but only for two sets of qualitative properties. In the next section, we will introduce a theorem to extend these results to a whole class of model functions. We shall also use this theorem to demonstrate our test on several more complicated models, in order to show that it is not only applicable to extremely simple models such as the Rosenzweig-MacArthur model.

# Chapter 4

# Projection from an $\varepsilon_Q$-neighbourhood to the generalised bifurcation space in the case of an unknown function with $n$ inflection points

*This chapter is based on parts of the paper (Adamson and Morozov, 2014a)*

## 4.1 Introduction

In this chapter, we extend the results found in Chapter 3 regarding sensitivity analysis of stationary states of the model. Focusing on structural sensitivity in the case where unknown functions are functions of one variable belonging to a certain class of functions, we show how we can explore all perturbations of such functions and so analyse the structural sensitivity of a system with respect to the number and stability of its equilibria. Further, we suggest a method for considering any of a general class of functions with an arbitrary number of inflection points—thereby providing the required tools for a structural sensitivity analysis of any model with respect to variation of a function of this type. We then use the proposed method to demonstrate structural sensitivity with respect to predation terms—of Holling type II and III, respectively—in two recent ODE models of biological systems from highly cited papers, along with a delay-differential equation model. We demonstrate the existence of structural sensitivity in these models and show that conventional methods based solely on parameter sensitivity will often fail to do so.

The chapter is organized as follows. Section 4.2 recaps the general approach to the investigation of structural sensitivity with respect to the number and stability of stationary states of ODE-based models, which was presented in the last chapter. In section 4.3 we suggest a method of projecting the neighbourhood of a function in infinite-dimensional space onto a related finite-dimensional space in the case where we have a function with a finite number of known inflection points. In section 4.4 we use our method to investigate structural sensitivity in several well-known multicomponent

ecological models. Section 4.5 provides a discussion of a few important aspects of structural sensitivity in biological models, in particular, how we should define the 'degree' of structural sensitivity in a model, and what the potential relation is between structural sensitivity of models and the underlying biological systems.

## 4.2 General approach of the investigation

We consider a continuous-time system $(M)$ given by the differential equations

$$\dot{x} = G\left(g_1(x), \dots, g_m(x), \tilde{h}_1(x), \dots, \tilde{h}_p(x)\right), \quad x \in \mathbb{R}^n, \tag{4.1}$$

where $g_1, \dots, g_m, \tilde{h}_1, \dots, \tilde{h}_p \in C^1(\mathbb{R}^n)$. Here $G: \mathbb{R}^{m+p} \to \mathbb{R}^n$ is a linear function representing the overall 'structure' of the model $(M)$ in terms of the various model functions, detailing how the growth rates, mortality terms, functional responses, etc. are used to build the full model. Of these model functions, we assume that $g_1, \dots, g_m$ are of known analytical form, and so only require a choice of parameters to be fully determined, while we assume that $\{\tilde{h}_1(x), \dots, \tilde{h}_p(x)\}$ is the set of functions with unknown parameterisations. Usually we have some prior theoretical or experimental knowledge concerning this set of functions, and so we can use this knowledge to specify a class of function sets $Q = \{Q_1, \dots, Q_p\}$, $Q_i \subsetneq C^1(\mathbb{R}^n)$ which $\{\tilde{h}_1(x), \dots, \tilde{h}_p(x)\}$ must belong to, and therefore eliminate any irrelevant choices of functions. In this way we define $(M)$ as a 'partially specified model' (Wood, 2001). We also require that $Q$ includes bounds on the second derivatives of its constituent functions for the reasons mentioned in Section 2.2.

To complete our model $(M)$, we first need to make an arbitrary initial choice of parameterisation of the functions $\tilde{h}_1, \dots, \tilde{h}_p$, which we shall denote by $h_1, \dots, h_p$. We call these functions the 'base functions', and their exact form does not matter, provided that they are taken from $Q$ and are fitted to available experimental data. To fully determine whether or not $(M)$ is $\varepsilon$-structurally sensitive or not (for the given base functions), we first need to obtain a value for $\varepsilon$—the accuracy of the available experimental data, and then check the entirety of $B_\varepsilon(M; d_Q)$ for models which predict behaviour that differs qualitatively from the behaviour predicted by $(M)$. The main difficulty in such an investigation is the requirement that we cover all functions of $B_\varepsilon(M; d_Q)$: since this is generally infinite dimensional (even when we only have a single unknown model

function $h$)—it is the space of function sets in $Q$ that take values within $\varepsilon$ of those of the base function set—it is obviously impossible to directly check this neighbourhood as can be done in variation-of-parameters investigations. However, as an alternative to considering neighbourhoods in function space directly, we note that several properties of a dynamical system are completely determined by a few specific values of the model functions and their derivatives, rather than the entire functions. These specific local values can be treated as parameters, and make up what is called the 'generalised bifurcation space'. The main idea of the general structural sensitivity analysis is then to determine the region of generalised bifurcation space corresponding to $B_\varepsilon(M; d_Q)$, or the $\varepsilon_Q$-neighbourhood of $M$, by projecting the initial infinite dimensional neighbourhood $B_\varepsilon(M; d_Q)$ into this space. By thoroughly exploring the projected region, we will be able to make exhaustive conclusions about the presence or absence of structural sensitivity in the model with regards to the given system properties.

In this way, the problem of covering $B_\varepsilon(M; d_Q)$ in function space is reduced to the problem of determining whether or not a function in $B_\varepsilon(M; d_Q)$ exists which, when added to the model, will yield certain values—specifically certain equilibrium values—and values taken by the function and its derivative at these equilibria. This is a nontrivial problem, and depends on the base function and the function class $Q$ which the unknown functions in the model $(M)$ must belong to: using the $d_Q$ distance requires that functions taking the given set of local values must also be within a distance $\varepsilon$ of the base function set across the entire domain $\Omega$, and therefore the problem is a *nonlocal* one. However, once this problem has been solved the rest of the analysis is straightforward, and so methods for constructing the necessary and sufficient conditions for the existence of functions taking a given set of local values whilst remaining in $B_\varepsilon(M; d_Q)$ are very powerful tools for structural sensitivity analysis.

In the previous chapter we presented and proved the necessary and sufficient conditions for the existence of a function $\tilde{h}$ in $B_\varepsilon(M; d_Q)$ yielding certain equilibrium values $x^*$ and taking values $\tilde{h}(x^*)$ and $\tilde{h}'(x^*)$ for two cases: where the function is positive and monotonically increasing (e.g. a functional response of Holling type II) and when it is monotonically decreasing (e.g. a logistic growth function). In the next section, we expand on these results, and present a general method for obtaining such conditions in the case that our base function has $n$ arbitrary inflection points. Since the vast majority

of functions generally considered in biological models are of such a form, this should enable us to analyse structural sensitivity—with respect to variation in a single function changing the stability of equilibria—in a large number of contemporary biological models.

## 4.3 Determining the necessary and sufficient conditions for the existence of a function with $n$ predetermined inflection points in the $\varepsilon_Q$-neighbourhood

In a wide variety of cases, we require processes to be modelled by one-dimensional functions which are convex/concave over several ranges, and therefore possess a certain set of inflection points—for example, sigmoid functions, or in the most basic case, saturating functions such as a Holling type II functional response. The requirement for a function to be concave up/down over certain domains can be deduced either from theoretical reasoning or—to a basic extent—from experimental data. Although the exact inflection points are usually themselves unknown, we can consider them as generalised parameters of our investigation, along with the derivatives of unknown functions at equilibrium, etc. We show an example of such a function as the base function in Figure 4.1, with six inflection points denoted as $a_1, \dots, a_6$. We should note, however, that a function with so many inflection points is quite exotic, and included here merely as a reference, to demonstrate the generality of our approach - in practice, aside from oscillators it is rare to use functions even with two or more inflection points. The main goal of this section is to provide a tool to be able to check for a given value of a function, $\tilde{h}(x^*)$, at an equilibrium point $x^*$ and for a given value $\tilde{h}'(x^*)$ of the derivative at this point, whether or not there exists at least one function passing through this point and remaining in the neighbourhood $B_\varepsilon(M; d_Q)$. Here we provide such a tool, which is formulated by Theorem 4.1.

Mathematically speaking, given a base function $h: \mathbb{R} \to [0, x_{\max}]$, and values $X, hX$ and $DH$, we want to determine whether or not there exists a function $\tilde{h}: \mathbb{R} \to [0, x_{\max}]$ with continuous derivative that satisfies the following criteria:

(i) $\exists$ a partition $0 < a_1 < \cdots < a_n < x_{\max}$ such that either:
$0 < \tilde{h}''(x) < A_2$ for $x \in [0,a_1) \cup (a_2, a_3) \cup \dots \cup (a_{2k}, a_{2k+1}) \cup \dots$

and $A_1 < \tilde{h}''(x) < 0$ for $x \in (a_1, a_2) \cup (a_3, a_4) \cup \ldots \cup (a_{2k+1}, a_{2k+2}) \cup \ldots$,

or

$A_1 < \tilde{h}''(x) < 0$ for $x \in [0, a_1) \cup (a_2, a_3) \cup \ldots \cup (a_{2k}, a_{2k+1}) \cup \ldots$
and $0 < \tilde{h}''(x) < A_2$ for $x \in (a_1, a_2) \cup (a_3, a_4) \cup \ldots \cup (a_{2k+1}, a_{2k+2}) \cup \ldots$,

(ii) $\tilde{h}(X) = hX$ and $\tilde{h}'(X) = DH$, (4.2)

(iii) $\tilde{h}(0) = 0$,

which is in the $\varepsilon$-neighbourhood of the base function $h$, defined in terms of either absolute or relative distance. That is, if $h_{\varepsilon+}$ and $h_{\varepsilon-}$ are the functions giving the upper and lower boundaries of the $\varepsilon$-neighbourhood of $h$ (if we are using the absolute definition of distance, $h_{\varepsilon+}(x) = h(x) + \varepsilon$ and $h_{\varepsilon-} = h(x) - \varepsilon$, while if we are using the relative definition of distance, $h_{\varepsilon+}(x) = \frac{h(x)}{1+\varepsilon}$ and $h_{\varepsilon-} = (1 - \varepsilon) \cdot h(x)$) then $h_{\varepsilon-}(x) \leq \tilde{h}(x) \leq h_{\varepsilon+}(x)$ $\forall\, x \in [0, x_{\max}]$. We note that the base function $h$ should also itself satisfy conditions (4.2i) and (4.2iii): these define the function class $Q$ from which we should choose any appropriate function. In practice, $X$ will usually denote a parameter corresponding to an equilibrium point, and condition (4.2ii) simply states that $hX$ corresponds to the value taken by the unknown function at this equilibrium point and that $DH$ corresponds to the value taken by its derivative at this point. Condition (i) states that we want our function to be alternatingly concave up and concave down across the given partition, which forms the set of the function's inflection points. Condition (4.2iii) simply states that the function should pass through the origin – as is required for most functions (growth rates, for example) to make biological sense.

In order to determine the existence of such a function, we note that given any function $g$ that satisfies criteria (4.2) and that at some point $y \in (a_k, a_{k+1})$ assumes the value $g(y)$ with derivative $g'(y)$, upper and lower bounds for such a function can be defined across the entire domain $[0, x_{\max}]$ as follows (see the blue curves in Figure 4.1 for an example):

1) If criterion (4.2i) requires $0 < \tilde{h}''(x) < A_2$ for $x \in [a_k, a_{k+1}]$, as is the case in Fig. 4.1, then the upper bound of $g$ across $[a_k, a_{k+1}]$ is given by $g(x) \leq \mathrm{Upp}_{y,g(y),g'(y)}(x) = g(y) + g'(y) \cdot (x - y) + \frac{A_2}{2}(x - y)^2$—i.e. the parabola with

maximal second derivative $A_2$ tangent to $g$ at $y$—and the lower bound of $g$ across the same interval is given by $g(x) \geq \text{Low}_{y,g(y),g'(y)}(x) = g(y) + g'(y) \cdot (x - y)$ – i.e. $g$ must lie above its own tangent at $y$ since it is concave up over this interval. Similarly, if criterion (4.2i) requires $A_1 < \tilde{h}''(x) < 0$ for $x \in (a_k, a_{k+1})$, then the upper bound of $g$ across $[a_k, a_{k+1}]$ is given by $\text{Upp}_{y,g(y),g'(y)}(x) = g(y) + g'(y) \cdot (x - y)$ and the lower bound is given by $\text{Low}_{y,g(y),g'(y)}(x) = g(y) + g'(y) \cdot (x - y) + \frac{A_1}{2}(x - y)^2$. Furthermore, these inequalities are strict except at $y$ itself.

2) We now extend our upper and lower boundaries to the adjacent intervals $[a_{k-1}, a_k]$ and $[a_{k+1}, a_{k+2}]$. Consider $[a_{k-1}, a_k]$, and assume that we have the case where $0 < \tilde{h}''(x) < A_2$ for $x \in (a_k, a_{k+1})$, as in Figure 4.1. We already have a value for the upper bound at $a_k$: $\text{Upp}_{y,g(y),g'(y)}(a_k) = g(y) + g'(y) \cdot (a_k - y) + \frac{A_2}{2}(a_k - y)^2$, so we can continue the upper bound by following step 1), replacing $y, g(y)$ and $g'(y)$ with $a_k$, $\text{Upp}_{y,g(y),g'(y)}(a_k)$ and $\text{Upp}'(a_k)$, where $\text{Upp}'(a_k) = g'(y) + A_2(a_k - y)$ is the (right hand side) derivative of the curve $\text{Upp}_{y,g(y),g'(y)}(x)$ at $a_k$. Since in this case, $A_1 < \tilde{h}''(x) < 0$ for $x \in (a_{k-1}, a_k)$, we can define $\text{Upp}_{y,g(y),g'(y)}$ across $[a_{k-1}, a_k]$ as the tangent line to $\text{Upp}_{y,g(y),g'(y)}(a_k)$. In a similar way, we can continue the lower bound across this interval, starting from $\text{Low}_{y,g(y),g'(y)}(a_k) = g(y) + g'(y) \cdot (a_k - y)$ and $\text{Low}'(a_k) = g'(y)$, and following the parabola of second derivative $A_1$ that is tangent to $\text{Low}_{y,g(y),g'(y)}(a_k)$. Essentially we are proceeding exactly as per step 1), but using $\text{Upp}_{y,g(y),g'(y)}(a_k)$ and its right-derivative as initial values. This can be seen clearly from Figure 4.1, where the upper and lower bounds over $[a_2, a_3]$ are the line and parabola, respectively, continuing from the upper and lower bounds already defined over $[a_3, a_4]$. We use exactly the same approach over $[a_{k+1}, a_{k+2}]$, and the alternative case, in which $A_1 < \tilde{h}''(x) < 0$ over the original interval $x \in [a_k, a_{k+1}]$, can be dealt with in a similar manner.

3) Using the values and derivatives of $\text{Upp}_{y,g(y),g'(y)}$ and $\text{Low}_{y,g(y),g'(y)}$ at $a_{k-1}$ and $a_{k+2}$, we can extend $\text{Upp}_{y,g(y),g'(y)}$ and $\text{Low}_{y,g(y),g'(y)}$ in the same way over the intervals $[a_{k-2}, a_{k-1}]$ and $[a_{k+2}, a_{k+3}]$. We can then proceed to define $\text{Upp}_{y,g(y),g'(y)}$ and $\text{Low}_{y,g(y),g'(y)}$ inductively across the whole of the domain $[0, x_{\max}]$.

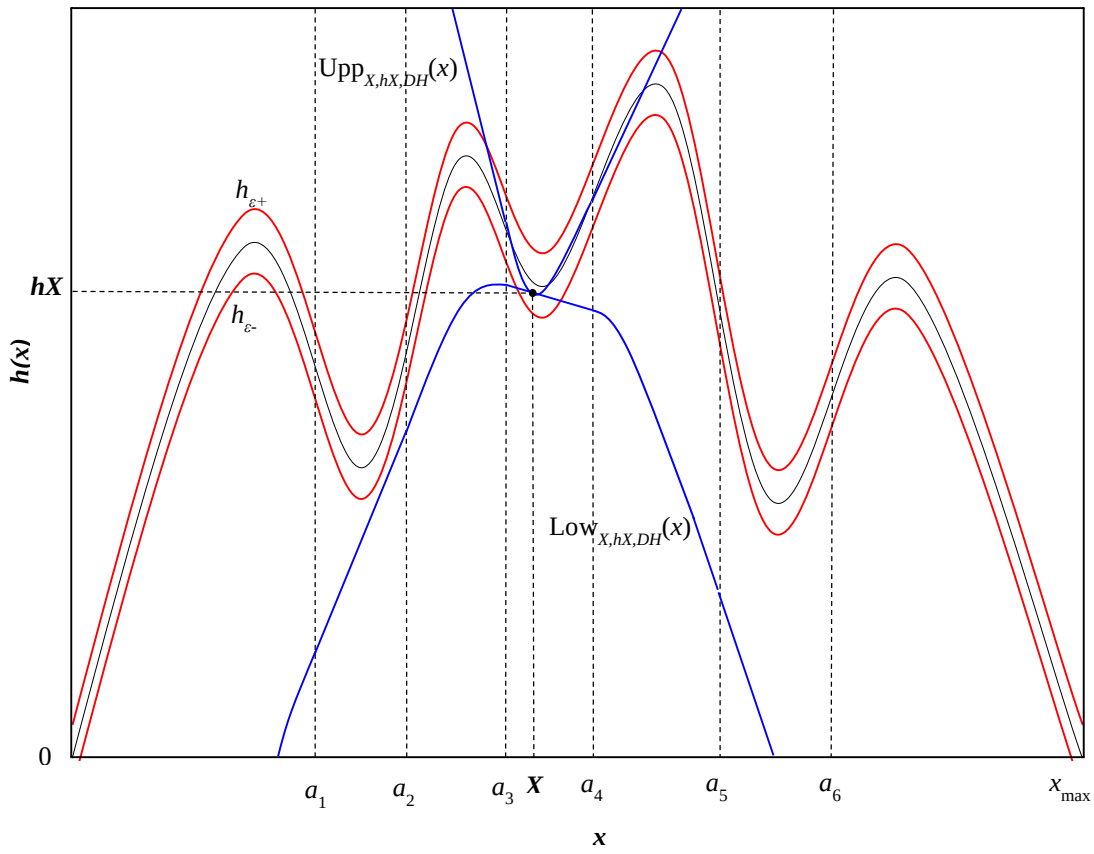


Figure 4.1: The $\varepsilon_Q$-neighbourhood of a base function $h$ with six inflection points $a_1, \ldots, a_6$, together with the upper and lower bounds $\mathrm{Upp}_{X,hX,DH}(x)$ and $\mathrm{Low}_{X,hX,DH}(x)$ of any functions satisfying conditions (i)-(iii) in Section 4. The base function is shown in black, while the upper and lower bounds $h_{\varepsilon+}$ and $h_{\varepsilon-}$ are shown in red and $\mathrm{Upp}_{X,hX,DH}(x)$ and $\mathrm{Low}_{X,hX,DH}(x)$ are shown in blue.

To derive conditions for the existence of a function $\tilde{h}$ satisfying (4.2) in the $\varepsilon$-neighbourhood of $h$, we must first create the $\mathrm{Upp}_{y,g(y),g'(y)}$ and $\mathrm{Low}_{y,g(y),g'(y)}$ functions using steps 1)-3), starting with $y = X$, $g(y) = hX$ and $g'(y) = DH$. This will give us the upper and lower bounds for any viable function $\tilde{h}$. We now put forward the following:

**Theorem 4.1:**

There exists a function $\tilde{h}: \mathbb{R} \to [0, x_{\max}]$ that satisfies criteria (4.2) if and only if

$$\mathrm{Upp}_{X,hX,DH}(x) > h_{\varepsilon-}(x) \;\; \forall\, x \in [0, x_{\max}],\ \mathrm{Upp}_{X,hX,DH}(0) \geq 0, \tag{4.3}$$

$$\text{and } \mathrm{Low}_{X,hX,DH}(x) < h_{\varepsilon+}(x) \;\; \forall\, x \in [0, x_{\max}],\ \mathrm{Low}_{X,hX,DH}(0) \leq 0,$$

where $\mathrm{Upp}_{X,hX,DH}$ and $\mathrm{Low}_{X,hX,DH}$ are the upper and lower bound functions defined in steps 1)-3) above.

**Proof**

Clearly such a function cannot exist unless conditions (4.3) are satisfied, and so they are necessary conditions, but it remains to be proved that they are sufficient conditions for the existence of a function satisfying criteria (4.2). In order to do this, we shall construct a valid function assuming only these conditions. To follow the proof, it is helpful to refer to Fig. 4.1, which shows an example base function and its $\varepsilon$-neighbourhood (red boundaries) together with the corresponding $\mathrm{Upp}_{X,hX,DH}$ and $\mathrm{Low}_{X,hX,DH}$ (blue curves).

We first choose some $0 < \delta < \varepsilon$ which is sufficiently close to $\varepsilon$ that the condition $\mathrm{Upp}_{X,hX,DH}(x) > h_{\delta-}(x)$ and $\mathrm{Low}_{X,hX,DH}(x) < h_{\delta+}(x) \;\; \forall\, x \in [0, x_{\max}]$ still holds, and some $0 < \gamma \ll 1$ such that if we construct $\mathrm{Upp}_{X,hX,DH}$ and $\mathrm{Low}_{X,hX,DH}$ using slightly relaxed bounds on the second derivative—$\gamma < \tilde{h}''(x) < A_2 - \gamma$ and $A_1 + \gamma < \tilde{h}''(x) < -\gamma$ instead of $0 < \tilde{h}''(x) < A_2$ and $A_1 < \tilde{h}''(x) < 0$—then conditions (4.2) are still satisfied, and furthermore, that the second derivatives of $h_{\delta-}$ and $h_{\delta+}$ are still within these new bounds. It is easy to verify that such $\delta$ and $\gamma$ must exist through the continuity of the construction of $h_{\delta+}$, $h_{\delta-}$, $\mathrm{Upp}_{X,hX,DH}$ and $\mathrm{Low}_{X,hX,DH}$. Hereon, whenever we talk of $\mathrm{Upp}_{y,g(y),g'(y)}$ and $\mathrm{Low}_{y,g(y),g'(y)}$, we shall refer to the upper and lower bounds constructed using the slightly modified limits of the second derivative.

Starting from $X$, we initially define $\tilde{h}$ for x<$X$ by setting $\tilde{h}(x)$=$\mathrm{Upp}_{X,hX,DH}(x)$. We note that, by the 3 steps of construction, $\mathrm{Upp}_{y,g(y),g'(y)}(x)$ and $\mathrm{Low}_{y,g(y),g'(y)}(x)$ are both continuous with respect to the initial values $y$, $g(y)$ and $g'(y)$. Therefore at every point $x$ over which we've already defined $\tilde{h}$, the new upper and lower bounds formed by starting from $x, \tilde{h}(x)$ and $\tilde{h}'(x)$ vary continuously. We can use this fact to construct a valid function $\tilde{h}$ piece by piece without violating any of the conditions it must satisfy. Let us initially consider the interval $[0, X]$. Since $\mathrm{Low}_{X,hX,DH}(x) < h_{\delta+}(x)$, and $\mathrm{Low}_{X,hX,DH}(0) \leq 0$, then if we check $\mathrm{Low}_{x,\tilde{h}(x),\tilde{h}'(x)}$ at each point of $\tilde{h}(x)$=$\mathrm{Upp}_{X,hX,DH}(x)$, then there must come a point $x_1 \in [0, X]$ for which either $\mathrm{Low}_{x_1,\tilde{h}(x_1),\tilde{h}'(x_1)}(0) = 0$ whilst $\mathrm{Low}_{x_1,\tilde{h}(x_1),\tilde{h}'(x_1)}$ remains below $h_{\delta+}$ over $[0, x_1]$, or at which $\mathrm{Low}_{x_1,\tilde{h}(x_1),\tilde{h}'(x_1)}$ is tangent to $h_{\delta+}$ at some point $x_2$. In the first case, we note that $\mathrm{Low}_{x_1,\tilde{h}(x_1),\tilde{h}'(x_1)}$ cannot pass below $h_{\delta-}$ in the interval $(0, x_1]$, because $h_{\delta-}(0) \leq 0$ and the curve of $\mathrm{Low}_{x_1,\tilde{h}(x_1),\tilde{h}'(x_1)}$ is everywhere more concave than that of $h_{\delta-}$ by definition—$\mathrm{Low}_{x_1,\tilde{h}(x_1),\tilde{h}'(x_1)}$ cannot lie beneath $h_{\delta-}$ over any interval because on the left hand side of any such interval, we would necessarily have $\mathrm{Low}'_{x_1,\tilde{h}(x_1),\tilde{h}'(x_1)}(x) < h'_{\delta-}(x)$, whilst on the right hand side we would need $\mathrm{Low}'_{x_1,\tilde{h}(x_1),\tilde{h}'(x_1)}(x) > h'_{\delta-}(x)$, which would violate $\mathrm{Low}''_{x_1,\tilde{h}(x_1),\tilde{h}'(x_1)}(x) > h''_{\delta-}(x)\ \forall x \in [0, x_{\max}]$. Therefore we can set $\tilde{h}(x) = \mathrm{Low}_{x_1,\tilde{h}(x_1),\tilde{h}'(x_1)}(x)$ for $x \in [0, x_1]$, and we will have successfully defined $\tilde{h}$ over $[0, X]$.

In the second case, we set $\tilde{h}$ equal to $h_{\delta+}$ for $x < x_1$, noting that regardless of our definition of distance, $h_{\delta+}$ and $h_{\delta-}$ both satisfy condition (4.2i) since $h$ does. If we are using Definition 2.24 of distance between functions (i.e. relative error), then $h_{\delta+}(0) = 0$ so we set $\tilde{h}(x) = h_{\delta+}(x)\ \forall x \in [0, x_1]$ and we are done. If we are using Definition 2.23 (absolute error), we note that since the construction of $\mathrm{Low}_{y,g(y),g'(y)}(x)$ is continuous, there must be a point $x_3$ such that $\mathrm{Low}_{x_3,h_{\delta+}(x_3),h'_{\delta+}(x_3)}(0) = 0$. $\mathrm{Low}_{x_2,h_{\delta+}(x_2),h'_{\delta+}(x_2)}(x)$ cannot pass below $h_{\delta-}$ over the interval $(0, x_2]$, again because it is everywhere more concave than $h_{\delta-}$, so assuming otherwise would cause a contradiction. Therefore we set $\tilde{h}(x) \coloneqq \mathrm{Low}_{x_3,h_{\delta+}(x_3),h'_{\delta+}(x_3)}(x)\ \forall\ x \in [0, x_2]$, and we have successfully defined $\tilde{h}$ over $[0, X]$.

We define $\tilde{h}$ across the interval $[X, x_{\max}]$ in a similar way. We initially set $\tilde{h}(x) = \mathrm{Upp}_{X,hX,DH}(x)$ for $x > X$, we check $\mathrm{Low}_{x,\tilde{h}(x),\tilde{h}'(x)}$ at each point, and note that there must

come a point $x_4$ at which either $\text{Low}_{x_4,\tilde{h}(x_4),\tilde{h}'(x_4)}(x)$ lies tangent to $h_{\delta+}$ at some further point $x_5$, or $\text{Low}_{x_4,\tilde{h}(x_4),\tilde{h}'(x_4)}(x_{\max}) < h_{\delta+}(x_{\max})$. Either way, we note that as before, $\text{Low}_{x_4,\tilde{h}(x_4),\tilde{h}'(x_4)}(x)$ must lie above $h_{\delta-}$ over the interval $[x_4, x_{\max}]$, so in the latter case, we can set $\tilde{h}(x) = \text{Low}_{x_4,\tilde{h}(x_4),\tilde{h}'(x_4)}$ over the interval $[x_4, x_{\max}]$, and we are done. In the former case, we set $\tilde{h}(x) = \text{Low}_{x_4,\tilde{h}(x_4),\tilde{h}'(x_4)}$ over the interval $[x_4, x_5]$, and then $\tilde{h}(x) = h_{\delta+}(x)\ \forall x \in (x_5, x_{\max}]$, and we are done.

We have successfully proved that, provided that conditions (4.3) are satisfied, it is always possible to construct a $C^1$ function satisfying criterion (4.2). Therefore conditions (4.3) are precisely the necessary and sufficient conditions for there to exist at least one function in the $\varepsilon$-neighbourhood of $h$ that satisfies criterion (4.2) ■

Using this result, we can determine a projection of the $\varepsilon_Q$-neighbourhood of $h$ from function space into the generalised bifurcation space composed of the values $X = x^*$, $hX = \tilde{h}(x^*)$ and $DH = \tilde{h}'(x^*)$, but we need to know the inflection points $a_1, \dots, a_n$ beforehand. In practice, however, we are rarely sure of the exact value of the inflection points—even if we can theoretically justify their existence and number. Because of this, we should add the inflection points themselves as parameters of our sensitivity investigation. From here we can either consider these $n$ inflection values as extra parameters in the generalised bifurcation space (already consisting of the values $X = x^*$, $hX = \tilde{h}(x^*)$ and $DH = \tilde{h}'(x^*)$) in which we will conduct our investigation, or we can simply consider our overall projected $\varepsilon_Q$-neighbourhood in the original $(X, hX, DH)$-space as the union of the projected neighbourhoods in $(X, hX, DH)$-space over all possible sets of inflection points. The latter approach has the advantage that it is more computationally efficient and much easier to visualise, but does carry the risk that some information will be lost when it comes to computing the volume of regions in the neighbourhood, as is necessary if we wish to *quantify* the sensitivity of a system.

In order to demonstrate how to use the result of Theorem 4.1 to investigate structural sensitivity in biological models, we shall next consider three different complex models from the literature, and explore the structural sensitivity of these models.

## 4.4 Examples of structural sensitivity analysis

We now demonstrate the approach outlined in sections 3.2 and 3.3 by implementing such a test on several mathematical models taken from the literature.

### 4.4.1 Age-structured Predator-prey model in a chemostat with nutrient

We consider the four dimensional system modelling predator-prey-nutrient dynamics in a chemostat from (Fussmann et al., 2000):

$$\frac{\mathrm{d}N}{\mathrm{d}t} = \delta(N_i - N) - \tilde{F}_c(N)C, \tag{4.4}$$

$$\frac{\mathrm{d}C}{\mathrm{d}t} = \tilde{F}_c(N)C - \frac{F_B(C)B}{\varepsilon} - \delta C, \tag{4.5}$$

$$\frac{\mathrm{d}R}{\mathrm{d}t} = F_B(C)R - (\delta + m + \lambda)R, \tag{4.6}$$

$$\frac{\mathrm{d}B}{\mathrm{d}t} = F_B(C)R - (\delta + m)B. \tag{4.7}$$

Here $N$ is the nutrient concentration, $C$ is the concentration of a unicellular green algae, $R$ is the concentration of planktonic rotifer that are still of reproductive age, and $B$ is the total concentration of the planktonic rotifer. $\tilde{F}_C(N)$ and $F_B(C)$ are the functional responses of the algae and the rotifer, respectively, which Fussmann et al. consider to be Monod functions $\tilde{F}_C(N) \coloneqq \frac{b_C N}{K_C + N}$ and $F_B(C) \coloneqq \frac{b_B C}{K_b + C}$. See Fussmann et al. (2000) for full explanation of the model parameters and discussion of the model's dynamical behaviour. The key bifurcation parameter in the system is the dilution rate $\delta$.

We shall check for structural sensitivity in this system with respect to the functional response of the algae, $\tilde{F}_c(N)$, and we assume that the parameterisation of the functional response of the rotifer is fixed as $F_B(C) \coloneqq \frac{b_B C}{K_b + C}$. We require that $\tilde{F}_c$ be a function satisfying the following conditions:

$$\tilde{F}_c(0) = 0, \tag{4.8}$$

$$\tilde{F}_C'(N) > 0 \quad \forall\, N \in [0, N_{\max}], \tag{4.9}$$

$$A < \tilde{F}_C''(N) < 0 \quad \forall\, N \in [0, N_{\max}]. \tag{4.10}$$

That is, $\tilde{F}_c$ is a functional response of Holling type II: an increasing, saturating function passing through the origin. We take the base function of $\tilde{F}_c$ as $F_C(N) \coloneqq \frac{b_C N}{K_C + N}$, with the

same parameters, $b_C = 3.3$ and $K_C = 4.3$, as are used in Chapter 3, and consider only functions that are within an absolute distance $\varepsilon$ of this base function $F_C$, that is

$$\left|\tilde{F}_c(N) - F_C(N)\right| < \varepsilon \quad \forall\, N \in [0, N_{\max}].$$

This can also be expressed as $\tilde{F}_c(N) < F_c^{\varepsilon+}(N) = F_C(N) + \varepsilon$, and $\tilde{F}_c(N) < F_c^{\varepsilon-}(N) = F_C(N) - \varepsilon$.

Now finding an equilibrium of system (4.4)-(4.7) is an underdetermined problem, since it entails solving four isocline equations for five unknowns, $N^*$, $C^*$, $R^*$, $B^*$ and $FN$ - where $FN = \tilde{F}_c(N^*)$—so we let $N^*$ follow $\Xi$, an unspecified parameter of our investigation. Given a choice of $\Xi$, we can then substitute in $N^* = \Xi$ into (4.4)-(4.7), and then determine the values $C^*$, $R^*$, $B^*$ and $FN$. Similarly, when performing a linear stability analysis, the unknown value $\tilde{F}_C'(N^*)$ will feature in the Jacobian matrix of (4.4)-(4.7) at $(N^*, C^*, R^*, B^*)$, so we let this value follow the parameter $DF$. Once a value of $DF$ is chosen, we can set $\tilde{F}_C'(N^*) = DF$, and conditions for the eigenvalues of the Jacobian to have negative real parts can be derived analytically to determine whether $(N^*, C^*, R^*, B^*)$ is a stable equilibrium or not.

Now we need to derive the necessary and sufficient conditions for there to exist a function $\tilde{F}_c: [0, N_{\max}] \to \mathbb{R}$ satisfying conditions (4.8)-(4.10) such that $N^* = \Xi$ and $\tilde{F}_C'(N^*) = DF$ hold for a given point $(\Xi, dF)$. These specific conditions were previously derived and proved in Chapter 3, but can also be derived from Theorem 4.1 in the case that there is no inflection point: since a Holling-type II function is concave down across the whole domain, the proof remains valid.

In this case, the upper and lower bounds of $\tilde{F}_c$ are as follows:

$$\mathrm{Upp}_{\Xi,FN,DF}(N) = FN + DF(N - \Xi),$$

$$\mathrm{Low}_{\Xi,FN,DF}(N) = FN + DF(N - \Xi) + \frac{1}{2}A(N - \Xi)^2,$$

and by Theorem 4.1 the conditions for the existence of such a function $\tilde{F}_c$ are:

$$FN + DF(N - \Xi) > F_c^{\varepsilon-}(N) \quad \forall\, N \in [0, N_{\max}],$$

$$FN + DF(N - \Xi) + \frac{1}{2}A(N - \Xi)^2 < F_c^{\varepsilon+}(N) \quad \forall\, N \in [0, N_{\max}],$$

$$FN - \Xi \cdot DF > 0 \text{ and } FN - \Xi \cdot DF + \frac{1}{2}A \cdot \Xi^2 < 0,$$

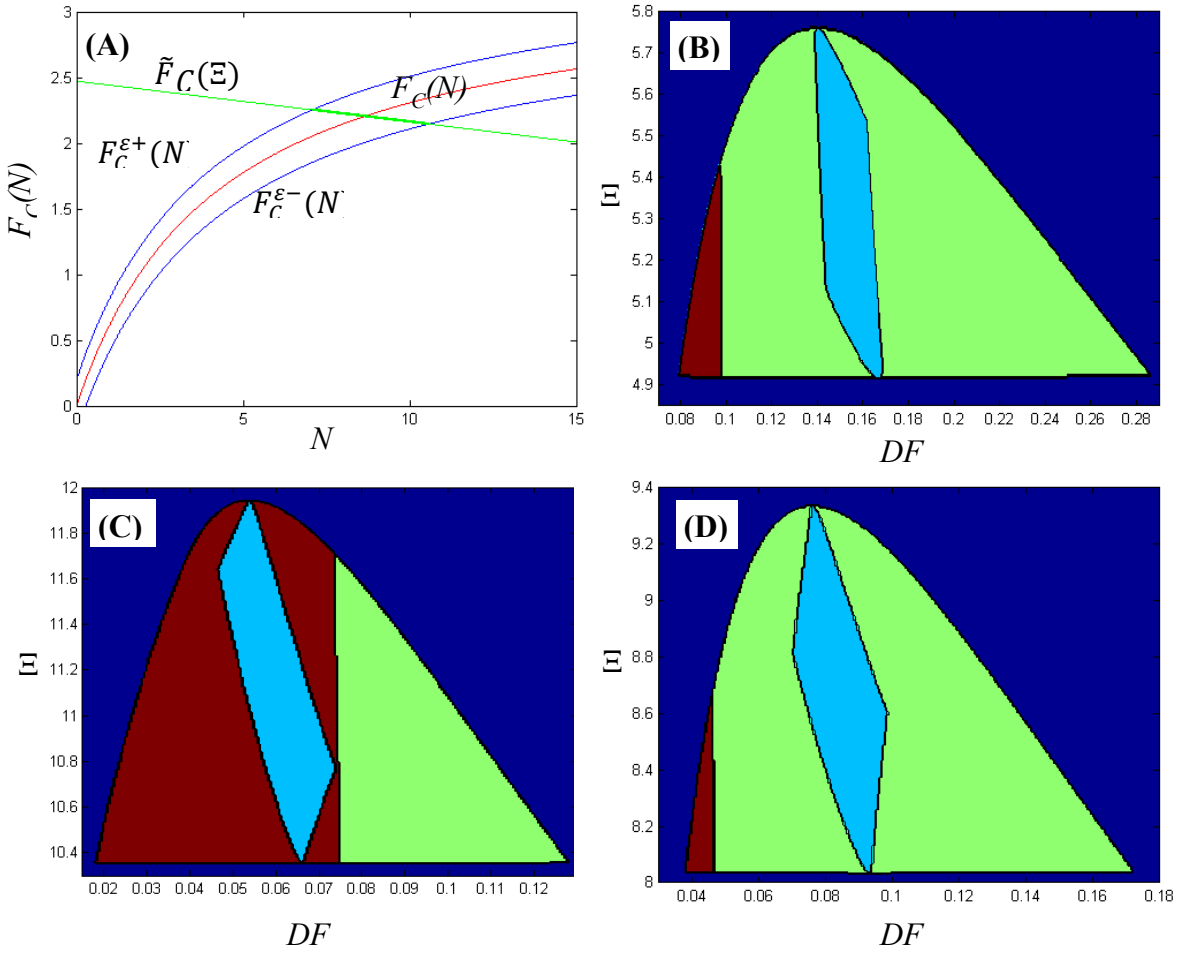


Figure 4.2: Structural sensitivity investigation of the nutrient-algae-reproducing rotifer-total rotifer system (4.4)-(4.7). (A) The base function $F_C(N) := \frac{b_C N}{K_C + N}$ and its $\varepsilon$-neighbourhood. $F_C$ is given by the red curve, while the boundaries of its $\varepsilon$-neighbourhood are given by the blue curves. The green curve is derived from isocline analysis of the system, and gives us the equilibrium value $\tilde{F}_C(\mathrm{N}^*)$, as a function of the equilibrium parameter $\Xi$. (B)-(D) Stability portraits of the $\varepsilon_Q$-neighbourhood of the base functional response of the algae, $F_C$, divided into regions of stability and instability of the interior equilibrium point, for three different values of the chemostat dilution rate, $\delta$. The green regions consist of points that correspond to a system with stable equilibrium, and the red regions of points which correspond to a system with unstable equilibrium. Dark blue indicates that there is no valid model function in the $\varepsilon_Q$-neighbourhood of $F_C$ such that the system with this function has equilibrium values $N^* = \Xi$ and $\tilde{F}_C'(N^*) = DF$. Azure regions indicate that the point $(\Xi, DF)$ can be covered by keeping the formulation of the base function and varying its parameters. The parameters are $N_i = 80$; $K_B = 15$; $b_B = 1.95$; $\epsilon = 0.25$; $m = 0.055$; $\lambda = 0.4$. The dilution rate $\delta$ takes the values: (B) $\delta = 0.175$. (C) $\delta = 0.5$. (D) $\delta = 0.75$.

We now proceed by scanning the $(\Xi, DF)$-space, and using these conditions to check each point for the existence of a corresponding function satisfying (4.8)-(4.10), as well as using the Jacobian to check whether or not the interior equilibrium in the system with such a function would be stable or unstable. The results of such investigations are shown in Fig. 4.2B-D constructed for three values of the chemostat dilution rate, $\delta$. In Fig. 4.2A we show the base function, the lower and upper bounds as well as the curve $\tilde{F}_c(\Xi)$ showing the dependence of $\tilde{F}_c(N^*)$ on the parameter $\Xi$—since this curve has negative derivative, it is clear that we can only have a single equilibrium value $N^*$ for a given functional response, since all functional responses have positive derivative. The parameters used are identical to those found in Fussmann et al. (2001) except for the maximum per-capita algae-consumption rate of the rotifer, $b_B$, which we change from $b_B = 2.25$ to $b_B = 1.95$—since with the original parameters there is little structural sensitivity present for us to discuss. We note, however, that the new parameters are still well within the values reported in the literature (e.g. Halbach and Halbach-Keup, 1974). With the new parameter set, we see that when $\delta = 0.175$ the system exhibits very little structural sensitivity (Fig. 4.2B), as almost the entire domain is covered by the region of stability, but we see that for intermediate values of $\delta$, shown in Figure 4.2C for $\delta = 0.5$, there are significant regions of both stability and instability in the $(\Xi, DF)$ domain.

In this figure, the fact that the azure region is located entirely within the domain of instability indicates that fixing $\tilde{F}_c = \frac{b_C N}{K_C + N}$ and varying the parameters $b_C$ and $K_C$ will give the misleading impression that the interior equilibrium is unstable for all possible functional responses. In figure 4.2D we see the domain with $\delta = 0.7$ is once again dominated by the stable region. Overall, the formulation of the functional response fixed as a Monod function, a variation-of-parameters investigation will uncover a pair of forward and backwards supercritical Hopf bifurcations with respect to the parameter $\delta$, but the continued presence of a green domain indicates that there may well be a different functional response parameterisation which is just as valid as the original function with regards to qualitative properties and data fitting, but for which the interior equilibrium is stable for all values of $\delta$. Thus for some functional responses, variation in the dilution rates will not result in a Hopf bifurcation, which was originally suggested in Fussmann et al., 2000.

### 4.4.2 Nutrient-Phytoplankton-Zooplankton Model with Detritus

We consider the nutrient-phytoplankton-zooplankton-detritus model given by

$$\frac{\mathrm{d}N}{\mathrm{d}t} = -\frac{N}{(e+N)}\frac{a}{(b+cP)}P + \beta\tilde{h}(P)\,Z + \gamma dZ^2 + \varphi D + k(N_0 - N), \tag{4.11}$$

$$\frac{\mathrm{d}P}{\mathrm{d}t} = \frac{N}{(e+N)}\frac{a}{(b+cP)}P - rP - \tilde{h}(P)Z - (s+k)P, \tag{4.12}$$

$$\frac{\mathrm{d}Z}{\mathrm{d}t} = \alpha\tilde{h}(P)Z - dZ^2, \tag{4.13}$$

$$\frac{\mathrm{d}D}{\mathrm{d}t} = rP + (1-\alpha-\beta)\tilde{h}(P)Z - (\varphi+\psi+k)D, \tag{4.14}$$

where the state variables *N*, *P*, *Z* and *D* represent the concentrations of nutrient, phytoplankton, zooplankton and detritus in the well-mixed upper layer of the ocean respectively, as first proposed in (Edwards, 2001), where a detailed description of the model and its parameters can be found. In particular, we are interested in the function $\tilde{h}(P)$, which is the functional response of the zooplankton—i.e. the per-capita rate at which zooplankton consume phytoplankton as a function of phytoplankton density. We take the precise formulation of this function to be unknown, but require it to be a $C^1$-function having the following properties (based on the classical definition of Holling type III in the literature, see Gentlemen et al., 2003):

$$\tilde{h}(0) = 0\,, \tag{4.15}$$

$$\tilde{h}'(P) > 0 \;\; \forall\, P \in [0, P_{\max}], \tag{4.16}$$

$$\exists P_0 \in (0, P_{\max}) \text{ such that } 0 < \tilde{h}''(P) < A_1 \;\; \forall\, P \in [0, P_0], \tag{4.17}$$

$$\text{and } A_2 < \tilde{h}''(P) < 0 \;\; \forall\, P \in [P_0, P_{\max}]. \tag{4.18}$$

That is, $\tilde{h}$ is an increasing sigmoid function over $[0, x_{\max}]$ that passes through the origin; $A_1$ and $A_2$ are parameters characterizing the values of the second derivative (these can be estimated based on the base function, but several values should be considered). We further require that $\tilde{h}$ be an absolute distance of less than $\varepsilon$ from the base function $h(P)$, which we take to be the functional response used in (Edwards, 2001): $h(P) = \frac{\lambda P^2}{\mu^2 + P^2}$, with $\lambda = 0.6$ and $\mu = 0.035$. That is

$$\left\|\tilde{h}(P) - h(P)\right\| < \varepsilon \quad \forall\, P \in [0, P_{\max}].$$

Now, finding the equilibrium densities in (4.11)-(4.14) requires us to solve a system of four equations for five unknown variables, so we allow the equilibrium density of the prey, $P^*$, to follow $P^* = \Phi$, where $\Phi$ is a parameter of the investigation, and then

we can solve the four equations for $N^*$, $Z^*$, $D^*$ and $hP$—where $hP = \tilde{h}(P^*)$ denotes the value of the functional response at the equilibrium—in the usual way. Figure 4.3A shows the base functional response in red and the upper and lower limits—in blue—of any viable function $\tilde{h}$, together with the curve showing the dependence of $hP$ on the parameter $\Phi$ (n.b. this should not be confused with the dependence of $\tilde{h}(P)$ on $P$, which remains unspecified throughout).

In order to find the stability of the equilibrium point $(N^*, P^*, Z^*, D^*)$, we can carry out the usual linear stability analysis by calculating the Jacobian from (4.11)-(4.14) at $(N^*, P^*, Z^*, D^*)$ and checking the sign of the real parts of its eigenvalues, but the Jacobian depends on the value $\tilde{h}'(P^*)$, which is unknown, and so we allow this value to follow $\tilde{h}'(P^*) = DH$, where $DH$ is another investigation parameter. Further, we note that the inflection point of our sigmoid function $\tilde{h}$ is unknown, and so needs to be treated as a further parameter of our investigation, $P_0$, as was discussed in the concluding paragraph of Section 4.3. In this instance, we shall consider a wide range of values of $P_0$ and superimpose the resulting projected $\varepsilon_Q$-neighbourhoods to obtain the total $\varepsilon_Q$-neighbourhood.

It is easy to obtain the necessary and sufficient conditions for there to exist a sigmoid function in the $\varepsilon_Q$-neighbourhood corresponding to the given values $(\Phi, DH)$ by applying Theorem 4.1. Following the process outlined in Section 4.3, for given values $\Phi$, $\Xi$ and $P_0$, we can compute the upper and lower bounds of our sigmoid function as follows.

If $\Phi \geq P_0$,

$$Upp(P) \coloneqq \begin{cases} hP + DH \cdot (P - \Phi) + \dfrac{A_1}{2}(P - P_0)^2 : P \in [0, P_0] \\ hP + DH \cdot (P - \Phi) \qquad\qquad : P \in [P_0, P_{\max}] \end{cases},$$

and

$$Low(P) \coloneqq \begin{cases} hP + DH \cdot (P - \Phi) + A_2\left(\dfrac{(P - \Phi)^2}{2} + (P_0 - \Phi)(P - P_0)\right) : P \in [0, P_0] \\ hP + DH \cdot (P - \Phi) + \dfrac{A_2}{2}(P - \Phi)^2 \qquad\qquad : P \in [P_0, P_{\max}] \end{cases}.$$

If $\Phi < P_0$,

$$Upp(P) \coloneqq \begin{cases} hP + DH \cdot (P - \Phi) + \dfrac{A_1}{2}(P - \Phi)^2 \qquad\qquad : P \in [0, P_0] \\ hP + DH \cdot (P - \Phi) + A_1(P_0 - \Phi)\left(P - \dfrac{1}{2}(P_0 + \Phi)\right) : P \in [P_0, P_{\max}] \end{cases},$$

and

$$Low(x) \coloneqq \begin{cases} hP + DH \cdot (P - \Phi) & : P \in [0, P_0] \\ hP + DH \cdot (P - \Phi) + \dfrac{A_2}{2}(P - P_0)^2 & : P \in [P_0, P_{\max}] \end{cases}.$$

From Theorem 4.1, we can obtain the necessary and sufficient conditions for values $\Phi$ and $dH$ to correspond to a valid function $\tilde{h}$ to be as follows:

If $\Phi \geq P_0$

$hP + DH \cdot (P - \Phi) + \dfrac{A_1}{2}(P - P_0)^2 > h_{\varepsilon-}(P) \ \forall P \in [0, P_0]$;

$hP + DH \cdot (P - \Phi) > h_{\varepsilon-}(P) \ \forall P \in [P_0, P_{\max}]$;

$hP + DH \cdot (P - \Phi) + A_2\left(\frac{1}{2}(P - \Phi)^2 + (P_0 - \Phi)(P - P_0)\right) < h_{\varepsilon+}(P) \ \forall P \in [0, P_0]$;

$hP + DH \cdot (P - \Phi) + \frac{A_2}{2}(P - \Phi)^2 < h_{\varepsilon+}(P) \ \forall P \in [P_0, P_{\max}]$;

$hP - DH \cdot \Phi + \frac{A_1}{2}{P_0}^2 > 0$,

and $hP - DH \cdot \Phi + A_2\left(\frac{1}{2}\Phi^2 - P_0 \cdot \left(P_0 - \tilde{P}\right)\right) < 0$.

If $\Phi < P_0$

$hP + DH \cdot (P - \Phi) + \dfrac{A_1}{2}(P - \Phi)^2 > h_{\varepsilon-}(P) \ \forall P \in [0, P_0]$;

$hP + DH \cdot (P - \Phi) + A_1(P_0 - \Phi)\left(P - \dfrac{1}{2}(P_0 + \Phi)\right) > h_{\varepsilon-}(P) \ \forall P \in [P_0, P_{\max}]$;

$hP + DH \cdot (P - \Phi) < h_{\varepsilon+}(P) \ \forall P \in [0, P_0]$;

$hP + DH \cdot (P - \Phi) + \dfrac{A_2}{2}(P - P_0)^2 < h_{\varepsilon+}(P) \ \forall P \in [P_0, P_{\max}]$;

$hP - DH \cdot \Phi + \dfrac{A_1}{2}\Phi^2 > 0$,

and $hP - DH \cdot \Phi < 0$.

Now we have these conditions, we can cover the ($\Phi$-$DH$) parameter space numerically checking whether each point $(\Phi, DH)$ has a corresponding sigmoid function in the $\varepsilon_Q$-neighbourhood of $h$ with an equilibrium and derivative taking these values. At the same time, if $(\Phi, DH)$ does correspond to such a function, we can numerically check the real parts of the eigenvalues of the Jacobian to determine the stability of the corresponding equilibrium point $(N^*, P^*, Z^*, D^*)$.

Such an investigation gives us portraits as in Fig. 4.3B-D. Here the dark blue regions give us the domain for which there is no function $\tilde{h} \in \varepsilon_Q(h)$ such that the resulting system satisfies $P^* = \Phi$ with $\tilde{h}'(P^*) = DH$. The remaining region—the projection of the $\varepsilon_Q$-neighbourhood of $h$ onto ($\Phi$-$DH$) space—is divided into areas in which the equilibrium is stable (green) and unstable (red). The overlying azure region is the range across which a function $\tilde{h}$ of the same form as the base function corresponds to the point $(\Phi, DH)$—i.e. this is the region which can be covered by fixing the parameterization as $\tilde{h}(P) = \frac{\lambda P^2}{\mu^2 + P^2}$, and simply varying the parameters $\lambda$ and $\mu$.

The figure shows us the results of a structural sensitivity analysis for the system with three different choices of the parameter $d$—the rate of predation on zooplankton by higher trophic levels. For $d = 1.0$ (Fig. 4.3B), we see that the azure region entirely overlies the green stability region, indicating that the conventional parameter variation approach used in (Edwards, 2001) would indicate no structural sensitivity for this system. However, our analysis reveals that there is still a significant region of instability in the system, which would be missed by the conventional approach. As $d$ is increased to 1.7, the azure region moves to straddle the bifurcation line (Fig. 4.3C), but when it is increased further to 2.1 the azure region moves back towards the stability domain. In the system with fixed base function $h(P) = \frac{\lambda P^2}{\mu^2 + P^2}$, this behaviour is shown to manifest itself as a pair of forward and backward Hopf bifurcations (Edwards, 2001), but we can see from Fig. 4.3D that when all possible parameterisations are taken into consideration, in fact the ratio between the areas of the stable and unstable regions remains relatively unchanged, which was somewhat overlooked in the initial publication by (Edwards, 2001). However, we note that since the azure region straddles the bifurcation line in this instance, a full variation of the parameters $\lambda$ and $\mu$ would also reveal this possibility to an extent.

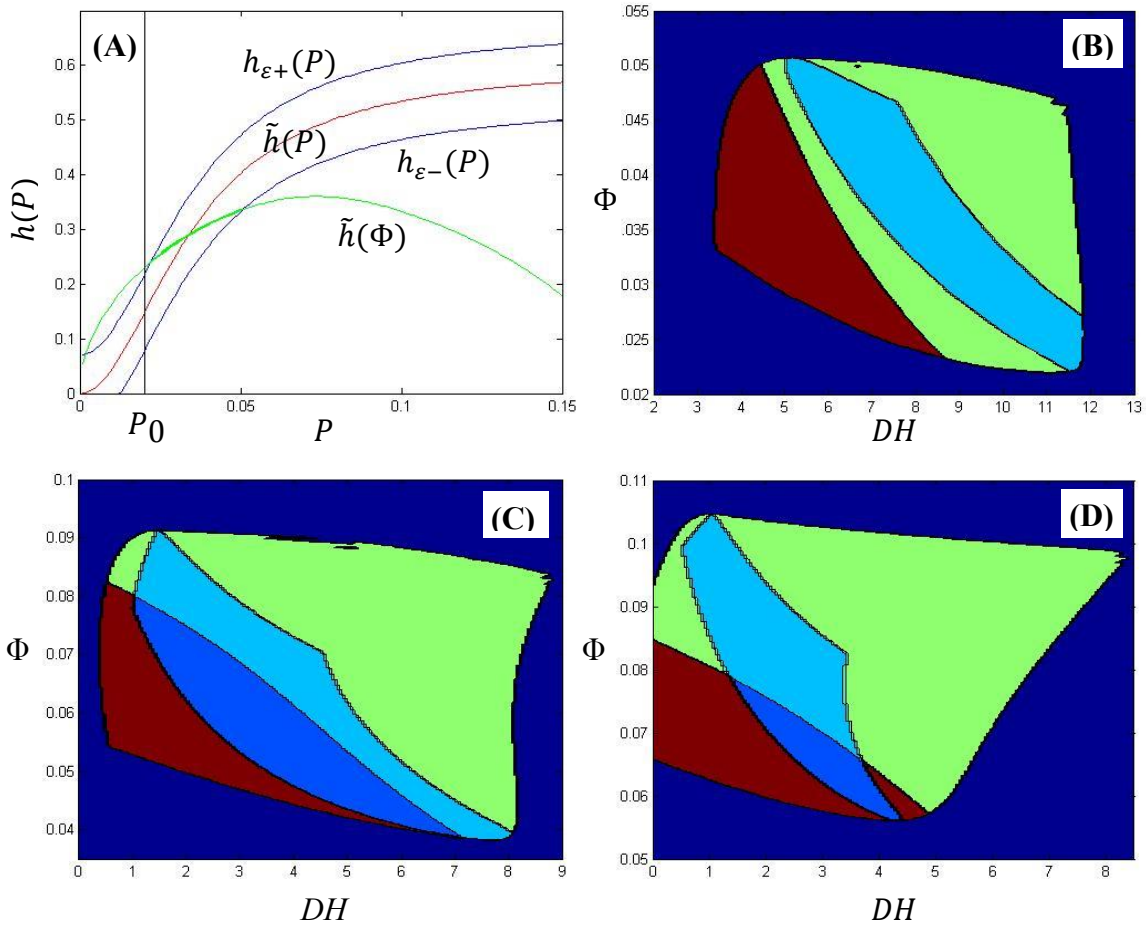


Figure 4.3: Structural sensitivity investigation of the nutrient-phytoplankton-zooplankton-detritus system (4.11)-(4.14). (A) The base function $h(P) = \frac{\lambda P^2}{\mu^2 + P^2}$ and its $\varepsilon$-neighbourhood. $h$ is given by the red curve, while the boundaries of its $\varepsilon$-neighbourhood are given by the blue curves. The green curve is derived from isocline analysis of the system, and gives us the equilibrium value $\tilde{h}(P^*)$, as a function of the equilibrium parameter $\Phi$. (B)-(D) Stability portraits of the $\varepsilon_Q$-neighbourhood of the base functional response, $h$, divided into regions of stability and instability of a specific equilibrium point, for three different values of the zooplankton predation rate, $d$. The green regions consist of points that correspond to a system with stable equilibrium, and the red regions of points which correspond to a system with unstable equilibrium. Dark blue indicates that there is no valid model function in the $\varepsilon_Q$-neighbourhood of $h$ such that the system with this function has equilibrium values $P^* = \Phi$ and $h'(P^*) = DH$. Azure regions indicate that the point $(\Phi, DH)$ can be covered by keeping the formulation of the base function and varying its parameters. The parameters are $e = 0.03$; $a = 0.2$; $b = 0.2$; $c = 0.4$; $\beta = 0.33$; $\gamma = 0.5$; $\phi = 0.1$; $k = 0.05$; $r = 0.15$; $s = 0.04$; $\alpha = 0.25$; $\psi = 0.08$ and $N_0 = 0.6$. The zooplankton predation rate in each figure is: (B) $d = 1.0$. (C) $d = 1.7$. (D) $d = 2.1$.

### 4.4.3 Tri-trophic food chain model with time delay

As an example of how the structural sensitivity analysis framework can work on delay-differential equation models, we consider the following system

$$\frac{\mathrm{d}x_1(t)}{\mathrm{d}t} = x_1(t)(1 - x_1(t)) - ax_1(t)x_2(t), \tag{4.19}$$

$$\frac{\mathrm{d}x_2(t)}{\mathrm{d}t} = -bx_2(t) + cx_1(t-\tau)x_2(t) - \tilde{h}\big(x_2(t)\big)x_3(t) - jx_2(t)^2, \tag{4.20}$$

$$\frac{\mathrm{d}x_3(t)}{\mathrm{d}t} = -fx_3(t) + k\tilde{h}\big(x_2(t-\tau)\big)x_3(t) - hx_3(t)^2, \tag{4.21}$$

representing a tri-trophic food chain model. Here $x_i$ is the density of the species in the trophic level *i*. A time delay takes place when food consumed by a predator is converted into its biomass, and, as in most time-delay systems, the length of this delay is a crucial bifurcation parameter. For details see (Kar, Ghorai and Batabyal, 2012). Notably, we allow the functional response of species $x_3$, $\tilde{h}$, to be an unspecified Holling type II function (i.e., it satisfies conditions (4.8)-(4.10) from Section 4.4.1), within a distance $\varepsilon$ of the base function given by the Monod parameterisation $h(x_2) \coloneqq \frac{dx_2}{x_2+e}$. We shall check for structural sensitivity in terms of the stability of a nontrivial equilibrium with respect to variation of this functional response. Finding the equilibria of system (4.19)-(4.21) is an underdetermined problem, as we need to solve three equations with four unknowns: $x_1^*$, $x_2^*, x_3^*$ and $hX$, where $hX = \tilde{h}(x_2^*)$, so we let $x_2^*$ follow $\Xi$, a parameter of our investigation. Given any choice of $\Xi$, we can substitute $x_2^* = \Xi$ into (4.19)-( 4.21) and the values $x_1^*$ and $x_3^*$ will be uniquely determined, while possible values $hX$ will be given by the positive roots of a quadratic equation (in all cases considered here, there is only one such positive root). Similarly, since $\tilde{h}'(x_2^*)$ is unspecified, we let it follow the parameter $DH$ so that we can carry out linear stability analysis. Once we have the equilibrium point $(x_1^*, x_2^*, x_3^*)$ and the values $\tilde{h}(x_2^*)$ and $\tilde{h}'(x_2^*)$, we can use the standard approach for evaluating the stability of an equilibrium point of a delay-differential equation. Details of this stability analysis are provided in Appendix B. Finally, we note that, by Theorem 3.1, the necessary and sufficient conditions for there to exist a function $\tilde{h}\colon [0, x_{2_{\max}}] \to \mathbb{R}$ satisfying conditions (4.8)-(4.10) such that $x_2^* = \Xi$, and $\tilde{h}'(x_2^*) = DH$ are the same as the conditions found in Section 4.4.1:

$$hX + DH(x_2 - \Xi) > h(x_2) - \varepsilon \quad \forall\, x_2 \in [0, x_{2_{\max}}],$$

$$hX + DH(x_2 - \Xi) + \frac{1}{2}A(x_2 - \Xi)^2 < h(x_2) + \varepsilon \;\; \forall\, x_2 \in \left[0, x_{2\max}\right],$$

$$hX - \Xi \cdot DH > 0 \text{ and } \; hX - \Xi \cdot DH + \frac{1}{2}A \cdot \Xi^2 < 0.$$

We can now carry out our approach by scanning the valid range of ($\Xi$-$DH$) space, using the above criteria to determine whether each point corresponds to a valid function $\tilde{h}$, and then finding the stability of the positive interior equilibrium for these values. The results of this analysis for several values of the time delay $\tau$ are shown in Fig. 4.4B-D. We see that, when $\tau$ is around 0.5, almost the entire domain exhibits a stable interior equilibrium, but as $\tau$ is increased the region of instability begins to grow until it occupies most of the domain at around $\tau = 1$. This is consistent with the findings of Kar, Ghorai and Batabyal (2012) who obtained a critical value of $\tau_0 \approx 0.9$ for the system with the Monod functional response as a base function.

One can see that in the case of a model with delay, the sensitivity analysis can be completed in a similar straightforward way as for systems without delay. Moreover, two things are of note with respect to the structural sensitivity of the particular model. Firstly, although the system clearly exhibits structural sensitivity for values of $\tau$ around 0.8, the range of values of $\tau$ for which we have structural sensitivity, i.e. between 0.5 and 1.15, is quite small. Secondly, in all cases where we have structural sensitivity, the region of the $\varepsilon_Q$-neighbourhood which can be explored by varying the parameters of the base function actually crosses the bifurcation line, and therefore any structural sensitivity in the system can be detected by a simple variation of parameters approach. This situation is therefore more favourable than the two examples previously discussed: it shows us that we don't always have extensive structural sensitivity around a local bifurcation point, and that it can be detected by parameter-based analysis in some cases, although we stress that this should not be taken for granted.

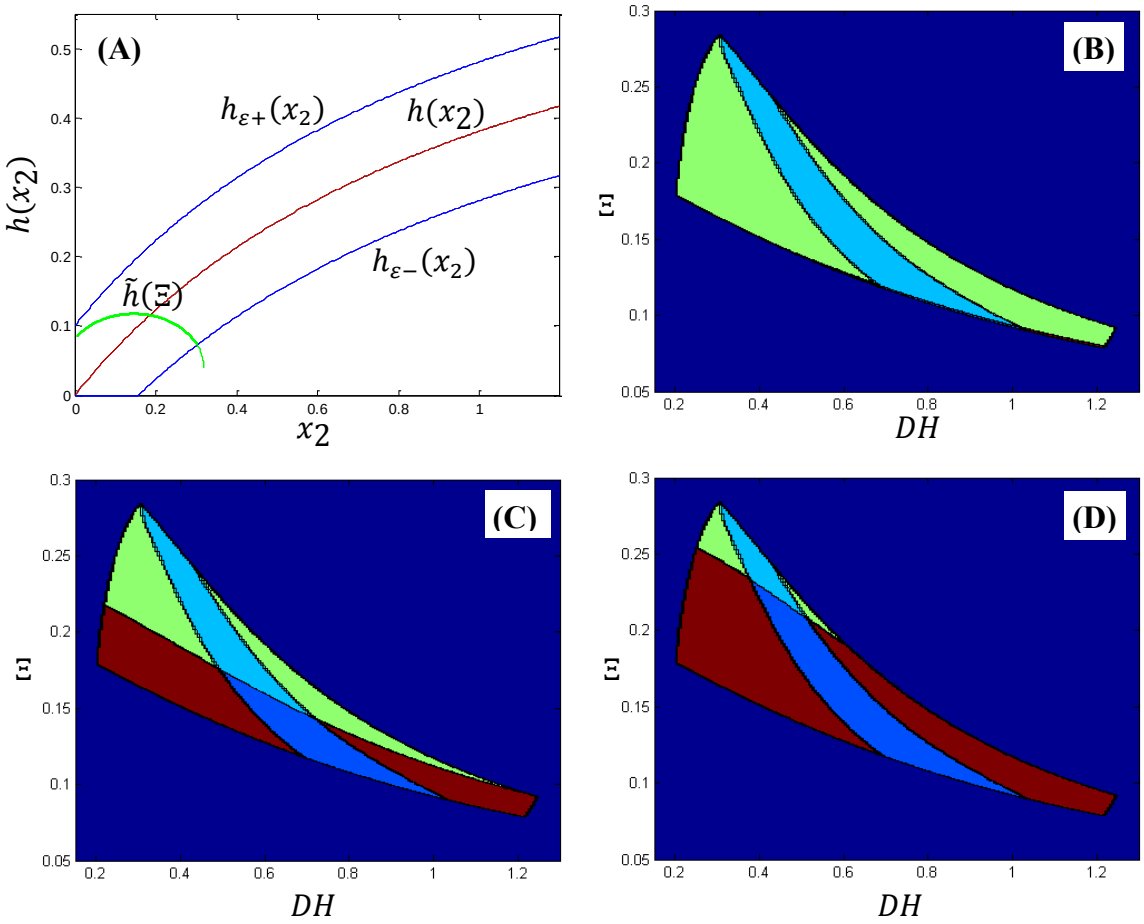


Figure 4.4: Structural sensitivity investigation of the tri-trophic model with delay given by (4.19)-(4.21). (A) The base function $h(x_2) = \frac{dx_2}{x_2+e}$ and its $\varepsilon$-neighbourhood. $h$ is given by the red curve, while the boundaries of its $\varepsilon$-neighbourhood are given by the blue curves. The green curve is derived from isocline analysis of the system, and gives us the equilibrium value $\tilde{h}(x_2^*)$, as a function of the equilibrium parameter $\Xi$. (B)-(D) Stability portraits of the $\varepsilon_Q$-neighbourhood of the base functional response, $h$, divided into regions of stability and instability of a specific equilibrium point, for three different values of the time delay, $\tau$. The green regions consist of points that correspond to a system with stable equilibrium, and the red regions of points which correspond to a system with unstable equilibrium. Dark blue indicates that there is no valid model function in the $\varepsilon_Q$-neighbourhood of $h$ such that the system with this function has equilibrium values ${x_2}^* = \Xi$ and $h'({x_2}^*) = DH$. Azure regions indicate that the point $(\Xi, DH)$ can be covered by keeping the formulation of the base function and varying its parameters. The parameters are $a = 1.5$; $b = 1.5$; $c = 3$; $f = 0.2$; $g = 2$; $j = 0.1$; $m = 0.6$ and $d = 0.8$; $e = 1.1$. The time-delay $\tau$ in each figure is: (B) $\tau = 0.5$. (C) $\tau = 0.8$. (D) $\tau = 1.0$.

## 4.5 Discussion and conclusions

In this chapter, we have extended the results of the previous chapter by providing and proving Theorem 4.1, which gives us such a projected neighbourhood for a function with $n$ inflection points—a common class of functions in biological modelling—when the concept of the $d_Q$-distance is used to defined the functional neighbourhood. This theorem allows us to obtain a projection from the $\varepsilon_Q$-neighbourhood of model functions into the generalised bifurcation space for a large class of highly biologically relevant functions, and therefore greatly aids the application of the framework outlined in Chapter 3. Further, we have considered several quite complicated models and used Theorem 4.1 to show that sensitivity takes place in these models within a large range of parameters, which can't always be observed using the conventional parameter-based analysis.

The widespread existence of structural sensitivity may require revisiting the entire concept of bifurcation analysis of biological models. Indeed, in such structurally sensitive systems, even in the case of variation of a well-defined model parameter (such as the dilution rate in the chemostat model in section 4.4.1), there is no particular value of this parameter for which a bifurcation occurs: the use of different functions will result in different bifurcation parameters. In this case we don't have any *concrete* bifurcations, and can only describe the model behaviour in terms of the probability of having a bifurcation. This idea can be illustrated using the stability diagrams in Figs 4.2-4.4: for instance, we can consider that a Hopf bifurcation in models occurs when the area corresponding to instability/stability exceeds a certain limit. The occurrence of a bifurcation may be described in this way based on the degree of sensitivity (Definition 3.1). Thus, in the chemostat model (4.4)-(4.7) proposed in (Fussmann et al., 2000), as opposed to the crossing of a Hopf bifurcation referenced in the title of the cited paper, it would be more correct to say that variation of the dilution rate $\delta$ shifts the system into a region where the probability of having oscillations becomes high compared to other ranges of $\delta$. In the next chapter, we expand upon this idea, and present a complete 'probabilistic bifurcation analysis' of a predator-prey model with ratio-dependent functional response in the case that the prey growth term is unspecified. The overall idea is to use the methods developed thus far to determine the probability that the Hopf bifurcation in a system will be supercritical or subcritical.

# Chapter 5

# Probabilistic bifurcation analysis of partially specified models

*This chapter is based on the paper (Adamson and Morozov, 2014b)*

## 5.1 Introduction

In this chapter we shall make a first step towards constructing a bifurcation portrait of a biological ODE-based model in the case where the constituent functions are generally uncertain but belong to a known *class of functions*, (Logistic growth type functions, or Holling type II functions for example). In this case, the given class of functions doesn't necessarily specify the bifurcation structure of the model completely: picking two different functions belonging to this class may result into two qualitatively different bifurcation portraits. Here we propose a method for determining the probability of a Hopf bifurcation in such a partially specified model being supercritical or subcritical. As an illustrative example we shall investigate the criticality of the Hopf bifurcation in a ratio-dependent predator-prey model with an unspecified prey growth function, but the same technique can be applied to a wide range of biological models with unspecified constituent functions.

Our illustrative example here is justified by the importance of predator-prey models with a ratio-dependent predator functional response, which have recently received a significant amount of attention. In such models, consumption of prey is a function of the ratio between the predator and the prey density, which is believed to be more ecologically relevant than the 'classical' prey dependent response in many cases (Arditi and Ginzburg, 1989; Arditi, Ginzburg and Akçakaya, 1991; Reeve, 1997; Bishop et al., 2006). There has been a considerable amount of research into bifurcation analysis of ratio-dependent predator-prey models (Kuang and Beretta, 1998; Berezovskaya et al., 2001; Hsu et al., 2001; Xiao and Ruan, 2001; Li and Kuang, 2007; Haque, 2009; Sen et al., 2012 as well as many other publications). In particular, it has been rigorously proved

that the stability loss in the case of the logistic growth function always takes place via a supercritical Hopf bifurcation with the appearance of a stable limit cycle, which signifies a non-catastrophic regime shift for the ecosystem. On the contrary, in the case where the prey growth rate is subject to an Allee effect (i.e. it increases at low population densities), it has been shown that the Hopf bifurcation in this system is actually subcritical (Sen et al., 2012), in which case the loss of stability of the coexistence equilibrium results in an eventual population collapse. However, all the above results were found for a *fixed* parameterisation of the growth term: it is not clear whether or not they are sensitive to the choice of this parameterisation.

Using the methods of sensitivity analysis outlined in the previous two chapters, we firstly show that all the previous theoretical results in the literature on the behaviour of ratio-dependent predator-prey models lack generality. In particular, we show that for a slightly different parameterization of the growth function—which we call 'generalized logistic growth'—the Hopf bifurcation can be subcritical, whereas for some different parameterization of an Allee effect, the Hopf bifurcation can be supercritical. Further we consider an $\varepsilon_Q$-neighbourhood—a general class of functions which contains an uncountable set of parametric families—of prey growth functions of logistic type, and for the given class of functions we determine how the probability of having a particular type of Hopf bifurcation in the model depends on $\varepsilon$, the degree of closeness between functions in the class. We show that even for very close prey growth functions there can be a large degree of uncertainty in the bifurcation structure of the model. Finally, we suggest a practical rule for concluding whether or not the uncertainty in the model functions results in uncertainty in the bifurcation portrait of the model, and whether or not it can therefore be analysed using the standard methods of bifurcation analysis.

## 5.2 Model equations

We shall investigate the following ratio-dependent predator-prey model as considered in (Berezovskaya et al., 2001; Sen et al., 2012 and a number of other works). For the sake of simplicity we already consider the dimensionless form of the model:

$$\dot{x} = x\tilde{r}(x) - \nu\frac{xy}{x+y}, \tag{5.1}$$

$$\dot{y} = \mu\frac{xy}{x+y} - \gamma y, \tag{5.2}$$

where $x$ is the prey density, $y$ is the predator density, $\nu$ is the maximal predation rate and $\mu$ is the maximal predator growth rate. The term $\frac{xy}{x+y}$ is the ratio-dependent functional response of the predator (Arditi and Ginzburg, 1989; Arditi, Ginzburg and Akçakaya, 1991; Reeve, 1997), and the unspecified function $\tilde{r}(x)$ is the growth rate of the prey, $\gamma$ is the mortality rate of the predator.

Model (5.1)-(5.2) with the prey growth $\tilde{r}(x)$ given by the classic logistic growth function $r_1(x) = s(1-x)$ has been studied in a large number of papers in almost every possible detail (Freedman and Mathsen, 1993; Jost et al., 1999; Kuang and Beretta, 1998; Berezovskaya at al., 2001; Hsu et al., 2001; Xiao and Ruan, 2001). In particular, it was shown that the system can have a unique interior equilibrium, signifying species coexistence, which can be either stable or unstable depending on parameters. Interestingly, the stability loss of this equilibrium always occurs via a supercritical Hopf bifurcation—that is, a small stable limit cycle emerges as a result (Kuang and Beretta, 1998). It has also been rigorously proved that in the case of a stable interior equilibrium, there can be no limit cycle in the system (Hsu et al., 2001; Xiao and Ruan, 2001; Haque, 2009). The complete set of bifurcation portraits of (5.1)-(5.2) with the logistic growth function $\tilde{r}(x)$ are provided in (Berezovskaya at al., 2001).

In the case where the prey growth is subject to the Allee effect (i.e. the per capita growth rate is an initially increasing function) Sen et al (2012) investigated the properties of the system for the parabolic parameterization of $r_2(x) = s(1-x)(\beta-1)$, which is the standard representation of the Allee effect used in the literature (Lewis and Kareiva, 1993; Owen and Lewis, 2001). It was found that in the case of the Allee effect, the stability loss of the coexistence equilibrium takes place only via a subcritical Hopf bifurcation, in this case the unstable limit cycle surrounding the stable equilibrium disappears and the trajectories will eventually go to the origin, which becomes the global

attractor in this system (Sen et al., 2012). This supercritical Hopf bifurcation is observed both in the case of a weak and a strong Allee effect, i.e., for $-1 < \beta < 1$, but for the case where the per capita growth function is always decreasing and can be considered as a generalized logistic function, i.e. $\beta < -1$, the Hopf bifurcation becomes supercritical again, as in the classical case $r_1(x) = s(1-x)$. This property allows us to hypothesize that well-known results obtained for the classic logistic function should be robust.

Below we shall show that this optimistic hypothesis is actually wrong, and the previously obtained results are in fact rather function-specific: the eventual type of Hopf bifurcation will strongly depend on the choice of function parameterization. In this paper, we mostly focus on the case of the logistic-like growth rate of the prey. However, similar techniques can be implemented in the case of an Allee effect in the prey growth as well (see the Discussion section of this chapter).

In this paper, we shall consider the following general definition of the logistic growth function of prey:

**Definition 5.1**

The prey growth is described by a logistic growth function in the case the per capita growth rate function $\tilde{r}: [0, x_{\max}] \to \mathbb{R}$ satisfies the two following properties:

(i) $\tilde{r}(0) > 0$,

(ii) $\tilde{r}'(x) < 0 \; \forall x \in [0, x_{\max}]$.

This definition is a generalization of the 'classical' logistic growth function based on common sense as well as some prior research (Gilpin and Ayala, 1973; Sibly et al., 2005; Freckleton et al., 2006). Similarly, for the prey growth subjected to the Allee effect, we propose the following definition. Here, for the sake of simplicity we consider that $x_{\max} = 1$.

**Definition 5.2**

The prey growth exhibits an Allee effect in the case where the per capita rate function $\tilde{r}: [0, x_{\max}] \to \mathbb{R}$ satisfies the three following properties. For some value $c \in (0, x_{\max})$ we have

(i) $\tilde{r}'(x) > 0 \; \forall \; x \in [0, c)$,

(ii) $\tilde{r}'(x) < 0 \; \forall \; x \in (c, x_{\max}]$,

(iii) $\tilde{r}(c) > 0$.

The above formulation is based on the ecological notion of the Allee effect (Hopf and Hopf, 1985; Wang and Kot, 2001; Berec et al., 2007).

## 5.3 Defining the type of a Hopf bifurcation for a general growth function

We will be mostly interested in determining the type, or criticality, of Hopf bifurcation depending on the parameterization of a model function. However, similar methods can be potentially used to address some other bifurcations, (see Section 5.5 for a discussion).

In order to investigate the Hopf bifurcation for a general per capita prey growth function $\tilde{r}(x)$, we can use the same approach as outlined in Chapters 3 and 4. The first step of this approach consists of leaving the function in question unspecified, and introducing generalised parameters to represent values taken by the system in the vicinity of a given equilibrium. We can then investigate local system properties in terms of these parameters (see also the related frameworks of generalised modelling, Gross and Feudel, 2006 and critical function analysis, Kisdi et al., 2013). From equations (5.1)-(5.2) we can easily find equations for the densities of species at a non-trivial equilibrium:

$$y^* = \frac{\mu-\gamma}{\gamma} x^*, \tag{5.3}$$

$$\tilde{r}(x^*) = \frac{\nu}{\mu}(\mu - \gamma). \tag{5.4}$$

We shall treat one of the values $x^*$and $y^*$ as an independent parameter of our investigation, since $\tilde{r}(x^*)$ is fixed due to the equilibrium condition (5.4). It is convenient to choose $x^*$ as a parameter since it is the dependent variable of the unknown function $\tilde{r}(x)$.

Here we shall consider the case that $\tilde{r}$ is a logistic function (see Definition 5.1). It is easy to see from equation (5.4) that if $\tilde{r}$ is monotonically decreasing, there is always a unique nontrivial equilibrium in the system. If we allow an Allee effect, the situation becomes somewhat more complicated, and the number of equilibria in the system will depend on how many inflection points the growth function takes.

In order to determine when a Hopf bifurcation takes place in the system (Kuznetsov, 2005), we need to consider the Jacobian matrix of the system. The appropriate computation of the Jacobian matrix at the interior equilibrium gives (after some simplification)

$$A = \begin{pmatrix} x^*\tilde{r}'(x^*) + \dfrac{\nu\gamma(\mu-\gamma)}{\mu^2} & -\nu\dfrac{\gamma^2}{\mu^2} \\ \dfrac{(\mu-\gamma)^2}{\mu} & -\dfrac{\gamma}{\mu}(\mu-\gamma) \end{pmatrix}, \tag{5.5}$$

where $\tilde{r}'(x^*)$ can also be considered as a generalised parameter. The conditions for a Hopf bifurcation are that a pair of complex conjugate eigenvalues must cross the imaginary axis, which can be expressed in terms of the determinant and trace of the Jacobian as $Tr(A) = 0$ and $Det(A) > 0$ (together with the standard transversality condition, see Kuznetsov, 2005). From those conditions we obtain after some simplification that at the Hopf bifurcation the value of $\tilde{r}'(x^*)$ is related to $x^*$as

$$\tilde{r}'(x^*) = \frac{1}{x^*}\left[\frac{\gamma}{\mu^2}(\gamma-\mu)(\nu-\mu)\right], \tag{5.6}$$

provided that the condition $\nu > \mu$ is satisfied (note that we always require that $\gamma < \mu$ to guarantee the existence of a positive equilibrium).

A non-degenerate Hopf bifurcation can be of two types, supercritical—in which a stable limit cycle appears when the equilibrium is destabilised—or subcritical—in which an unstable limit cycle *disappears* when the equilibrium is destabilised (Kuznetsov, 2005). We can determine the criticality of a given Hopf bifurcation by computing the first Lyapunov number $L_1$ of the system at the Hopf bifurcation point: we have $L_1 < 0$ for a supercritical Hopf bifurcation and $L_1 > 0$ for a subcritical Hopf bifurcation, since if the first Lyapunov exponent is positive, then the resulting limit cycle will be stable, and the Hopf bifurcation is supercritical. If the first Lyapunov exponent is negative, then the resulting limit cycle will be unstable and so the Hopf bifurcation will be subcritical (Kuznetsov, 2004).

In a general planar system at a Hopf bifurcation, given by the two dimensional system:

$$\dot{x} = ax + by + f(x,y),$$
$$\dot{y} = cx + dy + g(x,y)$$

with $f(x,y) = a_{20}x^2 + a_{11}xy + a_{02}y^2 + a_{30}x^3 + a_{21}x^2y + a_{12}xy^2 + a_{03}y^3$, and $g(x,y) = b_{20}x^2 + b_{11}xy + b_{02}y^2 + b_{30}x^3 + b_{21}x^2y + b_{12}xy^2 + b_{03}y^3$, the first

Lyanpunov number is given by the following expression (Bautin and Leontovich, 1976; Chow et al., 1994):

$$L_1 = -\frac{\pi}{4b\Delta^{\frac{3}{2}}}\{[ac(a_{11}^2 + a_{11}b_{02} + a_{02}b_{11}) + ab(b_{11}^2 + b_{11}a_{20} + b_{20}a_{11}) + c^2(a_{11}a_{02} + 2a_{02}b_{02}) - 2ac(b_{02}^2 - a_{20}a_{02}) - 2ab(a_{20}^2 - b_{20}b_{02}) - b^2(2a_{20}b_{20} + b_{11}b_{20}) + (bc - 2a^2)(b_{11}b_{02} - a_{11}a_{20})] - (a^2 + bc)[3(cb_{03} - ba_{30}) + 2a(a_{21} + b_{12}) + (ca_{12} - bb_{21})]\},$$

where $\Delta$ is the determinant of the Jacobian matrix.

Computation of $L_1$ requires the values of the third-order Taylor series expansion of the system about $(x^*, y^*)$, thus, in contrast to previous chapters, we now need to specify values for the second and third derivatives of $\tilde{r}$ at the equilibrium, i.e. $\tilde{r}''(x^*)$ and $\tilde{r}'''(x^*)$. We shall consider these values as independent parameters of the investigation, along with the value of $x^*$. The criticality of a Hopf bifurcation in the system with a given prey growth function will be entirely determined by these three values alone.

A typical dependence of the criticality of the Hopf bifurcation in system (5.1)-(5.2) is shown in Fig. 5.1 for three fixed values of the third derivative, $\tilde{r}'''(x^*)$, the other model parameters are $\nu = 2.7$; $\mu = 2$; $\gamma = 1.5$. We see that in these cases, there are substantial regions of both supercritical and subcritical Hopf bifurcations, thus we can both have a supercritical and subcritical bifurcation in the system with a logistic-type growth function. Note that the condition $\tilde{r}'(x^*) < 0$ is always satisfied for the given set of parameters (see expression (5.6)). An important immediate conclusion is that previous well-known works on ratio-dependent predator-prey models (see citations in Section 5.2) predicting only a supercritical bifurcation may not be generic, but instead might be artefacts of the particular choice of parameterization of $r(x)$. In particular, note that use of the standard logistic growth function with $r(x) = s(1 - x)$ immediately restricts us to the case $\tilde{r}''(x^*) = 0$, which, as can be seen from Fig. 5.1A, always lies in the supercritical Hopf bifurcation domain. Thus the necessity of a supercritical Hopf bifurcation in the ratio-dependent model may only arise because the per capita growth rate is a linear function.

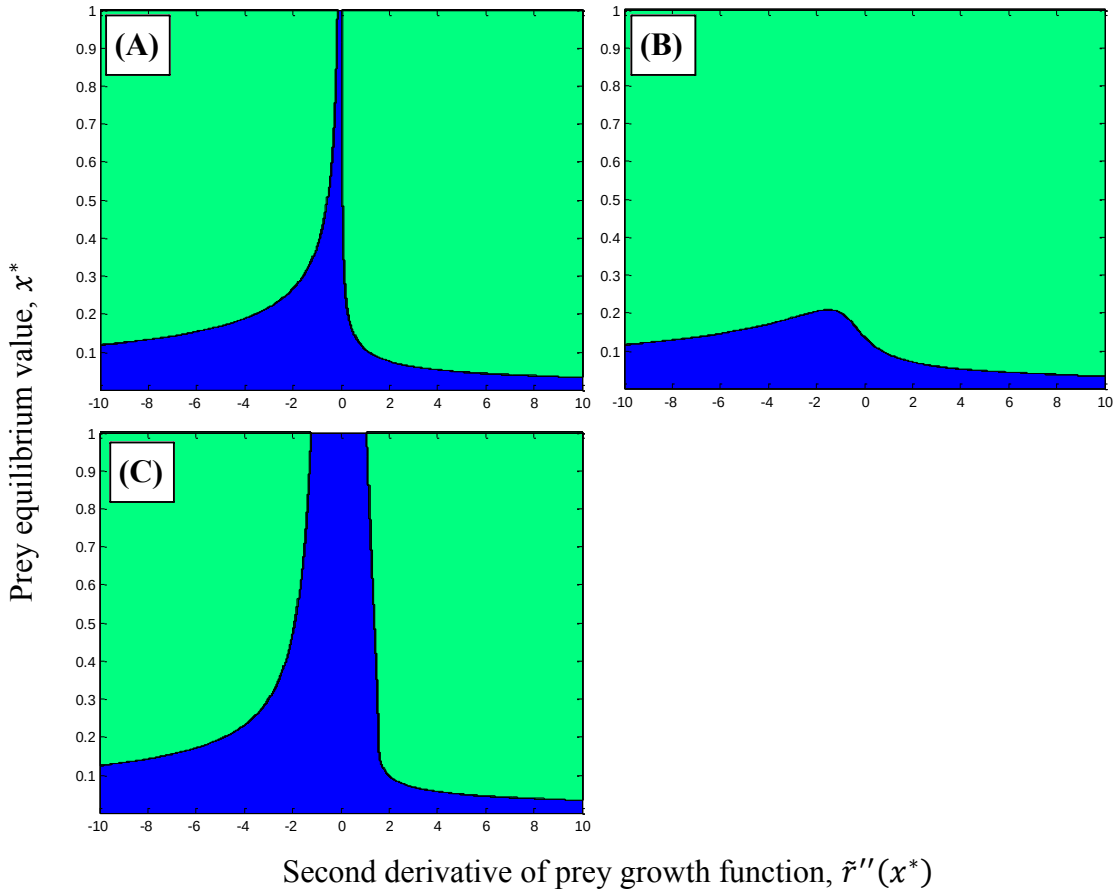


Figure 5.1: Plots of the regions of sub- and super-criticality of the Hopf bifurcation in system (5.1)-(5.2) in the space of values of prey equilibrium density, $x^*$, and the second derivative of the prey growth function at this density, $\tilde{r}''(x^*)$, for three different values of the third derivative, $\tilde{r}'''(x^*)$. Green regions correspond to a subcritical Hopf bifurcation, while blue regions represent a supercritical Hopf bifurcation. (A) $\tilde{r}'''(x^*) = 0$; (B) $\tilde{r}'''(x^*) = 5$. (C) $\tilde{r}'''(x^*) = -10$. The model parameters used to construct the figures are $\nu = 2.7; \mu = 2; \gamma = 1.5$.

We should also mention that for the linear parameterization of $r(x)$, a Hopf bifurcation can take place strictly speaking only for a specific combination of $\nu$, $\mu$ and $\gamma$: these parameters must be located on the Hopf bifurcation hypersurface. Indeed, the system of equations (5.3), (5.4) and (5.6) with $r(x) = s(1 - x)$ has no solution for an arbitrary choice of $\nu, \mu, \gamma$. In particular, for the parameters chosen in Fig. 5.1A no Hopf bifurcation is possible for the linear $r(x)$ and this fact provides a supplementary argument towards considering the general form of the growth rate function. On the other hand, direct computation confirms that the diagram remains similar (with $\tilde{r}''(x^*) = 0$ always being in the supercritical Hopf domain) even in the case where $\nu, \mu, \gamma$ actually satisfy the Hopf bifurcation criteria for the linear $r(x)$.

A similar discrepancy with the previous studies considering a particular parameterization for the Allee effect in prey growth rate for can be seen from Fig. 5.1 Indeed, for a generalized parameterization of the Allee effect (see Definition 5.2), the stability loss of the equilibrium can take place both via a supercritical and a subcritical Hopf bifurcation (cf. Sen et al., 2012).

Note that the influence of the criticality of a Hopf bifurcation is far more than a local matter: it has important implications for the global stability of an ecosystem. When a Hopf bifurcation is supercritical, the loss of the stability of an equilibrium is *noncatastrophic*, since for a limited parameter range trajectories are guaranteed to converge to the stable limit cycle which will be consequently formed in its vicinity. Provided the amplitude of this limit cycle is small, the ecosystem can still be considered to be stable, and moreover, if the bifurcation is reversed, the system will return to the original equilibrium. On the other hand, when a subcritical Hopf bifurcation takes place, an unstable limit cycle—which bounds the basin of attraction of the equilibrium—shrinks and disappears, and trajectories starting near to the equilibrium will leave its vicinity altogether. Therefore the loss of stability can be *catastrophic*, and can have a fatal effect on the persistence of species in the ecosystem, as trajectories may well converge to an extinction state.

The results demonstrated in Fig. 5.1 have some importance consequences which extend well beyond the particular ratio-depend model (5.1)-(5.2). How should we proceed in the case of such uncertainty? To somehow amend the situation and to go beyond well-known standard parameterizations, such as the logistic growth function $r(x) = s(1 - x)$ in (5.1)-(5.2), one can consider some other concrete parameterizations with the aim to conduct a thorough bifurcation analysis for each particular case by taking, for example, growth functions as $r(x) = s(1 - x^2)$, $r(x) = s\big(1 - \exp(x\alpha)\big)$, the theta-logistic function (Gilpin and Ayala, 1973), etc. The obvious drawback of this approach is that, in each case the investigation will be too specific and we cannot, of course, 'cover' all possible parameterizations by picking up some arbitrary functions of our preference. Alternatively, we can utilize the more general approach outlined in Chapters 3 and 4, by considering a generic function $r(x)$, for example, which satisfies Definition 5.1. In this case, we do not need to explore each concrete parameterization separately, but to be able to construct a *concrete* bifurcation portrait in such a generic case, we would need to restrict somehow the function $r(x)$, or else we may find ourselves in the situation where

there are several different types of bifurcation structure as in Fig. 5.1. One possible solution is to consider a narrow class of functions $r(x)$ that all provide equivalent bifurcation portraits. For instance, in system (5.1)-( 5.2), a possible constraint on the function $r(x)$ could be that we consider only those with a positive (or negative) Lyapunov exponent, $L_1$. However, to do this, we would need to impose some analytical constraints on our functions, which are difficult to verify empirically and have no clear biological meaning. Moreover, such constraints are strictly model-dependent: in the case of a prey-dependent functional response the condition $L_1 > 0$ will be given by a completely different equation. Thus, the above idea seems to lack any practicality.

In this chapter we suggest a novel approach to solving the problem raised above by applying the same approach as in Chapters 3 and 4. We still consider a generic growth rate function $r(x)$ satisfying Definition 5.1, but since the use of different parameterizations can result in uncertainty in the bifurcation portrait (e.g. in different scenarios of Hopf bifurcation), we describe the resultant qualitative bifurcation outcome in terms of a probabilistic framework. Given a certain class of model functions, we aim to calculate the probability of the model having a particular type of bifurcation scenario. In the next section we shall show how it can be possible in practice to evaluate the probability of having a supercritical Hopf bifurcation in model (5.1)-(5.2) for a generic class of functions $r(x)$ when a certain bifurcation parameter is varied.

## 5.4 Bifurcation analysis under uncertainty in model functions

### 5.4.1 Determining Functional Neighbourhoods

To proceed further with a bifurcation analysis of (5.1)-(5.2) with uncertain model functions it is necessary to further restrict the class of functions $r(x)$ which are allowed. This need follows in part from the fact that the class of functions satisfying Definition 5.1 is still quite broad and can include some 'exotic' biologically meaningless parameterizations in a qualitative sense, but when we consider the empirical background of the model, there is also a need for a quantitative restriction of our functions. When we fit a parameterisation to a certain experimental or observation data set, we should take into account experimental error and therefore consider alternative parameterisations within a given distance from the fitted function to be also valid (e.g. Cordoleani et al.,

2011), but if an alternative parameterisation passes too far away from the fitted function, and therefore the original data points, it should not be chosen as a viable alternative parameterisation. For this reason we should only compare bifurcation scenarios for functions which are relatively close to each other across the whole admissible range of $x$.

There exist various ways of constructing a class of functions with close values across the entire range of *x* (here we consider $x \in [0,1]$). In this paper, we shall use the same idea as in Chapters 3 and 4—the $\varepsilon_Q$-neighbourhood of a certain base function, constructed using the $d_Q$-distances, Definitions 2.6 and 2.7. To do this, we first require that the unknown function belongs to some class of functions, $Q$, which satisfy the qualitative properties which are supported by theory or conjecture, e.g. a class of logistic functions as in Definition 5.1. We then make an initial concrete choice of the unknown model function—the 'base function' $r_0(x)$, which we should fit to data as far as possible. The $\varepsilon_Q$-neighbourhood of this function is then defined as the subset of functions in $Q$ which are within a fixed distance of $\varepsilon$ from the base function. For more details, refer to Chapter 3.

As before, the problem of working with neighbourhoods of functions is that they are infinite-dimensional, while certain critical model properties in the vicinity of an equilibrium are often entirely determined by local values of the function and some of its derivatives in the vicinity of the equilibrium (see Section 5.3). Therefore it is important to relate the local function properties which are relatively easy to understand (see Fig. 5.1) and the global properties of the functions—their behaviour for any *x*. Our main idea is a projection of the infinite dimensional function space into a finite dimensional subspace of the local function values: $x^*$, $\tilde{r}(x^*)$, $\tilde{r}'(x^*)$, $\tilde{r}''(x^*)$ and $\tilde{r}'''(x^*)$. Note that $\tilde{r}(x^*)$ is always fixed by (5.4), and in the case that there is a Hopf bifurcation $\tilde{r}'(x^*)$ will be fixed by (5.6), so in such cases we will only need to consider a 3D domain consisting of $x^*$, $\tilde{r}''(x^*)$ and $\tilde{r}'''(x^*)$. Due to the non-local restriction of functions $r(x)$—they should belong to the $\varepsilon_Q$-neighbourhood of the base function $r_0(x)$—the values of $x^*$, $\tilde{r}'(x^*)$, $\tilde{r}''(x^*)$ and $\tilde{r}'''(x^*)$ cannot take arbitrary values, but will be located in the bounded domain. Here, as an illustrative example, we consider the standard linear function $r(x) = s(1-x)$ as the base function (with $s = 1$). We also impose bounds on the second derivative: $-A < \tilde{r}''(x) < A \; \forall x \in [0, x_{\max}]$, where $A$ is a positive parameter, in order to guarantee that the $d_Q$-distance is $C^1$, as in the previous chapters. Finally, to simplify the analytical work we consider that the actual function can be approximately

considered as a cubic function—with constant third derivative $\tilde{r}'''(x^*)$—over a small interval about the equilibrium, $(x^* - w, x^* + w)$. In this case, given the values $\tilde{r}(x^*)$, $\tilde{r}'(x^*)$, $\tilde{r}''(x^*)$ and $\tilde{r}'''(x^*)$ and $x^*$ we can derive the necessary and sufficient conditions for the existence of a function $\tilde{r}$ in the $\varepsilon_Q$-neighbourhood of the linear base function taking these values as follows.

Firstly, note that for $\tilde{r}$ to remain within the $\varepsilon_Q$-neighbourhood it must first satisfy

$$\tilde{r}(x) < r_{\varepsilon+}(x) = 1 + \varepsilon - x, \text{ and } \tilde{r}(x) > r_{\varepsilon-}(x) = 1 - \varepsilon - x.$$

Essentially, this means that $\tilde{r}(x)$ must remain between the red bounds in Figure 5.2 over the whole domain—it must remain within distance $\varepsilon$ of the base function.

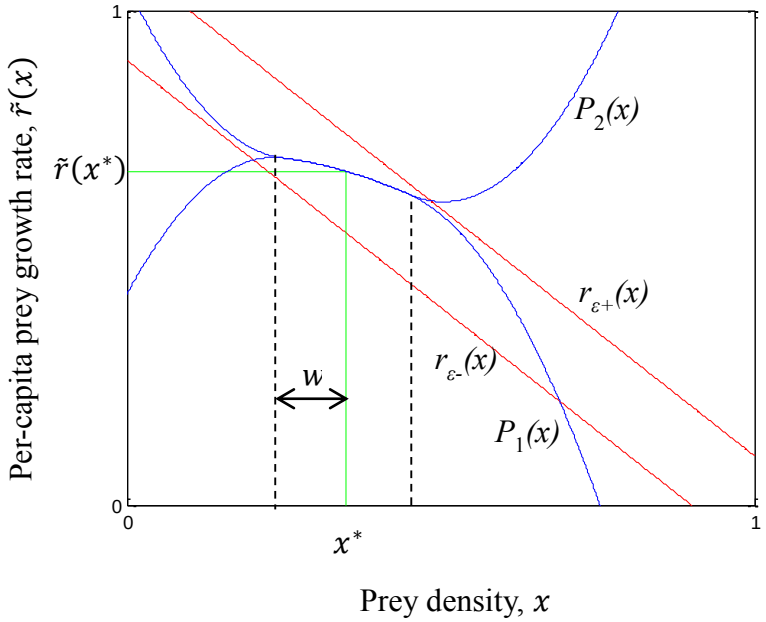


Figure 5.2: Projection of the $\varepsilon_Q$-neighbourhood into the generalised bifurcation space. The red lines $r_{\varepsilon-}$ and $r_{\varepsilon+}$ denote points a distance $\varepsilon$ from the (linear) base function. Any valid function must lie between these lines across the whole domain. The blue curves $P_1$ and $P_2$ represent the lower and upper bounds that necessarily hold for any function that belongs to the class $Q$. Valid functions must lie between these curves (and equal them across the domain $(x^* - w, x^* + w)$).

$\tilde{r}$ must also be in $Q$, so must further satisfy

$$\tilde{r}'''(x) = \tilde{r}'''(x^*) \ \forall x \in (x^* - w, x^* + w), \tag{5.7}$$

$$|\tilde{r}''(x)| < A \ \forall x \in [0, x_{\max}], \tag{5.8}$$

$$\tilde{r}'(x) < 0 \ \forall x \in [0, x_{\max}], \tag{5.9}$$

$$\tilde{r}(0) > 0 \tag{5.10}$$

Condition (5.7) tells us that across the interval $(x^* - w, x^* + w)$, $\tilde{r}$ is given by the cubic

$$\tilde{r}(x) = \tilde{r}(x^*) + \tilde{r}'(x^*)(x - x^*) + \tilde{r}''(x^*)(x - x^*)^2 + \frac{\tilde{r}'''(x^*)}{6}(x - x^*)^3 \qquad (5.11)$$

Therefore an initial necessary condition for the existence of a valid function $\tilde{r}$ attaining the values $x^*$, $\tilde{r}(x^*)$, $\tilde{r}'(x^*)$, $\tilde{r}''(x^*)$ and $\tilde{r}'''(x^*)$ is that this cubic must stay between $r_{\varepsilon-}$ and $r_{\varepsilon+}$ over this interval. In addition, this cubic must always have a negative first derivative, and not have a second derivative of magnitude greater than $A$. Furthermore, $\tilde{r}$ will be bounded above by the parabolas tangent to the above cubic at $x^* - w$ and $x^* + w$ with second derivative $A$, and will be bounded below by the tangent parabolas with second derivative $-A$. These are given by the blue curves in Figure 4.2. Taking these upper and lower bounds over the intervals $[0, x^* - w)$ and $(x^* + w, x_{\max}]$, together with the fact that $\tilde{r}$ must equal the cubic (5.11) over $(x^* - w, x^* + w)$, we can construct the following functions:

$P_1(x)$

$$= \begin{cases} B + C(x - x^* + w) - \dfrac{A}{2}(x - x^* + w)^2: & x \in [0, x^* - w) \\ \tilde{r}(x^*) + \tilde{r}'(x^*)(x - x^*) + \dfrac{\tilde{r}''(x^*)}{2}(x - x^*)^2 + \dfrac{\tilde{r}'''(x^*)}{6}(x - x^*)^3 : & x \in (x^* - w, x^* + w) \\ D + E(x - x^* - w) - \dfrac{A}{2}(x - x^* - w)^2: & x \in (x^* + w, x_{\max}] \end{cases}$$

and

$P_2(x)$

$$= \begin{cases} B + C(x - x^* + w) + \dfrac{A}{2}(x - x^* + w)^2: & x \in [0, x^* - w) \\ \tilde{r}(x^*) + \tilde{r}'(x^*)(x - x^*) + \dfrac{\tilde{r}''(x^*)}{2}(x - x^*)^2 + \dfrac{\tilde{r}'''(x^*)}{6}(x - x^*)^3 : & x \in (x^* - w, x^* + w) \\ D + E(x - x^* - w) + \dfrac{A}{2}(x - x^* - w)^2: & x \in (x^* + w, x_{\max}] \end{cases}$$

where:

$$B = \tilde{r}(x^*) - w\tilde{r}'(x^*) + \frac{w^2}{2}\tilde{r}''(x^*) - w^3\tilde{r}'''(x^*),$$

$$C = \tilde{r}'(x^*) - w\tilde{r}''(x^*) + \frac{w^2}{2}\tilde{r}'''(x^*),$$

$$D = \tilde{r}(x^*) + w\tilde{r}'(x^*) + \frac{w^2}{2}\tilde{r}''(x^*) + w^3\tilde{r}'''(x^*),$$

$$E = \tilde{r}'(x^*) + w\tilde{r}''(x^*) + \frac{w^2}{2}\tilde{r}'''(x^*).$$

For any function $\tilde{r} \in Q$, $P_1$ and $P_2$ necessarily form lower and upper bounds for $\tilde{r}$, since they are constructed as the extreme cases of functions in $Q$. So we have $P_1(x) \leq \tilde{r}(x) \leq P_2(x) \ \ \forall x \in [0, x_{\max}]$ (indeed, $\tilde{r}$, $P_1$ and $P_2$ coincide over the interval $(x^* - w, x^* + w)$), and therefore the conditions

$$\begin{aligned} &P_1(x) < r_{\varepsilon-}(x), \\ &P_2(x) > r_{\varepsilon+}(x), \\ &P_1'(x) < 0 \ \forall x \in (x^* - w, x^* + w), \\ &|P_1''(x)| < A \ \ \forall x \in (x^* - w, x^* + w), \end{aligned} \tag{5.12}$$

are necessary (note: $P_1$, $P_2$ and $\tilde{r}$ coincide over the interval $(x^* - w, x^* + w)$ and so are interchangeable in the 3rd and 4th conditions). In terms of the figure, these conditions can be interpreted as requiring that the red upper and blue lower bounds clearly cannot cross.

It remains to be shown that they are sufficient. In order to prove this, it is enough to provide a method to construct a valid function $\tilde{r}$ which remains between $r_{\varepsilon-}$ and $r_{\varepsilon+}$ given only these conditions. We already have $\tilde{r}$ equal to $P_1$ and $P_2$ over $(x^* - w, x^* + w)$, so only need to construct $\tilde{r}$ over $[0, x^* - w)$ and $(x^* + w, x_{\max}]$. To do this, we can in fact use the exact same approach as in the proofs of Theorem 3.1 and 4.1■

In Fig 5.3 we show examples of projections of the function space on the $x^* - \tilde{r}''(x^*)$ subspace for two different values of $\nu$ (n.b. we show a *cross-section* of the 3-dimensional projection, since $\tilde{r}'''(x^*)$ is fixed in the given diagram). The domain corresponding to all the possible functions is bounded, since for the points located in the black domain there is no corresponding function in the $\varepsilon_Q$-neighbourhood. We can also see that the domain of possible functions still contains both supercritical and subcritical Hopf bifurcations scenarios. Note that the size of the $\varepsilon_Q$-neighbourhood depends on the model parameters, and not solely on $\varepsilon$ or $A$. This follows from the fact that the values of $\tilde{r}(x^*)$ and $\tilde{r}'(x^*)$, which strongly influence the size of the $\varepsilon_Q$-neighbourhood, are not independent but are given by (5.4) and (5.6) and are therefore functions of $\nu$, $\mu$ and $\gamma$.

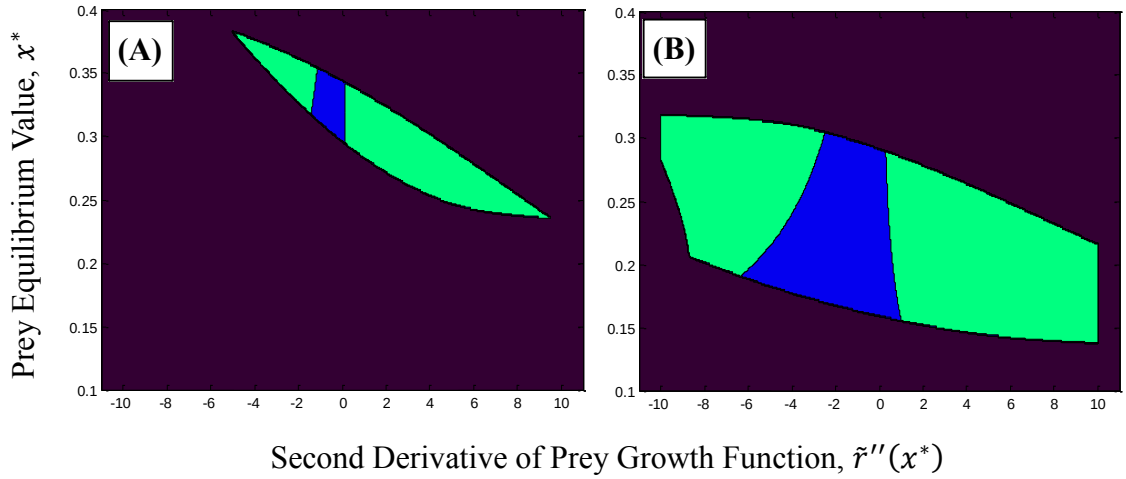


Figure 5.3: Regions of the $\varepsilon_Q$-neighbourhood in $x^* - \tilde{r}''(x^*)$ space showing a supercritical and subcritical Hopf bifurcation for two given bifurcation values, $\nu^*$. The dark blue region contains values outside the $\varepsilon_Q$-neighbourhood. Within the neighbourhood, green indicates the region in which the Hopf bifurcation will be supercritical, and red indicates the regions in which it will be subcritical. The two bifurcation values are (A) $\nu^* = 2.7$. (B) $\nu^* = 3.1$. $\gamma = 1.5; \mu = 2; \varepsilon = 0.1; A = 10; w = 0.1; \tilde{r}'''(x^*) = 0$.

### 5.4.2 Constructing the probability density function of a Hopf bifurcation

Figs 5.1 and 5.3, showing the different domains of criticality, are constructed under the assumption that we have a Hopf bifurcation for a given function for the parameters $\nu$, $\mu$, $\gamma$. In general, this will not be the case for an arbitrary function of class $Q$ in the $\varepsilon_Q$-neighbourhood of the base function. Therefore, to be able to evaluate the probability of having a particular type of Hopf bifurcation in the model we first need to determine the probability of having a Hopf bifurcation in the first place.

The probability of having a Hopf bifurcation in the system within a given range of parameters (regardless its criticality) will be determined by a certain probability density function (pdf). For the sake of simplicity, we fix two parameters ($\gamma$, $\mu$) and consider the maximal attack rate, $\nu$, as the sole bifurcation parameter in the system. For a given $\nu$, we can plot the neighbourhood in the space of values $x^*$ and $\tilde{r}'(x^*)$ corresponding to all functions in the $\varepsilon_Q$-neighbourhood, along with the Hopf bifurcation curve in this space (n.b. here we consider the union of neighbourhoods for all $-A < \tilde{r}''(x^*) < A$ so that we obtain a two-dimensional plot, rather than considering the 3-dimensional space $x^* - \tilde{r}'(x^*) - \tilde{r}''(x^*)$). Examples of this neighbourhood for two different values of $\nu$ are shown in Fig. 5.4A,B, where we show the stability/instability of

the stationary state for the given values of $x^*$and $\tilde{r}'(x^*)$, the value of $\tilde{r}(x^*)$ being fixed by (5.4).

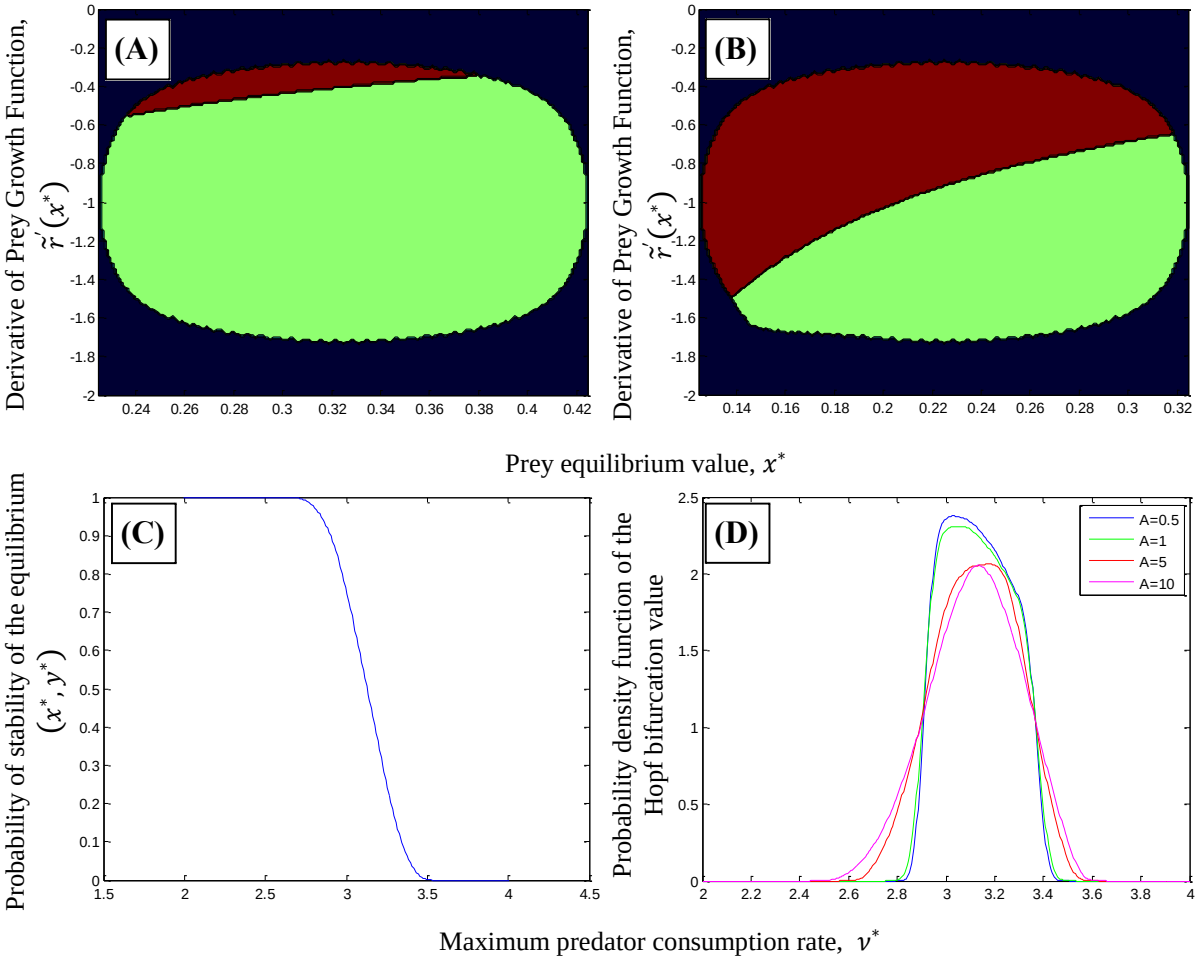


Figure 5.4: Constructing the probability distribution of the bifurcation value, $\nu^*$. (A),(B): Regions of stability and instability in the $\varepsilon_Q$-neighbourhood of the base function $r(x) = 1 - x$ shown in $x^* - \tilde{r}'(x^*)$ space. Dark blue regions correspond to points outside the neighbourhood. Within the neighbourhood, green regions indicate stability of the interior equilibrium and red regions indicate it is unstable. The parameters are (A) $= 2.7$; $\gamma = 1.5$; $\mu = 2$; $\varepsilon = 0.1$; $A = 10$; $w = 0.1$; $\tilde{r}'''(x^*) = 0$. (B) $\nu = 3.1$ all other parameters as in (A). (C): Dependence of the stable proportion of the $\varepsilon_Q$-neighbourhood on the asymptotic predation rate, $\nu$. All other parameters are the same as in (A). (D): Probability distribution of the bifurcation value, $\nu^*$. This is computed by taking the derivative of the stable proportion of the $\varepsilon_Q$-neighbourhood plotted in (C) with respect to $\nu$. All other parameters are the same as in Fig. 5.3A.

If we denote the area of the region of stability by $V_{\text{stable}}$, and the total area of the neighbourhood by $V$, then, using the assumption that functions are uniformly distributed in all neighbourhoods, we can define the probability of the equilibrium being stable for a given parameter value $\nu$ as simply the relative area of the stability region:

$$P_\nu(\text{Stable}) = \frac{V_{\text{stable}}(\nu)}{V(\nu)}. \tag{5.13}$$

In Fig. 4.4C we plot an example of how this probability changes with $\nu$. One can see that the probability of having stability monotonically decreases from one to zero as the value of $\nu$ increases: the Hopf bifurcation curve moves from the upper left corner to the lower right corner. The probability density function (pdf) of having a Hopf bifurcation is defined as:

$$p(\nu^* = \nu) \coloneqq -\frac{dP_\nu(\text{Stable})}{d\nu}, \tag{5.14}$$

The negative sign in this expression reflects the fact that the Hopf bifurcation is 'forward'—or destabilising with increasing $\nu$. We should note that defining the pdf in this straightforward way is only valid if the bifurcation curve in Figs 5.4A,B is shifted monotonically by a change in the parameter $\nu$, as is the case here. Otherwise, we may have the situation where the bifurcation curve 'rotates' and the advance and retreat of the curve in different regions cancel each other out to some extent.

In the case that we have a precisely specified growth function $\tilde{r}(x)$ (including the parameter values), then Fig. 5.4C will be a step function, and $p(\nu^* = \nu)$ will be a delta function centred at the exact bifurcation value $\nu^*$. To evaluate the probability of having a Hopf bifurcation in the range $[\nu_1, \nu_2]$ one needs to integrate the probability density function

$$P(\nu \in [\nu_1, \nu_2]) = \int_{\nu_1}^{\nu_2} p(\nu^* = \nu) d\nu \tag{5.15}$$

The range $[\nu_1, \nu_2]$ should be chosen so that a bifurcation definitely takes place within this interval, so that the integral across the whole range of $\nu$ will equal 1.

Fig. 5.4D shows this pdf constructed numerically for several values of the maximal admissible curvature of $\tilde{r}$, $A$. We see that as we restrict $A$ to lower values, and therefore restrict ourselves to increasingly linear functions, the range of possible bifurcation values diminishes, although note that even when $A$ is 0.5 there is still a wide range of potential bifurcation values.

### 5.4.3 Evaluating the probability of having a supercritical Hopf bifurcation

The next step in defining the probability of having a particular type of Hopf bifurcation is to derive the conditional probability of having a supercritical or subcritical bifurcation given that the bifurcation value is $\nu$, $P(\text{Supercritical}|\nu^* = \nu)$. We can compute $P(\text{Supercritical}|\nu^* = \nu)$ in a similar way to how we found $P_\nu(\text{Stable})$ in Section 5.4.2, i.e. by calculating the relative proportion of the area corresponding to the supercritical Hopf bifurcation in the total $\varepsilon_Q$-neighbourhood:

$$P(\text{Supercritical}|\nu^* = \nu) = \frac{V_{\text{supercritical}}(\nu)}{V(\nu)}, \tag{5.16}$$

in the diagrams shown in Fig. 5.3. Note that, although in this paper we fix $\tilde{r}'''(x^*) = 0$ to simplify the diagrams, in practice there is no reason why we could not also vary this to gain a more complete analysis. Here again we use the assumption that our functions are uniformly distributed in these neighbourhoods. In the Discussion we suggest how this assumption can be relaxed.

In Fig. 5.5 we plot the distribution of the conditional probability $P(\text{Supercritical}|\nu^* = \nu)$ for several values of maximum error, $\varepsilon$—recall that this term determines the width of the $\varepsilon_Q$-neighbourhood, or the maximum distance we allow $\tilde{r}$ to stray from the original logistic function while still being considered valid—and for several values of maximum curvature $A$—the largest absolute value of the second derivative of $\tilde{r}$, therefore giving a limit on how nonlinear $\tilde{r}$ can be. From Fig. 5.5A we see that, as $A$ is decreased and we restrict the second derivative more, $P(\text{Supercritical}|\nu^* = \nu)$ increases because we approach the case where $\tilde{r}$ is linear, in which case we will always have a supercritical bifurcation. In fact, when $A = 0.5$, we generally have $P(\text{Supercritical}|\nu^* = \nu) > 0.8$. Fig. 5.5B shows a similar result when we decrease the maximal error in our function $\tilde{r}$, although the shift towards a higher likelihood of a supercritical bifurcation is less drastic that with a restriction to more linear functions.

Finally, once we've computed the pdf of the Hopf bifurcation value $\nu^*$ and the conditional probability of having a supercritical bifurcation given this bifurcation value, the overall probability of having a supercritical Hopf bifurcation in the system will be given through the total probability theorem:

$$P(\text{Supercritical}) \coloneqq \int_{\nu_1}^{\nu_2} P(\text{Supercritical}|\nu^* = \nu) \cdot p(\nu^* = \nu)\, \mathrm{d}\nu, \tag{5.17}$$

where integration is done over all possible values of parameter $v$ for which a Hopf bifurcation of the interior equilibrium is possible.

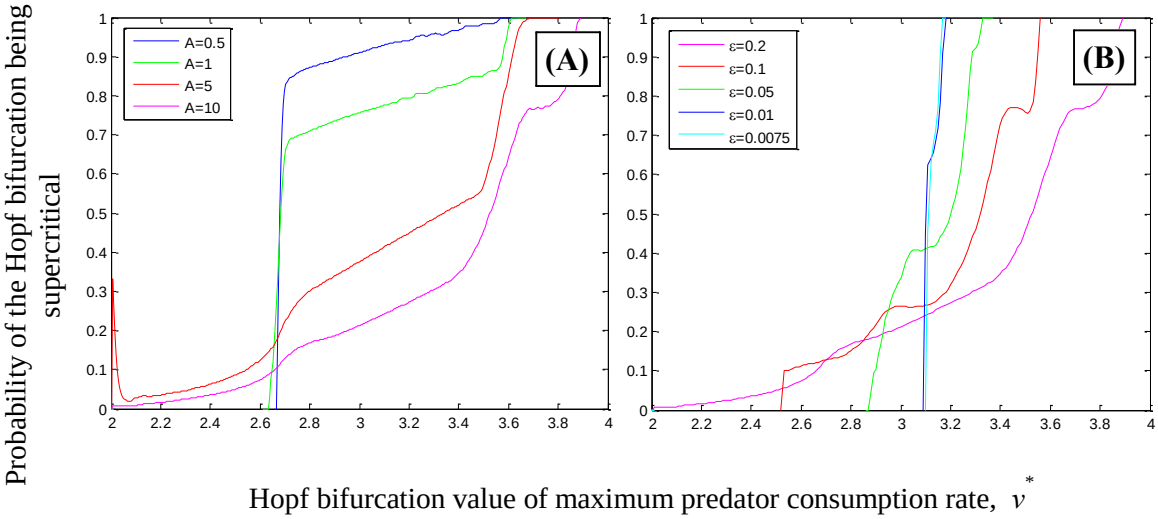


Figure 5.5: Conditional probabilities of the Hopf bifurcation being supercritical given the bifurcation parameter is $v^* = v$. (A) Dependendence on the maximum second derivative, $A$. All other parameters are the same as in Fig. 4.3A. (B) Dependence on the maximum error bound, $\varepsilon$. All other parameters are the same as in Fig. 5.3A.

In Fig. 5.6 we have plotted the total probability $P(\text{Supercritical})$ as a function of $\varepsilon$ for several values of $A$ using (5.17). These parameters have the following meaning: $\varepsilon$ describes the accuracy of our data—the bigger the error terms, the larger $\varepsilon$ should be; $\varepsilon$ therefore determines the uncertainty in our model functions as a result of inaccuracies in data. $A$, on the other hand is the limit on the magnitude of the second derivative of the prey growth function, which gives us the estimate of how fast our per capita growth function can decease with $x$. Unlike $\varepsilon$, the choice of $A$ is less straightforward and is more difficult to estimate from the data.

From Fig. 5.6 one can clearly see that in all cases the greater $\varepsilon$ is, and therefore the larger the error terms in our data (and the greater the uncertainty in our choice of functions), the probability of the Hopf bifurcation in the system being supercritical decreases, and the more likely we should regard a subcritical bifurcation. As regards $A$, an increase—reflecting a modeller's choice to allow more nonlinearity in the growth functions considered, preferably based on empirical observation if possible—should cause us to expect a higher likelihood of the Hopf bifurcation being subcritical. The reason for this shift towards an increased likelihood of a subcritical bifurcation with an

increase of $\varepsilon$ and $A$ is simply that linear functions always yield supercritical Hopf bifurcations since they restrict us to the line $\tilde{r}''(x^*) = 0$ in Fig. 5.1A, and so a relaxation of the linearity of our function—whether prompted by greater inaccuracy in our data or simply by modeller preference—increasingly allows the possibility of a subcritical Hopf bifurcation. Overall, in the case that $\varepsilon$ is relatively large (and in biology it generally is), we should question whether our restrictions on the linearity of the growth term are valid, as an artificially low value of $A$ can cause us to estimate an abnormally high probability of a supercritical Hopf bifurcation as a model artefact.

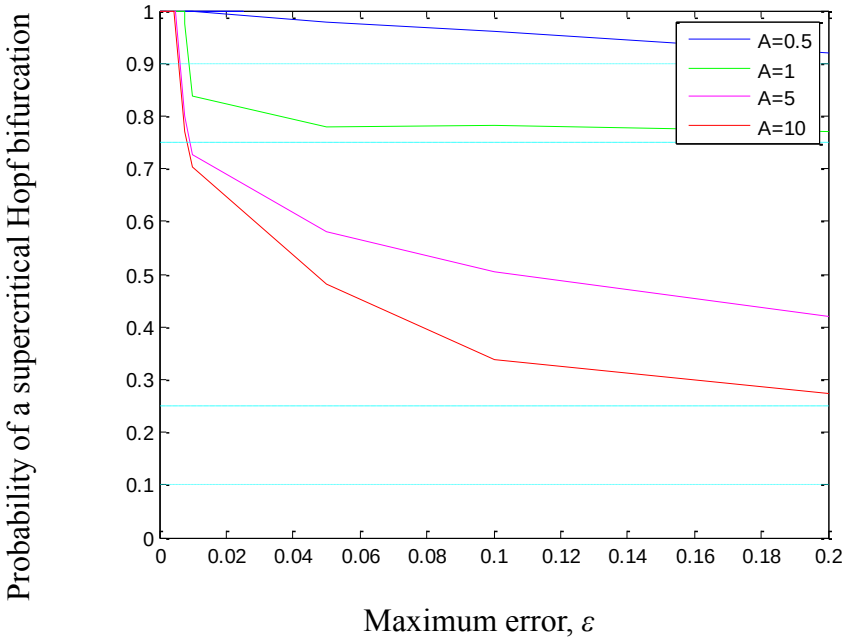


Figure 5.6: Total probability of the Hopf bifurcation being supercritical as a function of $\varepsilon$, plotted for several values of $A$.

The figure also shows that for a gradual increase of the accuracy (i.e. a decrease in $\varepsilon$) the probability of having a supercritical Hopf bifurcation will eventually tend to 1 and we can be more or less certain about the type of bifurcation. If we allow the second derivative to vary within broad intervals, however, a high degree of uncertainty in terms of the type of bifurcation will remain until relatively small error terms (corresponding to a relative error of $\varepsilon \approx$ 2.5-5%). Note that typically the error $\varepsilon$ is far greater than those values in any real biological experiments, thus a high uncertainty in the bifurcation structure will be unavoidable if we allow a large curvature of the growth rate function. To reduce this uncertainty, we need to obtain some extra information regarding the bounds on the second derivative $A$ (as well as the third derivative) of $r(x)$.

Another interesting result from Fig. 5.6 is what happens once the probability of the Hopf bifurcation being supercritical reaches 0.5. At this point, the chances of the bifurcation in the system being supercritical or subcritical are equally likely, so we have complete ambiguity with regards to which bifurcation type we should expect. Any further increase in $\varepsilon$ from this will cause the probability of a supercritical bifurcation to fall further and a subcritical bifurcation from this point will become increasingly more likely. This results in the almost paradoxical situation where greater uncertainty in our model functions should make us more, and not less confident in our model predictions.

Based on the probability plots shown in Fig. 5.6, we can classify the uncertainty in the bifurcation structure in model (5.1)-(5.2) by introducing a number of uncertainty levels. For instance, we can consider that in the case where $P(\text{Supercritical}) < 0.1$ or $P(\text{Supercritical}) > 0.9$, we do not have uncertainty in the bifurcation type and the model can be analysed using the standard methods of bifurcation analysis, despite the uncertainty in the model functions. In the case where we have $0.25 > P(\text{Supercritical}) > 0.1$ or $0.75 < P(\text{Supercritical}) < 0.9$, we can consider that a bifurcation of a certain type (i.e. either supercritical or subcritical) is to be *expected*, thus we can still use the deterministic framework, but we should always estimate the probability (i.e. the risk) of overlooking the other bifurcation structure. For $0.75 > P(\text{Supercritical}) > 0.25$ we can say that we more or less have *complete uncertainty* regarding the bifurcation structure and only probabilistic methods can be used in this case. We should stress that the given levels of uncertainty are flexible and can be varied depending on the modelling task.

## 5.5 Discussion

In this chapter, we have introduced a framework of how to include uncertainty in the parameterization of model functions into the construction of corresponding bifurcation diagrams. The main idea is to project the $\varepsilon_Q$-neighbourhood of valid model functions into the relevant generalised bifurcation space, and consider the probability of having a particular bifurcation diagram based on volumes in this projected neighbourhood. Because we embed uncertainty in the model functions into the specification of the $\varepsilon_Q$-neighbourhood, we find that even in a purely deterministic dynamical system, the uncertainty in the choice of functions results in a probabilistic description in terms of what type of bifurcation diagram we should expect given our a-priori information about

model functions. Here we have provided a concrete example (based on a ratio-dependent model with unknown growth rate function) of how such a probabilistic analysis may be done: we evaluated the probability of having a supercritical Hopf bifurcation in the system where the uncertainty was only in the criticality of the bifurcation.

One of the most surprising results of our investigation was that shown in section 5.4.3.—that an increase in the uncertainty in our model functions by increasing $\varepsilon$ can result in us being more certain in the model bifurcation structure. Although we should note that in the investigation, whenever we observed this situation there was still a great deal of uncertainty, it may be possible to have a situation where a standard bifurcation investigation would be appropriate for large $\varepsilon$, but more accurate data should increase the uncertainty and cause us to switch to a probabilistic investigation. How can we justify this? It seems to suggest that in certain cases, less accurate data is in fact desirable. However, we should always aim to obtain data that is as accurate as possible as a priority—if we artificially increase the error terms considered, and so decrease the uncertainty in the bifurcation structure in this way, then this would poorly represent the amount of uncertainty that there truly is in the model bifurcation structure.

One of the main assumptions we have made in this chapter is that the probability distribution in the generalised bifurcation space (the space of local function values) is uniform (c.f. the discussion of this probability distribution with respect to the degree of structural sensitivity in Section 3.2). This is, of course, far simpler than what we would expect in reality, and methods of constructing probability distributions should be improved. One approach is to couple our framework with the 'functional density' approach outlined in sections 3.2 and 3.4 by weighting the point $(x^*, \tilde{r}'(x^*), \tilde{r}''(x^*), \tilde{r}'''(x^*))$ by the functional density of these values. Recall that the functional density is the area of points in the $\varepsilon_Q$-neighbourhood that the graph of a function taking these values at $x^*$ can pass through. This approach could be further improved with little extra effort by assigning weights to the points in graph space according to a normal distribution centred on the middle of the neighbourhood when we are calculating this area. Another approach would be to derive a probability distribution of the local function values directly from the data points, but care must be taken to ensure that the resulting distribution is biologically relevant. Finally, we may aim to construct a more realistic distribution such as a Gaussian directly on the generalised bifurcation space, modified such that our $\varepsilon_Q$-neighbourhood gives the 90% confidence boundary, for

instance. The trouble with this is that it is still arbitrary as to what the mean point is etc., and an incorrect assumption may lead to the resulting distribution being even less realistic than the uniform distribution initially considered.

Here we have solely considered the case where the growth term in model (1)-(2) is logistic, and revealed that the standard result—that the Hopf bifurcation in the system will always be supercritical—in fact lacks generality when alternative functional forms are considered. The same question remains, however, with respect to the standard result that the Hopf bifurcation becomes subcritical when an Allee effect is introduced. Is this a general result, or simply an artefact of the particular functional forms of the growth rate used? Use of the standard Allee effect parameterisation $r(x) = (x - \beta)(1 - x)$ will automatically restrict us to the line $\tilde{r}''(x^*) = -2$ in Fig 5.1, for instance. Although this doesn't guarantee a subcritical Hopf bifurcation, certain resulting limitations on the equilibrium value $x^*$ do, but it is easy to see that a choice of an alternative functional form may lift this restriction to $\tilde{r}''(x^*) = -2$ and potentially cause a supercritical bifurcation to become possible. Therefore we can reasonably expect uncertainty in the criticality of the Hopf bifurcation which a standard bifurcation analysis will not be able to detect. Consider Definition 5.2 as opposed to Definition 5.1: since the growth function is initially increasing, and then subsequently decreasing, it is possible that the number of interior equilibria can be either one or two depending on the particular functional form chosen. We should generally expect the first interior equilibrium to be a saddle point, however, and we can investigate the number of equilibria using the framework outlined in Chapter 3. Note that if we consider alternative formulations of the Allee effect, for instance, ones which exhibit a 'double' Allee effect in which the per-capita growth function has two peaks (González-Olivares, 2011) this would complicate the possible bifurcation portraits significantly. Each extra peak allowed at the very least makes two additional interior equilibria possible.

Aside from a complete investigation into the Allee effect case, there are many other models which exhibit Hopf bifurcations, and it would be straightforward to implement a similar investigation of such systems to check the generality of their results. Furthermore, similar techniques can be applied to other local co-dimension one bifurcations, such as the saddle-node and transcritical bifurcations, for instance. We should also stress that there is no reason why we could not also consider co-dimension two bifurcations as well, such as Bogdanov-Takens bifurcations. Performing an

analogous investigation for nonlocal bifurcations would be a lot more challenging, however. The approach here makes much use of the fact that local bifurcations conditions can be derived solely in terms of a finite number of terms of the Taylor series expansion of the system evaluated at an equilibrium, which is not the case for nonlocal bifurcations. This should be the next step if we wish to develop a framework for combining investigation of the various individual bifurcations into a complete probabilistic description of a system's bifurcation portrait.

# Chapter 6

# General Discussion and Conclusions

The approaches to detecting and quantifying uncertainty in the dynamics of biological models that are presented here all share one thing in common: the use of partially specified models. Partially specified models (Wood, 2001) work by leaving uncertain functions unspecified apart from some local and global qualitative constraints and some error bounds which the functions must pass between. Working with partially specified models in general is, of course, far more difficult than working with fully specified models. If we limit ourselves to investigating model behaviour in the vicinity of an equilibrium, however, there is much that can be achieved. In order to analyse such models in terms of the number of equilibria and their stability, for instance, we can simply find the isocline equations and the Jacobian matrix as usual, and incorporate any values which are unknown due to the function being unspecified into a generalised bifurcation space. The crucial question then is how to link such an analysis to data.

In partially specified models, the data range considered—determined by the upper and lower bounds placed on valid model functions—is an integral part of the model, not something to be explored as a supplementary investigation, after the analysis is done. In fact, the partially specified models approach can be characterized as a quantitative extension of the classical Kolmogorov approach of investigating ecological models with general functions (Gause, 1934; Kolmogorov, 1936; Kuang and Freedman, 1988; Truscott and Brindley, 1994). All the methods presented in this thesis share the strategy of linking the generalised bifurcation analysis with the data range by somehow *projecting* the set of functions fitting the data range into the generalised bifurcation space. In this way, we reduce the problem of considering the entire infinite dimensional set of valid model functions into the problem of working in an equivalent region in the finite dimensional generalised bifurcation space, in which we can explore the model behaviour directly.

The question of projecting the set of valid model functions essentially boils down to being able to decide whether or not there exists a function that: i) satisfies the relevant constraints of biological realism, both global ones—e.g. positivity, monotonicity—and

local ones—$f(0) = 0$, for instance; ii) takes given derivatives at a specified point (e.g. an equilibrium point, $x^*$) *and* iii) remains between given upper and lower bounds across the whole domain. In general, however, this is an extremely difficult mathematical problem because it requires us to determine the existence of a function satisfying both various local constraints *and* global constraints. Here we have taken the strategy of using geometric methods to obtain the projection exactly, by finding necessary and sufficient conditions for such a function to exist.

In Chapters 3, 4 and 5, we considered geometric methods to obtain the projection. The main tools for determining the existence of a function satisfying the relevant local and global constraints are the inequalities which are constructed as necessary and sufficient conditions in Theorem 3.1, Theorem 3.2 and Theorem 4.1. These are extremely powerful theorems when applicable, because they allow us to achieve the projection (of the space of valid functions into the generalised bifurcation space) by checking some simple inequalities, which is extremely efficient computationally. However, these theorems all focus on the case that the upper and lower bounds are considered to be a fixed distance $\varepsilon$ from a fixed 'base function' that itself satisfied the constraints of biological realism. Therefore, the function bounds themselves satisfy the global constraints (or can be modified so that they do), and this can be seen to be crucial to the construction of an appropriate function in the proofs of those theorems.

A crucial extension of the partially specified model framework concerns the quantification of structural sensitivity in partially specified models. For instance, in the case where we reveal that the use of some functions can result in shifting stability or changing the number of equilibria in a system, can we somehow determine the 'relative proportion' of the functions yielding certain stability/equilibrium number predictions? To address the issue of quantifying uncertainty in partially specified models, we can use the degree of structural sensitivity, introduced in Definition 3.1. The degree of structural sensitivity is essentially derived from the probability of two model functions taken at random from the $\varepsilon_Q$-neighbourhood yielding different predictions for the stability of the equilibrium at hand when used in the model. Thus, the largest degree of sensitivity, $\Delta = 1$, corresponds to the maximal degree of uncertainty in the system: where the probabilities of stability and instability are equal to each other. In this case it is impossible to make any precise predictions based on the particular model: without more data concerning the

unknown model functions, the model essentially gives us no information about the stability of the chosen equilibrium.

The fact that biological models can be sensitive with respect to the choice of their constituting functions is well known in the literature, with a large number of examples provided (Myerscough et al., 1996; Wood and Thomas, 1999; Gross et al., 2004; Fussmann and Blasius, 2005; Gross et al., 2009; Poggiale et al., 2010; Anderson et al., 2010; Cordoleani et al., 2011; Gonzalez-Olivares et al., 2011; Adamson and Morozov, 2012a). Critically, however, structural sensitivity can be largely overlooked when using the conventional approach to sensitivity analysis, which is based only on a variation of parameters for fixed mathematical formulations of the functions (e.g. Bendoricchio and Jorgensen, 2001). This can be readily seen by looking at any of the stability plots—in Figs 3.5, 3.9, 4.2, 4.3, for example—and comparing the light blue domain—which corresponds to the region covered by varying the parameters of a fixed model functions—with the total projected domain corresponding to all valid functions. In all of these cases there are situations in which varying parameters will miss all of the structural sensitivity completely. Unfortunately, it seems to be quite common for modellers to simply use the most popular model functions unquestioningly, solely on the basis that such functions have been used so many times before. It should be kept in mind, however, that model functions usually become popular in the literature due to their analytical simplicity, rather than because they are supported by theoretical or empirical evidence. Checking for sensitivity by choosing a few concrete parameterizations of model functions and comparing the resultant outcomes in each case (e.g. Wood and Thomas, 1999; Fussmann and Blasius, 2005) is a more thorough approach, but can still be a rather subjective method, since it largely depends on the choice of the mathematical forms that are to be compared.

Our method is a more general alternative to parameter variation, and to other approaches such as fixing a few specific functional forms and proceeding as usual, then comparing the results, or combining them in a function $\alpha \cdot f(x) + (1-\alpha) \cdot g(x)$, and treating $\alpha$ as another parameter (Cordoleani et al. 2011). The advantage of our approach over standard parameter-based approaches (e.g. Bendoricchio and Jorgensen, 2001) is that it allows us to cover all function relations and not stick to any particular mathematical formulation—it therefore necessarily encompasses parameter variations, and goes beyond it; we cover the entire infinite dimensional space of valid model functions, rather than an arbitrary finite dimensional subset.

There are several existing frameworks which are related to our approach. Firstly, the framework of generalised modelling and the analogous structural kinetic modelling (Gross, Ebenhoh and Feudel, 2004; Gross and Feudel, 2006; Steuer et al., 2006.; Kuehn et al. 2012) shares with our method the use of unspecified functions which allow for a broad range of functional formulations to be considered, and the treatment of equilibrium values and the values of unknown functions/their derivatives as parameters in the Jacobian matrix of the system. However, instead of incorporating the whole data range into the model, and anchoring the generalised bifurcation space to this data range via a projection, in these approaches the initial model is *transformed* so that the generalised bifurcation analysis comes out in terms of general parameters which are more biologically interpretable and notionally more measurable than equilibrium densities, etc. A similar approach is taken in critical function analysis (de Mazancourt and Dieckmann, 2004; Kisdi, Geritz and Boldin, 2013). Critical function analysis is a branch of adaptive dynamics (Geritz et al. 1998; Morozov and Adamson, 2011)—whereby evolutionary trade-off curves are left unspecified, and the type of a hypothetical evolutionarily singular strategy (in terms of evolutionary stability, convergence stability etc.) is determined using the local curvature of the trade-off function taken at the trait values taken by this strategy.

However, in both of the above approaches there is no escaping the fact that all of the generalised parameters will necessarily be values that need to be measured at the *equilibrium density itself*. With the approach proposed here, using partially specified models and considering the whole data range, this dependence on measurements at a single density vanishes. The 'inputs' in our framework are not the local parameters corresponding to function values, elasticities etc. of the system at its equilibrium densities, as in generalised modelling, but global bounds such as the error bounds of the data range, the global qualitative restrictions of biological realism etc. Notably, we can still carry out parameter-based approaches if we like: if we are considering a data range determined by bounds at a distance $\varepsilon$ of a fixed base function, then the base function itself often has biologically interpretable parameters which can still be varied. In this case, varying the parameters will actually change the data range itself by shifting the upper and lower bounds of our function. Somewhat surprisingly, in this way we can investigate how our system responds to changes in a parameter of a function that is completely unspecified, and therefore has no parameters at all.

One crucial question concerns what we need to do in the case that we find a given model exhibits structural sensitivity. Certainly, we should be rather carefully regarding

the model's predictions—which may be quite inaccurate given the usual uncertainty of model functions and large scattering of points in laboratory experiments (Canale et al., 1973; DeMott, 1982; Hansen et al., 1990; Wood and Nisbet, 1991). One possible course of action could be to use data on the experimental population dynamics to reconstruct the unknown underlying model functions (Wood, 2001; Nelson et al., 2004; Nisbet et al., 2004; Cao et al., 2008). One can try to reconstruct as closely as possible the 'true' model functions which should be used in modelling of the given experimental mesocosm or ecosystem. However, in the case that we have structural sensitivity, an attempt to reveal such 'true' parameterisations for a given set of equations my simply be in vain. Functional relations that we use in models are often oversimplifications of a large number of factors—for instance, the functional response $h$ of a consumer is not only a function of food and/or the population density of the consumer itself, i.e. $h=h(P,Z)$—and even if the environmental conditions (temperature, light intensity, etc.) are kept fixed, other factors such as adaptation and evolution of the prey can influence the functional response (Yoshida et al., 2003; Kondoh, 2003; Jones et al., 2009). The influence of spatial scale can also be a crucial factor: implementing parameterizations obtained on a small spatial scale, such as are found in laboratory experiments, in modelling the dynamics over larger temporal and spatial scales can be erroneous for a number of reasons (Chesson, 1998; Pascual et al., 2001; Englund and Leonardsson, 2008, Morozov, 2010). As a result, the 'true' functional relation may simply not exist as a function of the given state variables of the model, and can be defined only up to a certain accuracy $\varepsilon$.

In this case, uncertainty in the choice of a parameterization may arise not because of some experimental errors, but as a result of internal drift of the functional relations in real ecosystems due to factors not included into the simplified model. For this reason, any case where an optimal parameterization of model functions mimics the experimental data well, but a close parameterisation results in a pronounced deviation, should be considered to be rather suspicious: if the data had been obtained another time, an entirely different optimal parameterisation may have been found. On the other hand, if the dynamics observed in a biological system appear to be relatively consistent, structural sensitivity in a corresponding model can be an indicator that something is wrong with the model construction, since we should expect some small variation in the biological functions which, according to a structurally sensitive model would result in significant variation in the population dynamics. In this case, we probably need to stop searching for a function providing us with a fantastic fitting and make necessary changes to the model

structure, by including adaptation and evolutionary factors, for instance (e.g. Yoshida et al., 2003; Jones et al., 2009).

One particularly interesting consequence of structural sensitivity in models is that it may help explain the apparent irregularity in the oscillations of species densities observed both in nature and in some experiments (e.g. Nicholson, 1957; Wolda, 1988; Giller and Doube, 1994; Smayda, 1998; Philippart et al., 2000; Guo et al., 2002; Valdes et al., 2007 and many other references). The widespread opinion is that irregular oscillations of species densities are a consequence of either internal chaotic dynamics (Hastings et al., 1993; Dennis et al., 2001), the influence of environmental noise (Greenman and Benton, 2003; Vasseur, 2007) or the interplay of both factors (Turchin and Ellner, 2000). The phenomenon of structural sensitivity allows us to propose another scenario of such irregular species oscillations, since in reality functional relations between system components are not fixed but slowly change in time. This can be a consequence of the fact that our models describe systems using a limited number of state variables, whereas the true relationships in the functions can depend on a large number of hidden variables which do not remain constant and change our model functions, but variation of model functions may also take place through processes of fast evolution and adaptation (Thompson, 1998; Duffy and Sivars-Becker, 2007; Kinnison and Hairston, 2007). This permanent variation can be visualized as an on-going random walk in the space of functions, which may translate itself into a large variation of the model outcomes due to the structural sensitivity of the system, and manifest as irregularity in the species population sizes, since small variations in functions may result in transitions between the stability and instability subdomains of the functional space and moreover, within the instability domain the amplitude as well as the period of resulting oscillations can prominently change through small variations in the model functions (Fussmann and Blasius, 2005; Cao et al., 2008; Cordoleani et al., 2011). In this way, small fluctuations in model functions may be amplified and result in large amplitude irregular oscillations of species densities, which may present themselves in the original biological system. Such a mechanism has been proposed in previous works (e.g. Beninca et al., 2011), but fluctuations in model functions were only considered to be due to variation in model parameters.

As a consequence of this mechanism, even simple 2-3 component classical ecological models may be able possess a large degree of complexity which is encoded in terms of structural sensitivity, complexity which will largely become hidden when one

uses only fixed parameterizations of model functions. We propose that structural sensitivity in our models may be strongly related to the complexity of the underlying real biological systems whose behaviour we wish to mimic. Structural sensitivity, in fact, should eventually entail a complete rethink of bifurcation theory in afflicted disciplines: due to uncertainty in the model functions, model dynamics can be defined only with certain probability. Therefore, as we saw in Chapter 4 with regards to Hopf bifurcations and their criticality, there are no longer concrete bifurcations in structurally stable systems, but rather there are probabilistic bifurcations—in which the probability of observing certain model behaviour undergoes a continuous change. Bearing this in mind, it is crucial to extend the framework of Chapter 5 and construct theory of probabilistic—or 'fuzzy'—bifurcation theory.

A crucial step towards a probabilistic bifurcation theory concerns how to consider probability distributions of regions in the generalised bifurcation spaces of partially specified models. Ideally, such a probability distribution should constitute a weighting of points in the generalised bifurcation space according to how well corresponding functions can fit the data range, but this is complicated by the very nature of the projection—we're projecting from an infinite-dimensional set of functions into a finite dimensional set, so every point in the projected region of generalised bifurcation space corresponds to an infinite class of possible valid function. As a pragmatic solution to this difficulty, we have introduced the notion of the 'functional density', which weights points in the generalised bifurcation space by the area of the data range which corresponding functions can pass through (see the end of Section 3.2, Section 3.4 and Section 6.3.4). However, in general the question of assigning more fitting probability distributions to generalised bifurcation spaces, and the related question of how we can assign measures to infinite dimensional sets is a difficult one, and should be given much more thought.

Finally, we can say a few words about how the framework proposed here can be extended. Firstly, our test is designed to detect qualitative changes to system dynamics, but structural sensitivity can also manifest itself in terms of large quantitative changes in a model's predictions, as in Defn. 2.2, (ii). Such 'quantitative' structural sensitivity can also have potentially calamitous consequences to the predictive power of a model (Wood and Thomas, 1999; Cordoleani et al., 2011), so developing methods to detect when this is the case would be in the interest of predictive modelling in a wide range of disciplines. In particular, one case in which the approach used here is not applicable is when we need to reveal the sensitivity of oscillatory dynamics (regular or chaotic) to the choice of the

model functions: for instance, the amplitude and period of any limit cycles may be sensitive to the choice of parameterization (Wood and Thomas, 1999; Fussmann and Blasius, 2005; Cordoleani et al., 2011). Another direction in which the framework could be extended would be the use of partially specified models to consider nonlocal bifurcations such as homoclinic and heteroclinic bifurcations, which are not determined by local approximations. Similarly, we could extend our framework to investigate the influence of functional variation on transient dynamics, rather than confining ourselves to asymptotic dynamics. At all three of these frontiers, we shall encounter the same general challenge: in these cases, the functions and their derivatives at a given locality don't give us enough information: we need to know the shape of the functions over a domain of positive measure. Therefore it is unlikely that a generalised bifurcation space of finite dimension will be sufficient to determine the entire range of model behaviour. Overall, we should say that the partially specified modelling framework is still a very young and growing research area. There are certainly many challenges ahead if it is to be extended to its full potential, but there is also great opportunity.

# Appendix A

# Computation of the area of the $\varepsilon_Q$-neighbourhood that can be covered by parameter variation

Here we analytically derive the conditions of when parametric-based analysis of structural sensitivity can provide the same result as the nonparametric test introduced in Chapter 3 (we assume the $\varepsilon_Q$ neighbourhood to be small). We consider a function $f: [P_1, P_2] \to \mathbb{R}$ with two parameters $\alpha$ and $\beta$, and aim to find a bound for the domain in $D - x$ space of functions in the $\mathcal{E}_Q$ neighbourhood of $f$ which can be explored by varying the parameters – which is the typical approach taken to structural sensitivity analysis.

First we note that taking the Taylor expansion of a function $f$ about $(x, \alpha_0, \beta_0)$ gives us

$$f(x, \alpha, \beta) \approx f(x, \alpha_0, \beta_0) + \Delta\alpha \cdot f_\alpha(x, \alpha_0, \beta_0) + \Delta\beta \cdot f_\beta(x, \alpha_0, \beta_0), \qquad (A1)$$

and differentiating w.r.t $x$ yields

$$f_x(x, \alpha, \beta) \approx f_x(x, \alpha_0, \beta_0) + \Delta\alpha \cdot f_{\alpha x}(x, \alpha_0, \beta_0) + \Delta\beta \cdot f_{\beta x}(x, \alpha_0, \beta_0). \qquad (A2)$$

where $\Delta\alpha = \alpha - \alpha_0$ , $\Delta\beta = \beta - \beta_0$ and $\Delta\alpha,\ \Delta\beta \ll 1$.

At $x = x^*$ we have

$$f(x^*, \alpha, \beta) \approx f(x_0, \alpha_0, \beta_0) + \Delta x \cdot f_x(x_0, \alpha_0, \beta_0) + \Delta\alpha \cdot f_\alpha(x_0, \alpha_0, \beta_0) + \Delta\beta \cdot f_\beta(x_0, \alpha_0, \beta_0) (A3).$$

where $\Delta x = x^* - x_0$ and $\Delta x \ll 1$.

Since we have $f(x_0, \alpha_0, \beta_0) = \frac{m}{k}$ and we require $f(x^*, \alpha_0, \beta_0) = \frac{m}{k}$, we obtain

$$-\Delta x \cdot f_x(x_0, \alpha_0, \beta_0) = \Delta\alpha \cdot f_\alpha(x_0, \alpha_0, \beta_0) + \Delta\beta \cdot f_\beta(x_0, \alpha_0, \beta_0), \qquad (A4)$$

by rearranging (A3).

If we introduce $\Delta D = f_x(x^*, \alpha, \beta) - f_x(x_0, \alpha_0, \beta_0)$, then by taking linear approximations to $f_x(x^*, \alpha_0, \beta_0)$, $f_{\alpha x}(x^*, \alpha_0, \beta_0)$ and $f_{\beta x}(x^*, \alpha_0, \beta_0)$ about $x^* = x_0$ in (A2) and discounting second order terms we get

$$\Delta D - \Delta x \cdot f_{xx}(x_0, \alpha_0, \beta_0) = \Delta\alpha \cdot f_{\alpha x}(x_0, \alpha_0, \beta_0) + \Delta\beta \cdot f_{\beta x}(x_0, \alpha_0, \beta_0). \qquad (A5)$$

Together, (A4) and (A5) form a linear system of two equations with – provided that we can find expressions for $\Delta\alpha$ and $\Delta\beta$ – two unknowns: $\Delta D$ and $\Delta x$. We can rearrange (A4) to find $\Delta x$, and substitute this into (A5) to get

$$\Delta x = -\Delta\alpha \cdot \frac{f_\alpha(x_0,\alpha_0,\beta_0)}{f_x(x_0,\alpha_0,\beta_0)} - \Delta\beta \cdot \frac{f_\beta(x_0,\alpha_0,\beta_0)}{f_x(x_0,\alpha_0,\beta_0)}, \text{ and}$$

$$\Delta D = \Delta\alpha \cdot \left(f_{\alpha x}(x_0,\alpha_0,\beta_0) - \frac{f_{xx}(x_0,\alpha_0,\beta_0)\cdot f_\alpha(x_0,\alpha_0,\beta_0)}{f_x(x_0,\alpha_0,\beta_0)}\right) + \Delta\beta \cdot \left(f_{\beta x}(x_0,\alpha_0,\beta_0) + \frac{f_{xx}(x_0,\alpha_0,\beta_0)\cdot f_\beta(x_0,\alpha_0,\beta_0)}{f_x(x_0,\alpha_0,\beta_0)}\right).$$

Now, provided that we can find an expression for the bounds of the region in $\alpha - \beta$ space which corresponds to functions in the $\mathcal{E}_Q$ neighbourhood of $f(x,\alpha_0,\beta_0)$, we can find the analogous region in $\Delta D - \Delta x$ space. To find such an expression we use conditions that depend on which definition of the $\mathcal{E}_Q$ neighbourhood of $f$ we are using. If we are using the absolute distance, the condition is that

$$|f(x,\alpha,\beta) - f(x,\alpha_0,\beta_0)| < \varepsilon \text{ for all } x \in [P_1,P_2], \qquad (A6)$$

so to find the bounds on $\alpha$ and $\beta$, we take the equality here, and using (A1) we obtain

$$\left|\Delta\alpha \cdot f_\alpha(\hat{x},\alpha_0,\beta_0) + \Delta\beta \cdot f_\beta(\hat{x},\alpha_0,\beta_0)\right| = \varepsilon, \qquad (A7)$$

where $\hat{x} \in [P_1,P_2]$ is the value at which the LHS takes its maximum. If we use relative distance, the condition becomes

$$\frac{|f(x,\alpha,\beta) - f(x,\alpha_0,\beta_0)|}{|f(x,\alpha_0,\beta_0)|} < \varepsilon, \qquad (A8)$$

and we need to consider

$$\frac{\left|\Delta\alpha \cdot f_\alpha(\hat{x},\alpha_0,\beta_0) + \Delta\beta \cdot f_\beta(\hat{x},\alpha_0,\beta_0)\right|}{|f(\tilde{x},\alpha_0,\beta_0)|} = \varepsilon, \qquad (A9)$$

where $\hat{x} \in [P_1,P_2]$ is again the value at which the LHS takes its maximum.

Note, however, that in both cases, $\hat{x}$ may be different for different values of $\Delta\alpha$ and $\Delta\beta$, so the resulting boundaries may be curvilinear. To avoid this, we choose $\hat{x} = P_2$ and use (A7) or (A9) to obtain explicit equations for the two boundary lines in $\Delta\alpha - \Delta\beta$ space. This will give us a linear boundary region, and since $\left|\Delta\alpha \cdot f_\alpha(P_2,\alpha_0,\beta_0) + \Delta\beta \cdot f_\beta(P_2,\alpha_0,\beta_0)\right| < \varepsilon$ is a necessary condition for (A6) to be satisfied, this linear region must contain the corresponding boundary region for the correct choice of $\hat{x}$. ■

# Appendix B

# Stability analysis of the delay differential equation (4.19)-(4.21)

Here we describe an approach to check the linear stability of an equilibrium of the system of delay-differential equations (4.19)-(4.21). Hereon we denote $x_i(t)$ by $x_i$, and $x_i(t-\tau)$ by $x_{i_\tau}$ for simplicity. We implement a standard technique of stability analysis of ODEs with delay (Dieudonne, 1960; Bairagi et al., 2008). We can let $\boldsymbol{x} = \boldsymbol{x}^* + \delta\boldsymbol{x}$, where $\delta\boldsymbol{x}$ is a small magnitude perturbation from the equilibrium $\boldsymbol{x}^*$, then use Taylor's theorem to obtain the linearization of the system

$$\dot{\delta\boldsymbol{x}} \approx \boldsymbol{J}_0\delta\boldsymbol{x} + \boldsymbol{J}_\tau\delta\boldsymbol{x}_{\boldsymbol{\tau}}, \tag{B1}$$

where $\boldsymbol{J}_0$ is the Jacobian matrix with respect to $\boldsymbol{x}$ and $\boldsymbol{J}_\tau$ is the Jacobian matrix with respect to $\boldsymbol{x}_{\boldsymbol{\tau}}$. If we assume that (B1) has exponential solutions, we can write $\delta\boldsymbol{x} = \boldsymbol{A}e^{\lambda t}$ and substitute this solution into (B1) gives us $\lambda\boldsymbol{A}e^{\lambda t} = \boldsymbol{J}_0\boldsymbol{A}e^{\lambda t} + \boldsymbol{J}_\tau\boldsymbol{A}e^{\lambda(t-\tau)}$. Dividing by $e^{\lambda t}$ yields

$$\lambda\boldsymbol{A} = \left(\boldsymbol{J}_0 + e^{-\lambda\tau}\boldsymbol{J}_\tau\right)\boldsymbol{A}. \tag{B2}$$

Since $\lambda$ is therefore an eigenvalue of the matrix $\left(\boldsymbol{J}_0 + e^{-\lambda\tau}\boldsymbol{J}_\tau\right)$, we know from the theory of linear algebra that (B2) holds if and only if the following holds:

$$\left|\boldsymbol{J}_0 + e^{-\lambda\tau}\boldsymbol{J}_\tau - \lambda\boldsymbol{I}\right| = 0, \tag{B3}$$

where $\boldsymbol{I}$ is the three-dimensional identity matrix. (A3) is called the *characteristic equation* of system (4.19)-(4.21), and can be calculated in this case as

$$\lambda^3 + P\lambda^2 + Q\lambda + (S\lambda + M)e^{-\lambda\tau} + N = 0, \tag{B4}$$

where $P = (c-1)x_1^* - 2jx_2^* - \left(\widetilde{H}'(x_2^*) + h\right)x_3^* - b$;

$Q = (x_1^* + hx_3^*)\left(b - cx_1^* + \widetilde{H}'(x_2^*)x_3^* + 2jx_2^*\right) + hx_1^*x_3^*$;

$S = k \cdot \widetilde{H}(x_2^*)\widetilde{H}'(x_2^*)x_3^* + acx_1^*x_2^*$;

$M = x_1^*x_3^*\left(k \cdot \widetilde{H}(x_2^*)\widetilde{H}'(x_2^*) + achx_2^*\right)$,

and $N = hx_1^*x_3^*\left(b - cx_1^* + \widetilde{H}'(x_2^*)x_3^* - 2jx_2^*\right)$.

Unlike the case of ODE systems, equation (B3) is not a polynomial over the complex numbers, but rather a quasi-polynomial: since the $e^{-\lambda\tau}$ term is periodic with respect to the complex part of $\lambda$, (B3) must have infinitely many complex solutions. Therefore the usual approach of directly finding the eigenvalues of (B3) and determining the conditions under which they all have negative real part cannot be used here. Instead, we need to choose a certain parameter – in this paper, we choose the time delay, $\tau$ – and determine the critical values for which the real part of $\lambda$ changes sign in order to detect bifurcations with respect to this parameter. At these critical values, the eigenvalues will take the form $\lambda = i \cdot \omega$ for some real $\omega$ (we assume, without loss of generality, that $\omega > 0$). Substituting $\lambda = i \cdot \omega$ into the characteristic equation (B4) and separating the real and imaginary parts yields

$$P\omega^2 - N = M\cos(\omega\tau) + S\omega\sin(\omega\tau), \quad \omega^3 - Q\omega = S\omega\cos(\omega\tau) - M\sin(\omega\tau) \quad \text{(B5)}$$

Squaring both equations and summing them results in

$$\omega^6 + (P^2 - 2Q)\omega^4 + (Q^2 - 2NP - S^2)\omega^2 + N^2 - M^2 = 0 \quad \text{(B6)}$$

which has at least one positive, real solution provided $N^2 < M^2$, since this implies the polynomial is negative at $\omega = 0$, while it tends to positive infinity as $\omega \to \infty$. Therefore, we can solve (B6) as a cubic equation with variable $\omega^2$ and take the positive roots of these solutions to obtain at most three positive roots of (B6). If we let $\omega_0$ denote any given positive root of (B6), then by rearranging both equations of (B5) in terms of $\sin\omega\tau$ and equating them, and then substituting in $\omega = \omega_0$, we obtain

$$\cos\omega_0\tau_C = \frac{S\omega_0^4 + (MP - QS)\omega_0^2 - MN}{S^2\omega_0^2 + M^2}, \quad \text{(B7)}$$

where $\tau_C$ are the critical values of the time delay, at which the real parts of $\lambda$ disappear. Therefore we obtain a countable family of critical time delays for each $\omega_0$:

$$\tau_{C_m} = \frac{1}{\omega_0}\cos^{-1}\left(\frac{S\omega_0^4 + (MP - QS)\omega_0^2 - MN}{S^2\omega_0^2 + M^2}\right) + \frac{m2\pi}{\omega_0}, \quad m \in \mathbb{Z}. \quad \text{(B8)}$$

Now we note that $\mathrm{Re}(\lambda) = 0$ is a necessary, but not sufficient condition for a stability change to take place. To prove that there will be such bifurcations at our critical values $\tau_{C_m}$, it is sufficient to prove that

$$\frac{\mathrm{dRe}(\lambda)}{\mathrm{d}\tau}|_{\lambda=i\omega_0} \neq 0,$$

**n.b.** This is not to say that $\frac{\mathrm{dRe}(\lambda)}{\mathrm{d}\tau}|_{\lambda=i\omega_0} \neq 0$ and $\mathrm{Re}(\lambda) = 0$ are necessary and sufficient conditions for a bifurcation at $\tau_{C_m}$: the sign of $\mathrm{Re}(\lambda)$ can still change when $\frac{\mathrm{dRe}(\lambda)}{\mathrm{d}\tau}|_{\lambda=i\omega_0} = 0$.

Note that $\mathrm{sign}\left\{\frac{\mathrm{dRe}(\lambda)}{\mathrm{d}\tau}|_{\lambda=i\omega_0}\right\} = \mathrm{sign}\left\{\mathrm{Re}\left(\left(\frac{\mathrm{d}\lambda}{\mathrm{d}\tau}\right)^{-1}|_{\lambda=i\omega_0}\right)\right\}$. Now by differentiating (B4) with respect to $\tau$, rearranging, substituting in $\lambda = i\omega_0$, taking the real part and simplifying, we obtain

$$\begin{aligned}\mathrm{sign}&\left\{\frac{\mathrm{dRe}(\lambda)}{\mathrm{d}\tau}|_{\lambda=i\omega_0}\right\}\\ &= \mathrm{sign}\{(Q-3\omega_0^2)(\omega_0^2-Q)(S^2\omega_0^2+M^2)\\ &\quad -2P(P\omega_0^2+N)(S^2\omega_0^2+M^2)-S^2(Q-3\omega_0^2)(\omega_0^2-Q)\\ &\quad -2PS^2(P\omega_0^2+N)\}.\end{aligned}$$

Provided that $\omega_0$ is not a root of this polynomial, there will be a bifurcation at each of the critical time delays, $\tau_{C_m}$, that are related to it, and this can easily be checked by substituting each of the $\omega_0$ into the polynomial.

Finally, once we have determined the bifurcation values of the time-delay, $\tau_{C_m}$, it is simple to check how many such bifurcations take place between $\tau = 0$ and a specified time-delay $\tau$, so we can determine the stability of our equilibrium for the system with this time-delay by computing the stability of the system in the case $\tau = 0$ (i.e. by using the standard stability analysis in the ODE case). If an equilibrium in the system without time-delay is stable, then it will be stable in the system with time-delay $\tau$ if $\#\{\tau_{C_m}|\tau_{C_m} \in (0,\tau)\}$ is even, and unstable if it is odd. If the equilibrium is unstable in the system without delay, this situation is reversed.

# Bibliography


Abrams, P.A. and Ginzburg, L. (2000) The nature of predation: prey dependent, ratio dependent, or neither? *Trends in Ecology and Evolution.* **15**, 337-341.

Adamson, M.W. and Morozov, A.Yu. (2012a) Revising the role of species mobility in maintaining biodiversity in communities with cyclic competition. *Bulletin of Mathematical Biology* **74**, 2004-2031.

Adamson, M.W. and Morozov, A.Yu. (2012b) When can we trust our model predictions? Unearthing structural sensitivity in biological systems. *Proc. R. Soc. A* **469**, 20120500

Adamson, M.W. and Morozov, A.Yu. (2014a) Defining and Detecting Structural Sensitivity in Biological Models: Developing a New Framework. *J. Math. Biol.***69**, 1815-1848.

Adamson, M.W. and Morozov, A.Yu. (2014b) Bifurcation analysis of models with uncertain function specification: how should we proceed? *Bull. Math. Biol.* **76**, 1218-1240.

Adamson, M.W., Morozov, A.Yu. and Kuzenkov, O.A. (2015) Quantifying uncertainty in partially specified biological models: How can optimal control theory help us? [*submitted*]

Anderson, T.R., Gentleman, W.C. and Sinha, B. (2010) Influence of grazing formulations on the emergent properties of a complex ecosystem model in a global Ocean general circulation model. *Progress in Oceanography* **87**, 201–213.

Arditi, R. and Ginzburg, L.R. (1989) Coupling in predator-prey dynamics: ratio-dependence. *J. Theor. Biol.* **139**, 311-326.

Arditi, R., Ginzburg, L.R. and Akçakaya, H.R. (1991) Variation in plankton densities among lakes: a case for ratio-dependent models. *American Naturalist* **138**, 1287-1296.

Arditi, R. and Saiah, H. (1992) Empirical evidence of the role of heterogeneity in ratio-dependent consumption. *Ecology* **73**, 1544-1551.

Bairagi, N., Sarkar, R.R. and Chattopadhyay, J. (2008) Impacts of incubation delay on the dynamics of an eco-epidemiological system-a theoretical study. *Bull. Math. Biol.* **70**, 2017–2038.

Bautin N. and Leontovich, Y. (1976) *Methods and Procedures for the Qualitative Investigation of Dynamical Systems in a Plane*. Moscow: Nauka.

Bazykin, A.D. (1998) *Nonlinear Dynamics of Interacting Populations.* Singapore: World Scientific.

Becks, L., Hilker, F.M., Malchow, H. and Jurgens, K.H.A. (2005) Experimental demonstration of chaos in a microbial food web. *Nature* **435**, 1226–1229.

Begon, M., Harper, J.L. and Townsend, C.R. (2002) *Ecology*. Blackwell Science, Oxford.

Bendoricchio, G. and Jorgensen, S. (2001) *Fundamentals of Ecological Modelling*. Amsterdam: Elsevier.

Benincà, E., Dakos, V., van Nes, E.H., Huisman, J. and Scheffer, M. (2011) Resonance of plankton communities with temperature fluctuations. *American Naturalist* **178**, E87-E95.

Berec, L., Angulo, E. and Courchamp, F. (2007) Multiple Allee effects and population management. TREE **22**, 185–191.

Berezovskaya, F., Karev, G. and Arditi, R. (2001) Parametric analysis of the ratio-dependent predator-prey model. *J. Math. Biol.* **43**, 221-246.

Bishop, M.J., Kelaher, B.P., Smith, M., York, P.H. and Booth, D.J. (2006) Ratio-dependent response of a temperate Australia estuarine system to sustained nitrogen loading. *Oecologia* **149**, 701-708.

Burden, R.L. and Faires, J.D. (2001) *Numerical Analysis*. Boston: Brooks/Cole.

Butler, G.J. and Wolkowicz, G.S.K. (1986) Predator-mediated competition in the chemostat. *J. Math. Biol.* **24**, 167–191.

Canale, R.P., Lustig, T.D., Kehrberger, P.M. and Salo, J.E. (1973) Experimental and mathematical modeling studies of protozoan predation on bacteria. *Biotech. and Bioeng.* **15**, 107–728.

Cao, J., Fussmann, G.F. and Ramsay, J.O. (2008) Estimating a predator-prey dynamical model with the parameter cascades method. *Biometrics* **64**, 959-967.

Chesson, P. (1998) 'Making sense of spatial models in ecology', in Bascompte, J. and Sole, R.V. (eds.) *Modeling Spatiotemporal Dynamics in Ecology* . New York: Springer, pp 151–166.

Chou, I. and Voit, E.O. (2009) Recent developments in parameter estimation and structure identification of biochemical and genomic systems. *Mathematical biosciences **219**,* 57-83.

Chow, S.-N., Li, C. and Wang, D. (1994) *Normal forms and bifurcation of planar vector fields*. Cambridge: Cambridge University Press.

Cordoleani F., Nerini D., Gauduchon, M., Morozov, A. and Poggiale J.-C. (2011) Structural sensitivity of biological models revisited. *J. Theor. Biol.* **283**, 82–91.

Cosner, C., DeAngelis, D.L., Ault, J.S. and Olson, D.B. (1999) Effects of spatial grouping on the functional response of predators. *Theor. Pop. Biol.* **56**, 65-75.

DeMott, W.R. (1982) Feeding selectivities and relative ingestion rates of *Daphnia* and *Bosmina*. L*imnology and Oceanography* **27**, 518–527.

Dennis, B., Desharnais, R. A., Cushing, J. M., Henson, S. M. and Costantino, R. F. (2001) Estimating chaos and complex dynamics in an insect population. *Ecol. Monographs* **71**, 277–303.

Dieudonne, J. (1960) *Foundations of Modern Analysis.* New York: Academic.

Duffy, M. A. and Sivars-Becker, L. (2007) Rapid evolution and ecological host–parasite dynamics. *Ecology Letters* **10**, 44–53.

Edwards, A.M. (2001) Adding detritus to a nutrient-phytoplankton-zooplankton model: a dynamical-systems approach. *J. Plankton Res.* **23**, 389-413.

Eichinger, M., Kooijman, S.A.L.M., Sempere, R., Lefevre, D., Gregori, G., Charriere, B. and Poggiale, J.-C. (2009) Consumption and release of dissolved organic carbon by marine bacteria in a pulsed-substrate environment: from experiments to modelling. *Aquat. Microb. Ecol.* **56**, 41–54.

Englund, G. and Leonardsson, K. (2008) Scaling up the functional response for spatially heterogeneous systems. *Ecology Letters* **11**, 440–449.

Freckleton, R.P., Watkinson, A.R., Green, R.E. and Sutherland, W.J. (2006) Census error and the detection of density dependence. *Journal of Animal Ecology*, **75**, 837–851.

Freedman, H.I. and Mathsen, R.M. (1993) Persistence in predator-prey systems with ratio-dependent predator influence. *Bull. Math. Biol.* **55**, 817-827.

Fussmann, G.F., Ellner, S.P., Shertzer, K.W. and Hairston Jr., N.G. (2000) Crossing the Hopf bifurcation in a live predator-prey system. *Science* **290**, 1358-1360.

Fussmann, G.F. and Blasius, B. (2005) Community response to enrichment is highly sensitive to model structure. *Biology Letters* **1**, 9–12.

Gause, G. F. (1934) *The struggle for existence.* New York: Hafner Publishing Company.

Gentleman, W., Leising, A., Frost, B., Storm, S. and Murray, J. (2003). Functional responses for zooplankton feeding on multiple resources: a review of assumptions and biological dynamics. *Deep-Sea Research II* **50**, 2847–2875.

Giller, P. S. and Doube, B. M. (1994) Spatial and temporal co-occurrence of competitors in Southern African dung beetle communities. *J. Anim. Ecol.* **63**, 629–643.

Gilpin, M.E. (1972) Enriched predator–prey systems: theoretical stability. *Science* **177**, 902–904.

Gilpin, M.E. and Ayala, F.J. (1973) Global models of growth and competition. *PNAS* **70**, 3590–3593.

González-Olivares, E., González-Yañez, B., Lorca, J.M., Rojas-Palma, A. and Flores, J.D. (2011a) Consequences of double Allee effect on the number of limit cycles in a predator–prey model. *Computers & Mathematics with Applications* **62**, 3449-3463.

González-Olivares, E., Lorca, J.M., Rojas-Palma, A. and Flores, J.D. (2011b) Dynamical complexities in the Leslie–Gower predator–prey model as consequences of the Allee effect on prey. *Appl. Math. Model.* **35**, 366–381.

Greenman J.V. and Benton T.G. (2003) The amplification of environmental noise in population models: Causes and consequences. *American Naturalist* **161**, 225-239.

Gross, T., Ebenhoh, W. and Feudel, U. (2004) Enrichment and food-chain stability: the impact of different forms of predator–prey interaction. *J. Theor. Biol.* **227**, 349–358.

Gross, T. and Feudel, U. (2006) Generalized models as a universal approach to the analysis of nonlinear dynamical systems. *Physical Review E* **73**, 016205.

Gross, T., Edwards, A., M. and Feudel, U. (2009) The invisible niche: Weakly density-dependent mortality and the coexistence of species. *J. Theor. Biol.* **258**, 148-155.

Guo, Q. F., Brown, J. H. and Valone, T. J. (2002) Long-term dynamics of winter and summer annual communities in the Chihuahuan desert. *J. Veg. Sci.* **13**, 575–584.

Halbach, U. and Halbach-Keup, G. (1974) Quantitative Beziehungen zwischen Phytoplankton und der Populationsdynamik des Rotators Brachionus calyciflorus Pallas. Befunde aus Laboratoriumsexperimenten und Freilanduntersuchungen. *Archiv fur Hydrobiologie* **73**, 273-307.

Hansen, B., Tande, K.S. and Berggreen, U.C. (1990) On the trophic fate of Phaeocystis pouchetii (Hariot). III. Functional responses in grazing demonstrated on

juvenile stages of *Calanus finmarchicus* (Copepoda) fed diatoms and *Phaeocystis*. *J. Plankton Res.***12**, 1173–1187.

Haque, M. (2009) Ratio-dependent predator-prey models of interacting populations. *Bull. Math. Biol.* **71**, 430-452.

Hastings, A., Hom, C. L., Ellner, S., Turchin, P. and Godfray, H. C. J. (1993) Chaos in ecology: is Mother Nature a strange attractor? *Annu. Rev. Ecol. Syst.* **34**, 1–33.

Holling, C.S. (1966) The functional response of vertebrate predators to prey density. *Mem. Entomol. Soc. Canada* **48**, 1–86.

Hopf., F.A. and Hopf., F.W. (1985) The role of the Allee effect in species packing. *Theor. Pop. Biol.* **27**, 25–50.

Hsu, S.-B., Hwang, T.-W. and Kuang, Y. (2001) Global analysis of the Michaelis–Menten-type ratio-dependent predator-prey system. *J. Math. Biol.* **42**, 489-506.

Janssen, P.H.M., Heuberger, P.S.C. and Sanders, R. (1994) UNCSAM: A tool for automating sensitivity and uncertainty analysis. *Environmental Software* **9**, 1–11.

Jassby, A.D. and Platt, T. (1976) Mathematical formulation of the relationship between photosynthesis and light for phytoplankton. *Limnol. Oceanogr.* **21**, 540–547.

Jeschke, J.M., Kopp, M. and Tollrian, R (2002) Predator functional responses: discriminating between handling and digesting prey. *Ecol. Monogr.* **72**, 95–112.

Jones, L., Becks, L., Ellner, S.P., Hairston, N., Yoshida, T. and Fussmann, G. (2009) Rapid contemporary evolution and clonal food web dynamics. *Phil. Trans. R. Soc. B*, **364**, 1579–1591.

Jost, C., Arino, O. and Arditi, R. (1999) About deterministic extinction in ratio-dependent predator-prey models. *Bull. Math. Biol.* **61**, 19-32.

Jost, C. and Ellner, S.P. (2000) Testing for predator dependence in predator-prey dynamics: A non-parametric approach. *Proc. R. Soc. B* **267,** 1611–1620.

Kar, T.K., Ghorai, A. and Batabyal, A. (2012) Global dynamics and bifurcation of a tri-trophic food chain model. *World J. of Modelling and Simuation* **8**, 66-80.

Kinnison, M.T. and Hairston Jr., N.G. (2007) Eco-evolutionary conservation biology: contemporary evolution and the dynamics of persistence. *Funct. Ecol.* **21**, 444–454.

Kisdi, E., Geritz, S.A.H. and Boldin, B. (2013) Evolution of pathogen virulence under selective predation: A construction method to find eco-evolutionary cycles. *J. Theor. Biol.* **339**, 140-150.

Kolmogorov, A.N. (1936) Sulla Teoria di Volterra della Lotta per l'Esistenza. *Giornale Instituto Italiani Attuari* **7**, 74–80.

Kondoh, M. (2003) Foraging adaptation and the relationship between food-web complexity and stability. *Science* **299,** 1388-1391**.**

Kuang, Y. and Freedman, H.I., (1988) Uniqueness of limit cycles in Gause-type models of predator–prey systems. *Mathematical Biosciences* **88**, 67–84.

Kuang, Y. and Beretta, E. (1998) Global qualitative analysis of a ratio-dependent predator-prey system. *J. Math. Biol.* **36**, 389–406.

Kuehn, C., Siegmund, S. and Gross, T. (2012) Dynamical analysis of evolution equations in generalized models. *IMA J. of Applied Math.* **78**, 1051-1077.

Kuznetsov, Y.A. (2004) *Elements of Applied Bifurcation Theory*. New York: Springer.

Lewis, M.A. and Kareiva, P. (1993) Allee dynamics and the spread of invading organisms. *Theor. Popul. Biol.* **43**, 141–158.

Li, B. and Kuang, Y. (2007) Heteroclinic bifurcation in the Michaelis-Menten type ratio-dependent predator-prey system. *SIAM J. Appl. Math.* **67**, 1453-1464.

Lim, J.T., Gold, H.J., Wilkerson, G.G. and Raper, C.D. (1989) Monte Carlo/response surface strategy for sensitivity analysis: application to a dynamic model of vegetative plant growth. *Appl. Math. Model.* **13**, 479–484.

de Mazancourt, C. and Dieckmann, U. (2004) Trade-off geometries and frequency-dependent selection. *American Naturalist* **164**, 765-778.

Morozov, A.Y., Arashkevich, E., Reigstad, M. and Falk-Petersen, S. (2008) Influence of spatial heterogeneity on the type of zooplankton functional response: a study based on field observations. *Deep-Sea Res. II* **55**, 2285–2291.

Morozov, A.Y. (2010) Emergence of Holling type III zooplankton functional response: bringing together field evidence and mathematical modelling. *J. Theor. Biol.* **265**, 45–54.

Morozov, A.Yu. and Adamson, M.W. (2011) Evolution of virulence driven by predator-prey interaction: possible consequences for population dynamics. *J. Theor. Biol.* **276**, 181-191.

Morozov, A.Y. (2012) 'Incorporating complex foraging of zooplankton in models: role of micro- and mesoscale processes in macroscale patterns.' In Lewis, M.A., Maini, P. and Petrovskii, S. (eds.) *Dispersal, Individual Movement and Spatial Ecology: A mathematical Perspective*. New York: Springer, pp 223-259.

Morris, W.F. (1990) Problems in detecting chaotic behavior in natural populations by fitting simple discrete models. *Ecology* **71**, 1849-1862.

Muller E.B., Kooijman S., Edmunds P.J., Doyle F.J. and Nisbet, R.M. (2009) Dynamic energy budgets in syntrophic symbiotic relationships between heterotrophic hosts and photoautotrophic symbionts. *J. Theor. Biol.* **259** 44–57.

Myerscough, M.R., Darwen, M.J. and Hogarth, W.L. (1996) Stability, persistence and structural stability in a classical predator-prey model. *Ecological Modelling* **89**, 31–42.

Nelson, W.A., McCauley, E. and Wimberta, J. (2004) Capturing dynamics with the correct rates: inverse problems using semiparametric approaches. *Ecology* **85**, 889–903.

Nicholson, A.J. (1957) The self-adjustment of populations to change. *Cold Spring Harbor Symposia on Quantitative Biology* **223**, 153-173.

Nisbet, R.M., McCauley, E., Gurney, W.S.C., Murdoch, W.W. and Wood, S.N. (2004) Formulating and testing a partially specified dynamic energy budget model. *Ecology* **85**, 3132-3139.

Oaten, A. and Murdoch, W.W. (1975) Functional response and stability in predator-prey systems. *Amer. Nat.*, **109**, 289–298.

Owen, M.R. and Lewis, M.A. (2001) How predation can slow, stop or reverse a prey invasion. *Bull. Math. Biol.* **63**, 655–684.

Pascual, M., Mazzega, P. and Levin, S. (2001) Oscillatory dynamics and spatial scale: the role of noise and unresolved pattern. *Ecology* **82**, 2357–2369.

Philippart, C.J.M., Cadee, G.C., van Raaphorst, W. and Riegman, R. (2000) Long-term phytoplankton–nutrient interactions in a shallow coastal sea: algal community structure, nutrient budgets, and denitrification potential. *Limnol. Oceanogr.* **45**, 131–144.

Poggiale, J.-C. (1998) Predator–prey models in heterogeneous environment: emergence of functional response. *Mathematical and Computer Modelling* **27**, 63–71.

Poggiale, J.-C., Michalski, J. and Arditi, R. (1998) Emergence of donor control in patchy predator-prey systems. *Bull. Math. Biol.* **60**, 1149-1166.

Poggiale, J.-C., Auger, P., Cordoléani, F. and Nguyen-Huu, T. (2009) Study of a virus-bacteria interaction model in a chemostat: application of geometrical singular perturbation theory. *Phil. Trans. R. Soc. A* **367**, 4685-4697.

Poggiale, J.-C., Baklouti, M., Queguiner, B., Kooijman, S. (2010) How far details are important in ecosystem modelling: the case of multi-limiting nutrients in phytoplankton–zooplankton interactions. *Phil. Trans. R. Soc. B* **365**, 3495–3507.

Reeve, J.D. (1997) Predation and bark beetle dynamics. *Oecologia* **112**, 48-54.

Rosenzweig, M.L. and MacArthur, R.H. (1963) Graphical representation and stability conditions of predator–prey interactions. *American Naturalist* **97**, 209–223.

Rosenzweig, M.L. (1971) Paradox of enrichment: destabilization of exploitation ecosystems in ecological time. *Science* **171**, 385–387.

Savageau, M.A. and Voit, E.O. (1987) Recasting nonlinear differential equations as S-systems: a canonical nonlinear form. *Mathematical biosciences* **87**, 83-115.

Sen, M., Banerjee, M. and Morozov, A. (2012) Bifurcation analysis of a ratio-dependent prey-predator model with the Allee effect. *Ecological Complexity* **11**, 12-27.

Sibly, R.M., Barker, D., Denham, M.C., Hone, J. and Pagel, M. (2005) On the regulation of populations of mammals, birds, fish, and insects. *Science*, **309**, 607–610.

Smayda, T.J. (1998) Patterns of variability characterizing marine phytoplankton, with examples from Narragansett Bay. *ICES J. Mar. Sci.* **55**, 562–573.

Steele, J.H. and Henderson, E. (1992) The role of predation in plankton models. *J. Plankton Res.* **14**, 157–172.

Steuer, R., Gross, T., Selbig, J. and Blasius, B. (2006) Structural kinetic modeling of metabolic networks. *PNAS* **103**, 11868-11873.

Sumner, S. (1996) Hopf bifurcation in pioneer-climax competing species models. *Math Biosci.* **137**, 1-24.

Thompson, J.N. (1998) Rapid evolution as an ecological process. *Trends Ecol. Evol.* **13**, 329–332.

Tischner, R. and Lorenzen, H. (1979) Nitrate uptake and nitrate reduction in synchronous Chlorella. *Planta* **146**, 287-92.

Truscott, J.E. and Brindley, J. (1994) Equilibria, stability and excitability in a general class of plankton population models. *Phil. Trans. R. Soc. A* **347**, 703–718.

Turchin, P. and Ellner, S.P. (2000) Living on the edge of chaos: population dynamics of Fennoscandian voles. *Ecology* **81**, 3099–3116.

Valdes, L. et al. (2007) A decade of sampling in the Bay of Biscay: what are the zooplankton time series telling us? *Progr. Oceanogr.* **74**, 98–114.

Vasseur, D.A. (2007) Populations embedded in trophic communities respond differently to coloured environmental noise. *Theoretical Population Biology* **72**, 186–196.

Wang, M.E., Kot, M. (2001) Speeds of invasion in a model with strong or weak Allee effects. *Math. Biosci.* **171**, 83–97.

Wolda, H. (1988) Insect seasonality: why? *Annu. Rev. Ecol. Syst.* **19**, 1–18.

Wood S.N. and Nisbet, R.M. (1991) *Estimation of Mortality Rates in Stage-Structured Populations*. New York: Springer Verlag.

Wood, S.N. and Thomas, M.B. (1999) Super-sensitivity to structure in biological models. *Proc. R. Soc. B* **266**, 565–570.

Wood, S. N. (2001) Partially specified ecological models. *Ecological Monographs* **71,** 1–25.

Xiao, D. and Ruan, S. (2001) Global dynamics of a ratio-dependent predator-prey system. *J. Math. Biol.* **43**, 268-290.

Yoshida, T., Jones, L.E., Ellner, S.P., Fussmann, G.F. and Hairston, N.G. (2003) Rapid evolution drives ecological dynamics in a predator-prey system. *Nature* **424,** 303–306.